BIOCHEMICAL RECONSTITUTION AND FUNCTIONAL CHARACTERIZATION OF THE WAVE REGULATORY COMPLEX

APPROVED BY SUPERVISORY COMMITTEE

Michael K. Rosen, Ph.D.

Joseph Albanesi, Ph.D.

Qinghua Liu, Ph.D.

Elliott Ross, Ph.D.

To my loving wife

and to the memory of my mother.

BIOCHEMICAL RECONSTITUTION AND FUNCTIONAL CHARACTERIZATION OF THE WAVE REGULATORY COMPLEX

by

AYMAN MOHAMED ISMAIL

DISSERTATION

Presented to the Faculty of the Graduate School of Biomedical Sciences

The University of Texas Southwestern Medical Center at Dallas

In Partial Fulfillment of the Requirements

For the Degree of

DOCTOR OF PHILOSOPHY

The University of Texas Southwestern Medical Center at Dallas

Dallas, Texas

June, 2009

Acknowledgments

I am greatly indebted to my mentor Michael K. Rosen. Almost everything I know about research and scientific thinking, I learned from him or from discussions I had while I was a member of his lab. He has been supportive and very patient throughout a project that required extreme attention to details and involved a lot of frustrating moments. While remaining realistic at all times, he was always optimistic and had the confidence that I can overcome all the hurdles in my project. If for nothing else, that made me push myself to try harder than ever and discover new limits of patience and perseverance. As I move on with my career, I will miss the most every single discussion we had, whether about my thesis or biology in general.

It is said that life is a school where you learn something new everyday. If the people I know are the books of my school of life, then current and former members of the Rosen lab formed libraries that enriched my experience and my life beyond measure. They were a group that relished scientific discussions. They are (in no specific order) Abi Seth, M.D., Ph.D., Gaya Amarasinghe, Ph.D., Shae Padrick Ph.D., Daisy Leung, Ph.D., Pilong Li, Ph.D., Eduardo Torres, Ph.D., Ilidio Martins, David Morgan, Ph.D., Sanjay Panchal, Ph.D., Takanori Otomo, Ph.D., Chinatsu Otomo, Mara Kreishman Deitrick, Ph.D., Xiaolan Yao, Ph.D., Hui-Chun Cheng, Ph.D., Junko Umetani, Lynda Doolittle, Baoyu Chen, Ph.D., Da Jia, Ph.D., Xiaocheng Chen, Ph.D., Sudeep Banjade, Zhucheng Chen, Ph.D., Zoltan Metlagel, Ph.D., Soyeon Kim, Elisha White and Dee Seres.

I thank my committee members, Joseph Albanesi, Ph.D., Elliott Ross, Ph.D., and Qinghua Liu, Ph.D. Their questions and suggestions always helped me shape the

direction of my next research. I also thank Kevin Gardner, Ph.D., the chair of the molecular biophysics graduate program for all his efforts, assisted by Jo Appleton, to make the program successful, and always responsive to the needs of its students.

I want to acknowledge all the support I received from my family. My trusted companion and my wife, Rita Sulahian, Ph.D., defines with her support to me the meaning of unconditional love and patience. She gets all the credit for keeping me sane during these years. My father, brother and sister in Lebanon have been supportive of all my career decisions, no matter how far those decisions removed me away from my country. They are always in my heart. Finally, I wish my mother was still with us to celebrate my achievements with me.

Publications

1. Ismail, A.M., Padrick, S.B., Chen, B., Umetani, J., and Rosen, M.K. (2009). The WAVE regulatory complex is inhibited. Nat Struct Mol Biol *16*, 561-563.

2. Padrick, S.B.*, Cheng, H.C.*, Ismail, A.M.*, Panchal, S.C., Doolittle, L.K., Kim, S., Skehan, B.M., Umetani, J., Brautigam, C.A., Leong, J.M., and Rosen, M.K. (2008). Hierarchical regulation of WASP/WAVE proteins. Mol Cell *32*, 426-438. (* equally contributing authors)

3. Talhouk, R.S., Mroue, R., Mokalled, M., Abi-Mosleh, L., Nehme, R., Ismail, A., Khalil, A., Zaatari, M., and El-Sabban, M.E. (2008). Heterocellular interaction enhances recruitment of alpha and beta-catenins and ZO-2 into functional gap-junction complexes and induces gap junction-dependant differentiation of mammary epithelial cells. Exp Cell Res *314*, 3275-3291.

BIOCHEMICAL RECONSTITUTION AND FUNCTIONAL CHARACTERIZATION OF THE WAVE REGULATORY COMPLEX

Ayman Mohamed Ismail, Ph.D.

The University of Texas Southwestern Medical Center at Dallas, 2009

Supervising Professor: Michael K. Rosen, Ph.D.

Members of the Wiskott-Aldrich syndrome protein (WASP) family (WASP, N-WASP, WAVE 1-3) have a central role in the transmission of the extracellular signals to the actin cytoskeleton. These proteins use their C-terminal VCA domain to stimulate the actin-nucleating activity of Arp2/3 complex in response to upstream signals from the Rho family GTPases Cdc42 and Rac1. While WASP regulation by GTPases and kinases is well characterized both biochemically and structurally, little is known about WAVE regulation.

WAVE exists as part of a five protein complex termed the WAVE Regulatory Complex (WRC). It consists of WAVE, Sra1, Nap1, Abi2 and HSPC300. Biochemical studies of WRC have been hampered by the difficulty of expressing WRC components in bacterial, insect or yeast expression systems. Baculoviruses yielding high expression of each component of WRC were obtained using a modified pFastBac vector, where translation is driven by the lobster tropomyosin promoter. Co-infection into Sf9 cells allowed efficient expression and purification of WRC and two sub-complexes, Sra-Nap and Abi2-WAVE1-HSPC300. We show that WRC is inactive toward Arp2/3 complex in pyrene based actin assembly assays. However, Abi2-WAVE1-HSPC300 heterotrimer is active and Sra1-Nap1 heterodimer inhibits it suggesting that WRC is autoinhibited.

A modified WRC complex, where WAVE1 has a PreScission protease site between its VCA domain (the active domain) and its N-terminus and is lacking the proline rich domain, is also inactive toward Arp2/3 complex. However, upon digestion with PreScission protease, this modified complex becomes active. This suggests that the affinity between VCA and the Sra-Nap heterodimer is inherently weak and the heterodimer requires the linkage provided by the Abi2-WAVE1-HSPC300 heterotrimer to VCA to efficiently inhibit it from activating the Arp2/3 complex. The same results are obtained using all Drosophila components. Finally, Rac1-GTP is able to activate WRC towards Arp2/3. However, no dissociation of the complex is detected upon activation by Rac1.

In addition to WRC regulation, we have established the mechanism for hyperactivation of VCA through dimerization. We found that a dimeric VCA construct binds Arp2/3 complex with a two VCAs to one Arp2/3 ratio. The affinity of dimeric

VCA for Arp2/3 is at least 100 fold higher than monomeric VCA. That explains the potentiation of VCA toward Arp2/3 observed upon VCA dimerization, and provides a mechanistic framework for a new model of WASP regulation superimposed upon allostery. We have also demonstrated that N-WASP and WRC may be able to form a hetero-VCA dimer through the interaction of Abi2 SH3 domain and N-WASP PRD. Such interaction increases the complexity and the signal integration potential of WASp family proteins.

Table of Contents

List of Figures

List of Tables

List of Appendices

List of Abbreviations

Abi	Abl Interactor
Arp2/3	Actin Related Protein 2/3
βME	Beta Mercaptoethanol
cAMP	Cyclic Adenosine Monophosphate
CNS	Central Nervous System
CYFIP	Cytoplasmic FMRP Interacting Protein
Da	Dalton
F-actin	Filamentous Actin
FMRP	Fragile X Mental Retardation Protein
G-actin	Globular (monomeric) actin
GAP	Guanine nucleotide Activating Protein
GBD	GTPase Binding Domain
GDB	Guanine Diphosphate
GEF	Guanine nucleotide Exchange Factor
GS4B	Glutathione Sepharose 4B
GST	Glutathione S-Transferase
GTP	Guanine Triphosphate
HSPC300	Hematopoietic Stem Progenitor Cells 300
HSQC	Heteronuclear Single Quantum Correlation
IRSp53	Insulin Receptor Substrate p53
kDa	kiloDalton
M	Molar

MALS	Multi-Angle Light Scattering
MEF	Mouse Embryonic Fibroblast
μM	Micromolar
mM	Millimolar
MS	Mass Spectroscopy
Nap	Nck Associated Protein
NBF	Nap Binding Fragment
nM	Nanomolar
NMR	Nuclear Magnetic Resonance
NPF	Nucleation Promoting Factor
N-WASP	Neuronal-WASP
PIP_3	Phosphatidylinositol 3,4,5-trisphosphate
ppm	Parts Per Million
PRD	Proline Rich Domain
PTM	Post Translational Modification
Rho	Ras Homology
Scar	Suppressor of Cyclic AMP Receptor
SDS-PAGE	Sodium Dodecil Sulfate-Polyacrylamide Gel Electrophoresis
Sf9	*Spodoptera Frugiperda* cells 9
SH2	Src Homology 2
SH3	Src Homology 3
Sra	Specifically Rac Associated
VCA	Verproline homology Central domain Acidic region

WASH	WASP and Scar Homologue
WASP	Wiskott Aldrich Syndrome Protein
WAVE	WASP homology Verprolin like protein
WH1	WASP Homology 1
WHAMM	WASP Homolog associated with Actin Membranes and Microtubules
WHD	WAVE Homology Domain
WRC	WAVE Regulatory Complex

Chapter One: Introduction

1.1. Actin cytoskeleton and the WASP family proteins

1.1.1. Actin cytoskeleton and the nucleation problem

The cellular cytoskeleton is a collection of filaments of different sizes and protein constituency that provide the cell with shape, structural rigidity/flexibility, movement and a framework for protein and vesicular trafficking. The cytoskeleton is generally divided into three distinct yet interconnected networks: microtubules, the intermediate filaments and the actin filaments. This work focuses on regulators of the actin cytoskeleton.

Actin is one of the most conserved proteins in nature. Its amino-acid sequence is fully identical in most mammals, including humans, cows, cat, rabbits, pigs and mice (Sheterline et al., 1998). Actin transits between two forms, a monomeric state known as G-actin and a polymeric state known as filamentous actin or F-actin. The latter state forms the actin cytoskeleton, a complex network of actin filaments that can be bundled into different shapes and structures due to the large number of proteins that interact with the actin filament. For example, α-actinin can assemble actin filaments into a contractile bundle; fimbrin can group them more tightly into a parallel bundle, while filamin enables the formation of a mesh-like network of filaments. These connections allow the cell to form different structures such as lamellipodia, filopodia and stress fibers, which in turn provide the cell with vital functions including migration, adhesion, establishment and maintenance of polarity, and vesicular trafficking (Egea et al., 2006; Evangelista et al., 2003; Pollard and Borisy, 2003; Rafelski and Theriot, 2004).

The actin cytoskeleton is a dynamic structure that undergoes cycles of filament polymerization and depolymerization. This process is highly regulated by proteins that can interact with either actin monomer or actin filament and regulate the actin monomer-polymer dynamics. Some of those proteins promote severing of the filaments and depolymerization, such as cofilin, villin, gelsolin and ADF, while others cap the ends of the filaments to prevent depolymerization like tropomodulin, AIP, CapG [extensive reviews in (dos Remedios et al., 2003; Paavilainen et al., 2004; Silacci et al., 2004)]. But perhaps the most important regulators are the actin nucleators because they enable quick response of the actin cytoskeleton to extra-cellular signaling by overcoming the actin nucleation problem and thus rapidly generating *de novo* actin filaments. The nucleation problem stems from the fact that actin filaments require the presence of an actin nucleus to start growing by the rapid addition of G-actin to that nucleus with a favorable affinity of 120 nM. The nucleus itself is made of three G-actin monomers. However, most G-actin in the cell is bound to profilin, which blocks nucleation. Moreover, the nucleus formation itself is a limiting step in *de novo* filament formation (Fig. 1.1A). Two G-actin monomers form a dimer with a modeled affinity of 4.6 M. A third G-actin binds to that dimer with an estimated affinity of 0.6 mM (Pollard, 1986; Sept and McCammon, 2001). Such spontaneous nucleation is infrequent, and it lacks the spatial and temporal control of filament generation needed for correct cellular response to signaling cues. Actin nucleators not only provide such control but also catalyze the thermodynamically unfavorable formation of the actin nucleus allowing new filaments to quickly form where and when needed. Formin(s), Spir(s), Leiomodin and the actin related protein 2/3 complex (Arp2/3 complex) constitute the groups of known actin nucleators in eukaryotes.

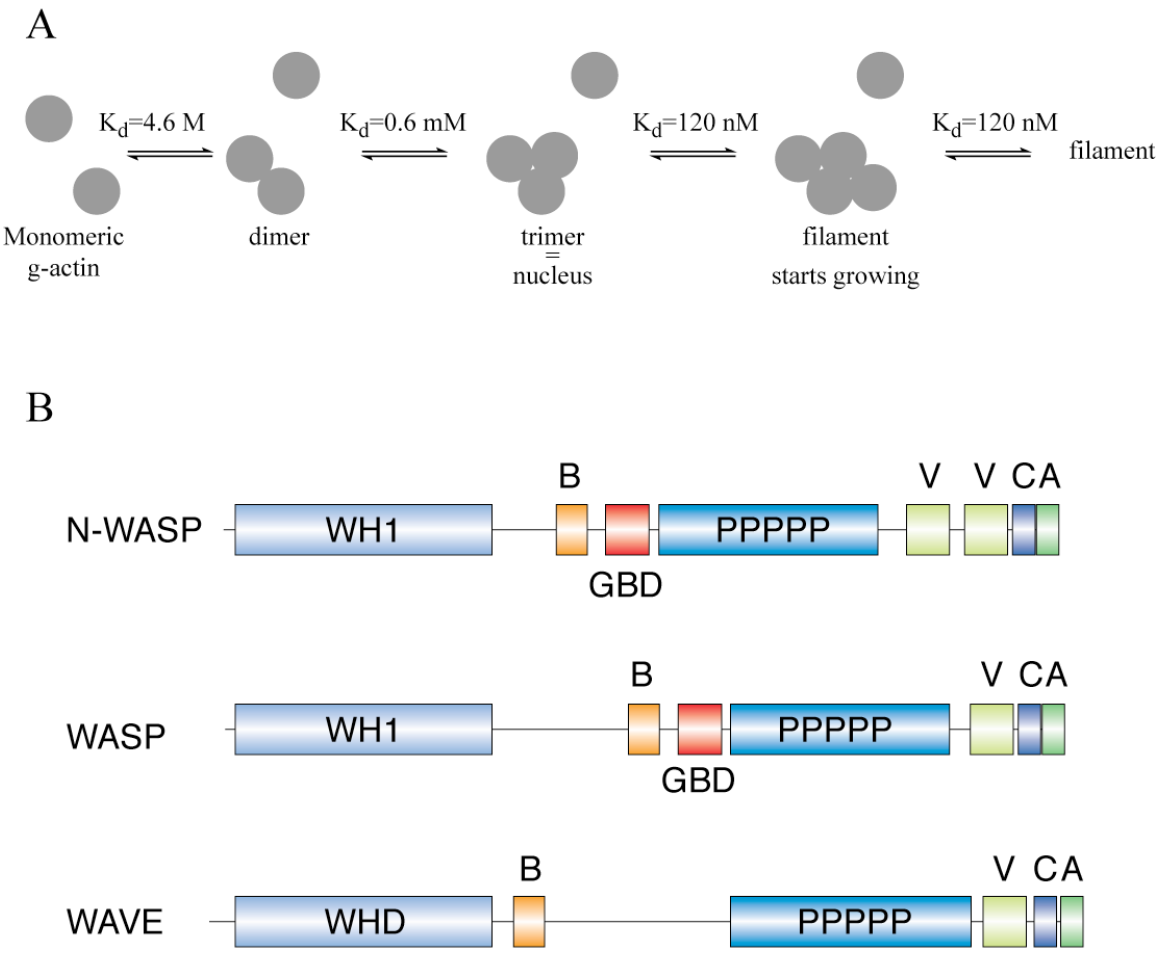

Figure 1.1: The actin nucleation problem and the WASP family proteins

(A) The dimerization of monomeric G-actin and the trimer formation are unfavorable reaction. However, once a nucleus is formed, G-actin can bind with high affinity, and a filament can polymerize rapidly. (B) The modular domain organization of N-WASP, WASP and WAVE

1.1.2. The WASP family proteins

The Arp2/3 complex is made of 7 different proteins (one copy each) that include the actin related protein 2 (Arp2) and Arp3, which are structurally similar to actin (Machesky et al., 1994; Robinson et al., 2001). In the active complex, Arp2 and Arp3 are thought to form an actin dimer-like structure that can accept a G-actin brought in by the Arp2/3 complex activator to form an actin nucleus. The complex is inactive in the absence of signaling. Among its activators (also known as nucleation promoting factors-NPF), the WASP family of proteins is the most studied. The family includes the Wiskott Aldrich Syndrome Protein (WASP), the ubiquitous neuronal WASP (N-WASP) and the three paralogues of the WASP family Verprolin homologous (WAVE) proteins, WAVE1, WAVE2 and WAVE3. Newly discovered members include the Wiskott Adrich syndrome protein and Scar Homologue (WASH) and WASP homolog associated with actin, membranes, and microtubules (WHAMM).

WASP family proteins are all characterized by a central segment rich in proline (PRD) followed by a C-terminal VCA segment (Verprolin homology, Central hydrophobic, and Acidic elements) (Fig. 1.1B). Arp2/3 complex binds the VCA, and the side of an existing actin filament. These interactions induce a rearrangement of Arp2 and Arp3 in the complex, whereby they adopt a conformation similar to a dimer of actin. A monomeric actin bound to the V segment of VCA is added to the actin-like dimer of Arp2 and Arp3 and completes the nucleus. The Arp2/3 complex is activated and nucleates a new filament. In addition to PRD and VCA, WASP and N-WASP also have a WH1 (WASP homology1) domain, followed by a basic region and a GTPase binding domain (GBD) N-terminal to their PRD region. Whereas isolated VCA can activate

Arp2/3 on its own in an actin assembly assay (the standard pyrene fluorescence based assay for actin assembly, see p58), full length WASPs have very low activity. Structural work done in our lab provided the explanation: The C segment of VCA forms an amphipathic helix that binds Arp2/3 complex on the hydrophobic face (Panchal et al., 2003). In the context of WASPs, this hydrophobic face binds intra-molecularly to the GBD (Fig. 1.2A), which prevents the A segment from activating the Arp2/3 complex, leading to WASPs auto-inhibition (Kim et al., 2000). The Rho GTPase Cdc42 transmits extra-cellular signals to WASPs by binding to the GBD and allosterically releasing VCA from GBD (Fig. 1.2B), enabling it to become active towards Arp2/3 complex (Abdul-Manan et al., 1999; Kim et al., 2000). Moreover, WASPs are capable of integrating multiple signaling cues. Phosphorylation of a tyrosine in the GBD creates a new signaling pathway where SH2 domain containing proteins can bind and activate WASPs (Torres and Rosen, 2003). SH3 domain containing proteins can bind PRD and activate WASPs. The phosphoinositide PIP_2 was demonstrated to bind the basic region preceding GBD and activate WASPs (Miki et al., 1996; Prehoda et al., 2000; Rozelle et al., 2000). However, the predominant mechanism for these classes of activators (SH3 containing proteins and phospholipids) may not be release of auto-inhibition, but rather dimerization of WASP and the resulting potentiation, as will be explained later.

WAVE proteins are regulated differently from WASPs. They do not have a GBD domain to intra-molecularly inhibit VCA (Fig. 1.1B), and indeed purified full length WAVE is active towards Arp2/3 complex in an actin assembly assay (Machesky et al., 1999). Despite their lack of a GBD, WAVE proteins were implicated as downstream effectors of Rac, another Rho GTPase, although no direct interaction between Rac (or

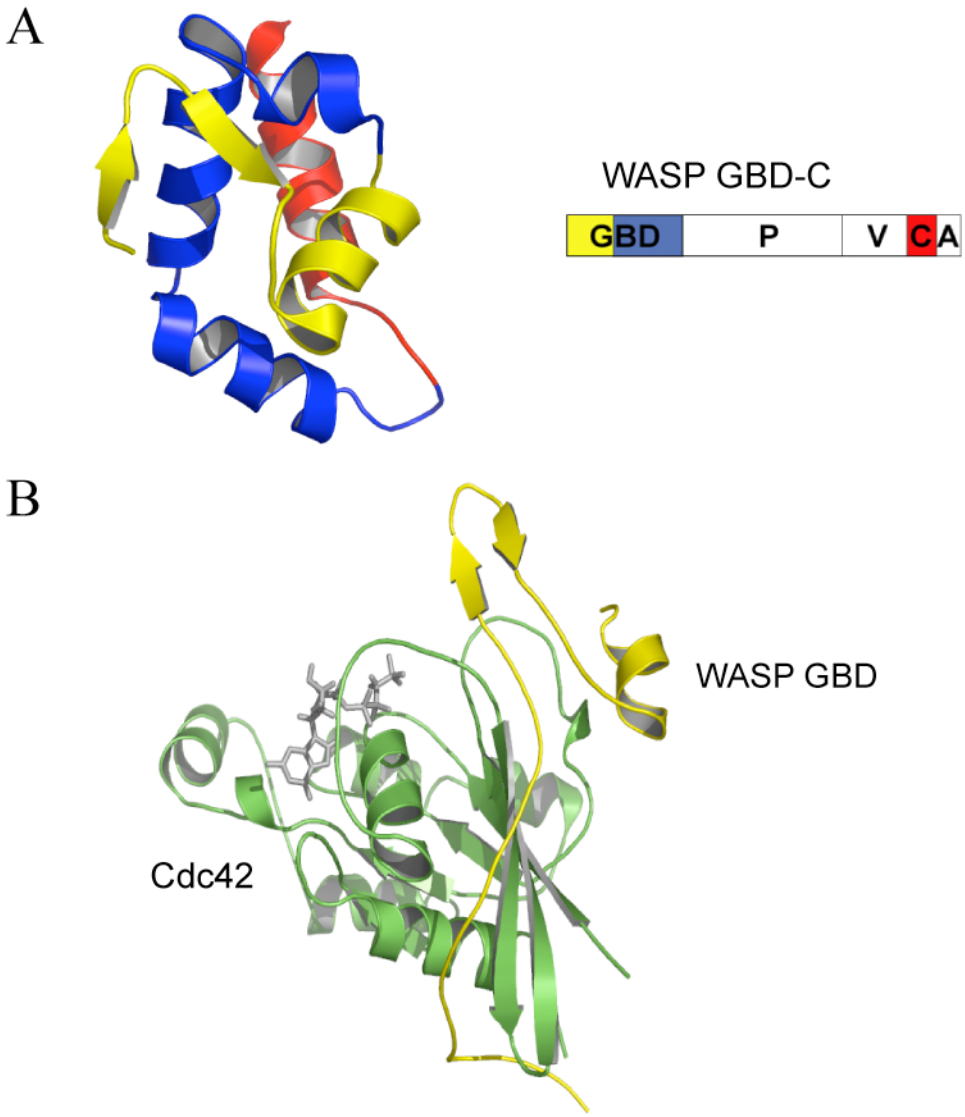

Figure 1.2: Autoinhibition and activation mechanisms of WASP

(A) The autoinhibited structure of a WASP construct comprising of the GBD and the C segment of VCA, tethered by a GGS linker. The structure is composed of a hairpin and 5 α-helix and resembles three stacked layers, with GBD forming the front 2 (yellow and blue), while C forms the third (red). (B) Cdc42 binds the CRIB motif (yellow layer in (A)), leading to unfolding of the GBD and release of VCA.

other Rho GTPases) and any of the three WAVEs has been established. The N-terminus of WAVEs is made of a Scar/WAVE homology domain (WHD) that is distinct from WH1 domain in WASP, and has not been assigned a function yet (Fig. 1.1).

Besides domain architecture, WAVE is also different than WASP in the nature of its existence in the cell. In 2002, a report detailed the purification and identification of a pentameric complex containing WAVE, along with PIR121, Nap, Abi and HSPC300 (Eden et al., 2002). We call this complex the WAVE Regulatory Complex or WRC. The discovery of the WRC was extremely important for a number of reasons. First, it grouped research interests on five seemingly unrelated protein into one field. Second, it provided the missing link between Rac and the actin cytoskeleton (Rac can bind PIR121). Third, it provided a potential regulatory framework for WAVE. Fourth, it oriented the research on WAVE toward the investigation of the function of WRC. The next sections of this chapter summarize the literature on the WRC.

1.2. WAVE Regulatory Complex (WRC)

Before the seminal 2002 paper by Eden *et.al.*, four of the five components of WRC were already identified independently. It is interesting that each of those was discovered in a different context, and only WAVE was directly linked Arp2/3 regulation.

1.2.1. Identification of the different components of the complex

1.2.1.1. WAVE1, 2, 3

The deletion of cAMP receptor2, a G-protein coupled receptor, causes morphogenic arrest before tip formation in *Dictyostelium discoidum* development. In a

search for genetic deletions that would suppress this phenotype, Bear *et.al.* identified a gene the deletion of which restores tip formation (Bear et al., 1998). The gene was thus named Suppressor of cAMP Receptor or *Dd*Scar. A sequence based homology search identified three human orthologues, *Hs*Scar1, *Hs*Scar2 and *Hs*Scar3, and one fruit fly orthologue, *Dm*Scar. It was also noted that Scar, like WASP, has a proline rich domain followed by a VCA domain. Scar was thus considered a new member in the WASP family of proteins.

In parallel and independent study, Miki *et.al.* were trying to identify new members of the WASP family by looking for proteins that contain the verproline homology region (the V segment of the VCA domain) in the human genome. They discovered a protein that has similar sequence structure to that of WASP but without a CRIB motif (Miki et al., 1998). It was therefore named WASP family Verproline Homologous protein or WAVE1. WAVE1 was shown to bind to profilin through its proline rich domain. It also co-immunoprecipitated with Rac but not Cdc42, although direct interaction could not be established. Actin reorganization induced by Rac but not Cdc42 was disrupted by the expression of a WAVE1-ΔV construct. From this work, The authors suggested for the first time that two parallel pathways existed for signaling to the actin cytoskeleton through Rho family of GTPases: one that goes through Cdc42-WASP and another that goes through Rac-WAVE.

Using sequence homology search, WAVE2 and WAVE3 were identified, their sequence aligned with WAVE1 and found to be 73% identical in the WHD N-ternimal domain and 83% identical in the VCA domain. Overall, the three sequences are 48% identical (Suetsugu et al., 1999). Further examination of sequences of WAVE1,

WAVE2, WAVE3 and Scar1, Scar2, Scar3 reveals that they are actually the same proteins, respectively. The literature uses Scar and WAVE interchangeably. Throughout this dissertation, I will only use the WAVE nomenclature. The initial mapping of tissue distribution determined that WAVE1 and WAVE3 are predominantly expressed in the brain and weakly in kidney and liver, while WAVE2 is ubiquitous (Suetsugu et al., 1999). A later study extended the profile of WAVE1 expression to lungs, placenta, liver and pancreas (Sossey-Alaoui et al., 2003).

1.2.1.2. Nap1

Nap was identified twice by the same group in two separate screens looking for binders of two separate proteins. The objective of the first screen was to look for proteins that would interact with one of the three SH3 domains of the adapter protein Nck, (Kitamura et al., 1996). Using immobilized GST-Nck-SH3, the authors were able to pull-down from bovine brain extract a 125-kDa protein and a 140-kDa protein that bound only to full length Nck and the first SH3 domain, but not to the second and third SH3 domains or to the control SH3 domains from Grb2 and p85α proteins. The 125-kDa protein was sequenced and a corresponding cDNA was isolated from rat brain. The protein was called Nck associated protein 1 or Nap1. Further studies with purified proteins failed to demonstrate direct interaction, suggesting that Nap1 may be a part of a complex to which Nck binds.

In a very similar study, the same group screened for proteins that bind Rac GTPase from bovine brain extract (Kitamura et al., 1997). Again they pulled down a 125-kDa and a 140-kDa protein. The 125-kDa protein was identified as Nap1. As with Nck, direct association of Rac and Nap1 could not be established using purified proteins.

Nap1 is ubiquitously expressed as its mRNA was found in all rat tissues that were screened with a Nap1 cDNA northern blot analysis. It also showed high identity score with a family of proteins of unknown function and no known domains called Hem. Nap1 was later called Hem2.

1.2.1.3. Sra1 and PIR121

A similar study looking for Rac binding proteins in the bovine brain cytosol again identified a 125-kDa and a 140-kDa protein (Kobayashi et al., 1998). The 125-kDa protein was none other than Nap1/Hem2. The 140-kDa protein was not a known protein; it was named Specifically Rac Associated 1 or Sra1. Interestingly, Sra1 co-sediments with F-actin but not G-actin, making it a potential candidate for the missing link between Rac signaling and the actin cytoskeleton.

Another screen was behind the identification of PIR121. A DNA micro-array chip was setup to look for proteins with increased levels of expression in a cell line that expresses the p53-121F mutant, a mdm2 independent apoptosis inducing p53 mutant (Saller et al., 1999). The protein identified in this screen was called 121F-specific p53 inducible RNA or PIR121. However, overexpression of PIR121 failed to induce apoptosis on its own. Originally, no link was suggested between PIR121 and the actin cytoskeleton. Later on, it was found to share 87.7% identity with Sra1 and was thus considered its homologue.

In 2001, a group was screening for proteins that interact with the fragile X mental retardation protein (FMRP), a protein involved in translational regulation, using a yeast two-hybrid system (Schenck et al., 2001). The screen identified a number of proteins, including one that the authors named Cytoplasmic FMRP Interacting Protein1 or

CYFIP1. After sequencing the protein, it was determined that it is actually the previously identified Sra1. *In vitro* translation and pull-downs confirmed the interaction. Given that PIR121 is the Sra1 homologue, Schenck *et.al.* tested its binding to FMRP and got positive results; they gave PIR121 a second name, CYFIP2. They also looked for interaction between CYFIP1 and 2 and the two FMRP related proteins FXR1 and FXR2. Only CYFIP1/Sra1 bound both FXR1 and FXR2. This study suggested that a cross-talk could exist between the translational control machinery and the actin rearrangement machinery. Such a link would be important especially in processes that require both dendritic extension and *de novo* protein synthesis such as synapse formation and neuronal plasticity.

The *C.elegans* orthologues of both Sra1 and Nap1 were determined by homology search to be Gex2 and Gex3, respectively (Soto et al., 2002). Gex2 and Gex3 are required for proper cell migration and organ development in the worm. When either of the two is knocked-down by RNAi, *C.elegans* die prematurely. The most pronounced phenotype is the presence of otherwise internal gut cells on the exterior side of the gut, because of the failure of dermal cell migration in the ventral enclosure. Gex, or Gut on the exterior proteins, were named after this phenotype. Interestingly, a yeast two hybrid assay established that Gex2 and Gex3 actually bind to each other, but only if both are full length. This could mean the folding of both proteins is sensitive to deletions. The result was confirmed by pull-downs from *C.elegans* lysate and from *in vitro* translated system.

1.2.1.4. Abi1, 2

Two studies published back to back established the existence of a family of proteins that bind to the tyrosine kinase c-Abl. The new proteins were called Abl

interactor 1 and 2, or Abi1 and Abi2 (Dai and Pendergast, 1995; Shi et al., 1995). Abi proteins have a homeo-domain like basic region at their N-terminus, followed by a proline rich domain and an SH3 domain at the C-terminus. The two groups demonstrated that the SH3 domain of c-Abl binds PRD in Abi and that the SH3 domain of Abi binds the C-terminal of c-Abl, which contains three proline rich segments.

Soon after, a yeast two-hybrid screen looking for proteins that bind Nap1 identified Abi1 as a hit that was called Nap1BP (Yamamoto and Behl, 2001). Pull-downs confirmed the interaction, which was mapped to amino acids 497 to 845 of Nap1. Despite the establishment of Sra1 and Nap1 binding (in the *C.elegans* system), the possibility of a complex that includes Sra1, Nap1 and Abi was not recognized.

1.2.1.5. HSPC300

HSPC300 stands for Hematopoietic Stem Progenitor Cells 300. It referred to a hypothetical protein expressed by the smallest open reading frame from a human gene fragment. The sequence was deposited in a gene databank without further description, and no research involving HSPC300 has been reported before the discovery of WRC.

1.2.2. Identification of the WAVE Regulatory Complex

The search for proteins that bind and regulate the activity of WAVE was motivated by the fact that full length WAVE1, unlike the auto-inhibited WASP, is constitutively active towards Arp2/3 complex. Starting with bovine brain tissue, Eden *et.al.* performed a series of purification steps that included high speed centrifugation, ammonium sulfate precipitation, immuno-precipitation and a number of liquid chromatography columns (Eden et al., 2002). Throughout the purification, they followed

the fractions containing WAVE1 by immuno-blotting with an antibody against WAVE1. After 13 purification steps WAVE1 still co-eluted with 4 other proteins. Those proteins were digested in-gel with trypsin, followed by mass determination using mass spectrometry. The resulting peptides were searched against non-redundant protein databases and the proteins were identified as being PIR121, Nap1, Abi2 and HSPC300. The five proteins thus form a complex that we refer to as the WAVE Regulatory Complex or WRC. The stoichiometry was estimated to be 1:1:1:1:1. Most importantly, when tested in actin polymerization assay, WRC, contrary to full length WAVE1, did not stimulate Arp2/3 complex. Moreover, GTP loaded Rac addition to the reaction activated WRC towards Arp2/3 complex. The existence of WRC was confirmed when the same complex was purified using a different approach (Innocenti et al., 2004).

A similar complex containing Sra1, Nap1, WAVE2, Abi1 and HSPC300 was purified using a similar method as Eden *et.al.* starting from HeLa-S3 cells (Gautreau et al., 2004). A complex with WAVE3 was also reported (Stovold et al., 2005). Although no plant WRC has been purified yet, all components of WRC have homologs in *Arabidopsis thaliana* that have been functionally linked to the Arp2/3 complex and proper and epidermal morphogenesis (Basu et al., 2004; Basu et al., 2005; Brembu et al., 2004; Djakovic et al., 2006; El-Assal Sel et al., 2004; Saedler et al., 2004; Zhang et al., 2005; Zimmermann et al., 2004). Earlier studies had already established interactions between PIR121 or Sra1 and Nap1 and Abi (Soto et al., 2002; Yamamoto et al., 2001), as well as binding of Rac to Sra1 (Kobayashi et al., 1998) and Rac signaling through WAVE to actin cytoskeleton (Miki et al., 1998; Miki et al., 2000). All these observations can now be finally put together in one context that clarifies the signaling

pathway from Rac to the actin cytoskeleton: WRC is a five protein complex that contains and inhibits WAVE. Activated Rac binds Sra, which is a component of WRC, and triggers WAVE activation towards Arp2/3 complex. The latter nucleates new actin filaments.

Although no structure of WRC or any of its components exists today, the architecture of the complex has been explored. Using ^{35}S-methionine radioactive labeling and *in vitro* translated proteins, Gautreau *et.al.* co-expressed all possible pairwise combinations of Sra1, Nap1, WAVE2, Abi1 and HSPC300, where they also systematically tagged one protein of each pair with the Hemaglutinin (HA) tag. Immuno-precipitation using HA antibody followed by autoradiography revealed all possible pairwise interactions. Sra1 binds Nap1, Nap1 binds Sra1 and Abi1. Abi1 binds Nap1, WAVE2 and HSPC300, while WAVE2 binds Abi1 and HSPC300. Obviously HSPC300 binds WAVE2 and Abi1 (Gautreau et al., 2004). The interaction between Abi and WAVE has been mapped to the first 78 amino acids of Abi and the first 180 amino acids of WAVE (Echarri et al., 2004; Innocenti et al., 2004; Leng et al., 2005; Stovold et al., 2005). This was confirmed by Shae Padrick, currently a post-doctoral fellow in our lab, who also mapped the interaction of Abi and Nap1 to amino acids 100-158 of Abi (personal communication, unpublished data). We call this segment the Nap Binding Fragment or NBF.

1.3. WRC Biochemistry

A series of papers have firmly established the direct interaction of the VCA domain of the WASP family proteins with the Arp2/3 complex and the resulting

activation of that complex (Blanchoin et al., 2000; Machesky and Insall, 1998; Machesky et al., 1999; Panchal et al., 2003). WASP regulation is largely understood, while WAVE regulation is still a matter of debate.

1.3.1. WRC activity

Along their discovery of the WRC, Eden *et.al.* reported that 100 nM of their WRC, purified from bovine brain, is inactive towards Arp2/3 complex in actin assembly assay. They also found that Rac could activate the complex. However, Rac was able to pull-down only PIR121, Nap1 and Abi2 but not WAVE1 and HSPC300 (Eden et al., 2002). These data suggested a possible mechanism for WRC activation where Rac dissociates an inactive WRC into two sub-complexes, one of which, WAVE1–HSPC300, is bearing the active WAVE. We call this model the dissociation model (Fig. 1.3). Reconstitution of a system from purified components has been long considered the strongest evidence that an understanding of that system has been achieved. However, the only known reconstitution of WRC drew a new model. Innocenti *et.al.* tried to assemble WRC using proteins purified from three different sources (Innocenti et al., 2004). PIR121–NAP sub-complex was purified from 293T cells transfected with Flag-tagged Nap1 and myc-tagged PIR121 using anti-Flag antibody to affinity purify the sub-complex. WAVE2–Abi1 or WAVE1–Abi1 sub-complexes were generated in *Spodoptera frugiperda* (Sf9) insect cell system by co-infection of baculoviruses expressing GST-tagged WAVE1 or WAVE2 and His-tagged Abi1. A GST-WAVE–Abi sub-complex was affinity purified over glutathione beads. Finally, HSPC300 was purified from *E. coli* BL21 bacterial cultures. The WRC was reconstituted by mixing equimolar amounts of the components, without any further purification (see below for the problem with this

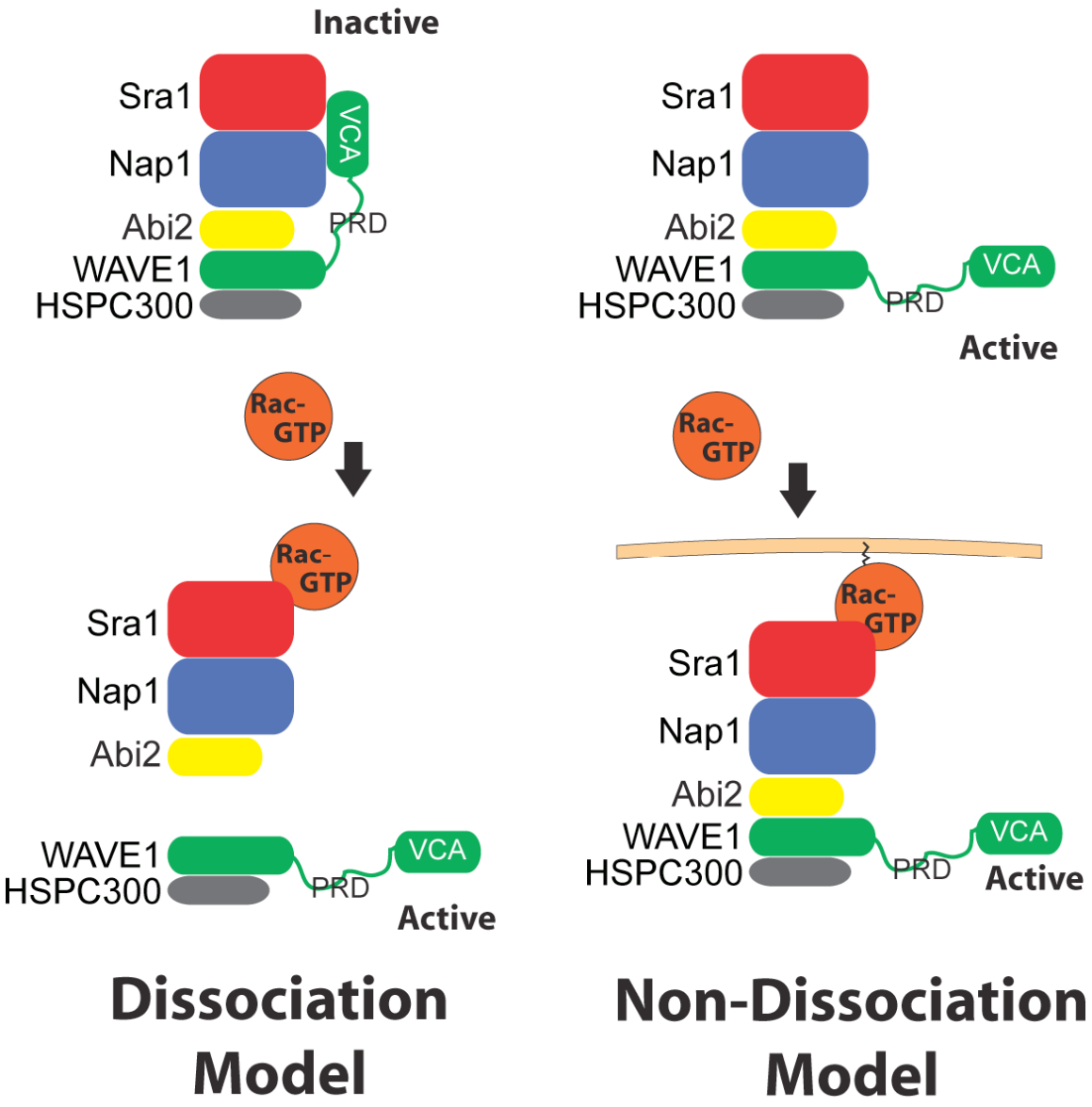

Figure 1.3: Current WRC regulation models

In the dissociation model on the left, Rac binds to Sra, leading to the dissociation of the inactive complex. One of the resulting sub-complexes contains the now active WAVE. In the non-dissociation model on the right, WRC is active. The binding to Rac simply localizes the complex to the membrane.

approach). The resulting WRC was active towards Arp2/3 in actin assembly assay. Moreover, an active Rac mutant, but not an inactive one, was immunoprecipitated with all WRC components pulled-down with Abi antibody. This implies that WRC in cells does not dissociate upon Rac binding. From these data, a new and contradictory model emerged where WAVE within WRC is constitutively active and Rac neither activates it further nor dissociates the complex. The authors suggest that Rac simply localizes WRC to the leading edge of lamellipodia. We call this model the non-dissociation model (Fig. 1.3).

The difference between the *in vivo* purified complex and the reconstituted complex could have been an inhibitory protein present in the purified complex that was not identified, and therefore was not included in the reconstitution. But the non-dissociation model gained more acceptance when Kim *et.al.* reported working with an active WRC. They purified the complex from rat brain following an almost identical protocol to the one that previously resulted in an inactive WRC (Kim et al., 2006). That complex was active towards Arp2/3 without the addition of Rac. An antibody against WAVE1 VCA blocked the activity of the complex without affecting the activity of WASP or N-WASP VCA domain, demonstrating that the WRC activity did not result from a WASP contamination. The group did not test the stability of the complex in the presence of Rac. Far from solving the difference between the dissociation and the non-dissociation models, these data only added to the confusion. If taken at face value, the results support the active WRC model. A deeper analysis of the work tells another story. The report identifies three residues in the PRD of WAVE1 that are phosphorylated in the purified complex. Once dephosphorylated, WRC substantially loses its activity. We do

not know if the complex purified by Eden *et.al.* was also phosphorylated. If it was, then Kim *et.al.* work contradicts the dissociation model. But if it was not, then Kim *et.al.* work suddenly supports that dissociation model. We just cannot tell.

Despite the fact that all aspects of the two WRC regulation models are contradictory, no attempt has been made to reconcile them. This is partially due to the difficulty in producing sufficient quantities of the different WRC components to perform biochemical reconstitution. The main aim of this dissertation has been to reconstitute several forms of WRC and to definitely determine whether WRC is active or inhibited. This is a crucial statement to make, because the interpretation of any work on the regulatory mechanisms of WRC has to be made in relation to the initial state of the complex, which is currently unknown.

1.3.2. WRC Phosphorylation

To date, among the five components of WRC, only Abi and WAVE proteins have been considered targets for regulation by phosphorylation. In fact, even before the discovery of WRC, Abi identification linked it to the tyrosine kinase c-Abl (Shi et al., 1995). Later data suggest that Abi1 and Abi2 are both a target for and a regulator of c-Abl. Abi1/2 as target for c-Abl was established in assays using purified proteins, and using pull-downs from cells expressing Abi and different variants of c-Abl (wild type and kinase deficient) followed by western blots to detect both Abi and phospho-tyrosine, both from mammalian and *Drosophila* cell lines (Juang and Hoffmann, 1999; Shi et al., 1995). The tyrosines targeted by c-Abl were identified as residues 148, 155, 248 and 285 in *Dm*Abi (Huang et al., 2007) (Fig. 1.4A). Abi Phosphorylation is proposed to regulate Abi protein levels in the cell and its localization (Huang et al., 2007).

Abi1/2 can also regulate the activity of c-Abl. The SH3 C-terminal domain of Abi is sufficient to activate c-Abl Phosphorylation of Abi and of Enabled (Ena) protein (Juang and Hoffmann, 1999). W426K, a mutation in Abi-SH3 that eliminates its binding to c-Abl PRD, abrogates this activation (Fig. 1.4A). Moreover Ena can bind to Abi through the interaction of its N-terminal EVH1 domain with the Abi-PRD (Tani et al., 2003) (Fig. 1.4A). Abi3, also known as NESH, can also bind Ena, but cannot pull-down c-Abl or activate it (Hirao et al., 2006). An examination of the sequence alignment of SH3 domain of Abi1, Abi2 and Abi3 shows that Abi3-SH3 is not highly similar to Abi1/2-SH3. Interestingly, c-Abl can phosphorylate other targets like c-Cbl regardless of the presence or absence of Abi. It is not clear whether Abi1/2, in the cellular context, activates c-Abl towards certain targets while remaining a component of WRC or as an independent protein. No such pool of independent Abi has been clearly established yet. It is worth noting that Abi residues 1 to 158, which are required for Abi integration into WRC, do not overlap with Ena binding site in the PRD, or with SH3 domain required for binding and activating c-Abl.

Phosphorylation has been reported for all three human WAVE orthologues (Fig. 1.4B). Src phosphorylates Tyr125 in the WHD of WAVE1 (Ardern et al., 2006), while P35/Cdk5 phosphorylates Ser310, Ser397 and Ser441 in PRD of WAVE1 (Kim et al., 2006). WAVE2 is phosphorylated on Tyr150 by Abl (Leng et al., 2005), on Ser 308, Ser343, Thr346 and Ser351 in the PRD by Erk (Danson et al., 2007; Nakanishi et al., 2007), and on Ser482, Ser484, Ser488, Ser 489 and Ser497 in the VCA domain by Casein Kinase 2 (CK2) (Pocha and Cory, 2009) or Erk (Nakanishi et al., 2007). WAVE3 is

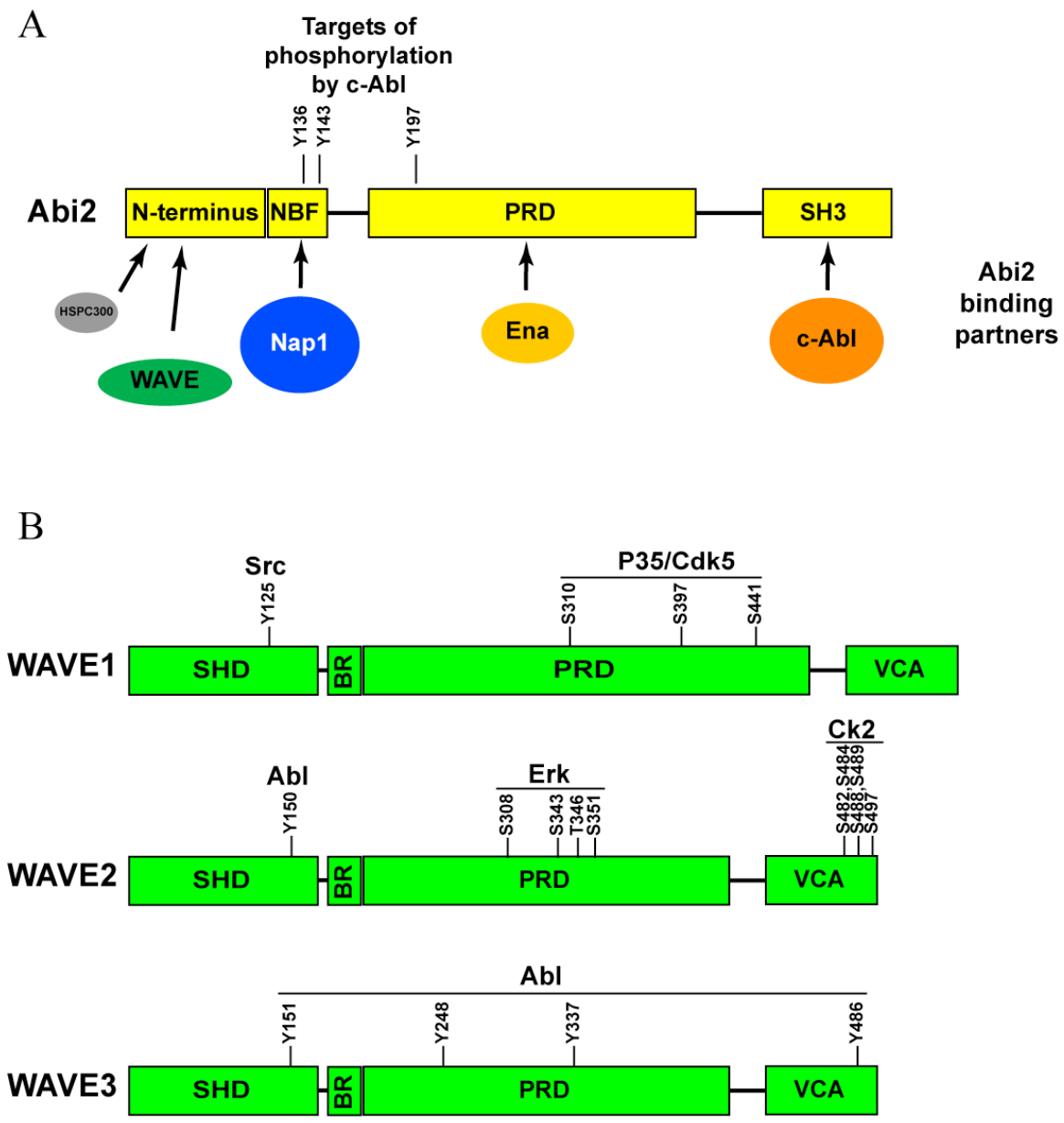

Figure 1.4: known phosphorylation sites on Abi2 and WAVE

(A) Mapping of known phosphorylation sites on the linear domain structure of Abi2. The binding site of some proteins on Abi2 is also shown for reference (A). Tyr136, Tyr 143 and Tyr197 in Abi2 correspond to Tyr148, Tyr155 and Tyr248 in DmAbi, respectively. Tyr285 in DmAbi is not conserved in Abi2. (B) Mapping of known phosphorylation sites on the linear domain structure of WAVE1, WAVE2 and WAVE3. Kinases targeting each residue are indicated above it. BR: basic region.

phosphorylated on Tyr151, Tyr248, Tyr337 and Tyr486 by Abl (Sossey-Alaoui et al., 2007)

The effect of these WAVE phosphorylations is still not clearly established. In primary hippocampal neurons harvested from mice, WAVE1 knock-down by RNAi disrupts spine morphogenesis. The phenotype can be reversed in these RNAi treated neurons with the expression of wild type WAVE1 or WAVE1-S310A, but not with WAVE1-S310D- a phosphorylation mimic (Kim et al., 2006), suggesting that phosphorylation in PRD impairs the proper control of WAVE1 and its efficient stimulation of Arp2/3, which is required for proper spin formation. On the contrary, WAVE3 tyrosine phosphorylation seems to be necessary for lamellipodia formation in COS7 cells, as well as their movement in *in vitro* migration assays (Sossey-Alaoui et al., 2007).

For WAVE2, actin assembly assays show opposing results based on the kinase used. Phosphorylation of WHD by Abl seems to enhance activity towards Arp2/3 complex (Leng et al., 2005), phosphorylation of PRD by Erk does not affect WAVE2 activity (Danson et al., 2007), whereas phosphorylation of VCA by CK2 or Erk substantially reduces the ability of WAVE2 to stimulate Arp2/3 complex (Nakanishi et al., 2007; Pocha and Cory, 2009). The physiological relevance of these phosphorylations is even less understood, as different phosphorylation mimics or phosphorylation deficient WAVE constructs expressed in cells fail to produce any detectable phenotype that can be correlated with the results from the actin assembly assays. Scratch wound healing assays using NIH-3T3 cells failed to establish a noticeable difference in migration speed or directional persistence between cells expressing wild type WAVE2 or phospho-defective

WAVE2 mutant (mutations to prevent phosphorylation in PRD) (Danson et al., 2007). Mutations of the serine residues in VCA also failed to produce statistically significant difference from wild type WAVE2 when measuring lamellipodia formation in mouse embryonic fibroblasts (MEF) (Nakanishi et al., 2007) and when measuring ruffles formation in NIH-3T3 cells (Pocha and Cory, 2009).

Those initial studies on WAVE phosphorylation suggest that WAVE regulation by kinases is different for the three human WAVE orthologues, although an extensive study mapping all the phosphorylation sites in all three WAVEs is still lacking. Nonetheless, some clear differences are already emerging. For example, two of the five serines phosphorylated in the VCA of WAVE2 are not conserved in WAVE1 and WAVE3. Also, WAVE1 and WAVE2 phosphorylation by Abl require Abi1 presence but WAVE3 does not (Sossey-Alaoui et al., 2007). But the main problem so far in interpreting the meaning of these modifications is the lack of a coherent testing method. In biochemical assays, what affects WAVE, as an individual protein, may not change its behavior in the context of the WRC. So far, no one tested the kinase effect on WRC in actin polymerization assays (all the previously mentioned assays were done using only WAVE and not WRC). Testing different WAVE constructs in cells also has its own perils. A low expression level of an unregulated VCA can induce membrane ruffling, while a high expression level can disrupt actin polymerization by sequestering G-actin (Machesky and Insall, 1998). In addition, testing for ectopic WAVE integration into the native WRC is necessary to distinguish impact of individual WAVE from effect of WAVE within WRC. This is especially true because no pool of WAVE has been found outside of WRC in the cell so far and ectopically expressed WAVE will not be regulated

the same way as the other components of the complex. In fact, overexpressed WAVE1, WAVE2 and WAVE3 have been shown to oligomerize with each other (Westphal et al., 2000), which could cause hyper-potentiation towards Arp2/3 (Padrick et al., 2008).

1.3.3. Association of WRC components with other proteins

Besides phosphorylation, WRC components can interact with a number of proteins that may regulate WRC activity. In addition to Abl binding, Abi1 can form a scaffold upon which three other proteins can bind simultaneously (Fig. 1.5A): an SH3 containing protein, Eps8, binds to PRD of Abi1, the SH3 of Abi1 binds Sos1 and the SH2 domain of the p85 regulatory subunit of PI3K binds to Abi1 Tyr407 if the latter is phosphorylated (Fan and Goff, 2000; Innocenti et al., 2003). This was demonstrated by a series of pull-downs of endogenous proteins from MEFs, as well as pull-downs of GST, HA or myc tagged proteins and identification of co-precipitants with immunoblots. Also, immunostaining shows p85 and Abi1 colocalizing in MEFs only when induced by PDGF. Put perhaps the most interesting protein is Sos1, a protein containing a PH domain and a DH domain. The former binds preferentially to PI3,4,5P which is the catalytic product of PI3K (Rameh et al., 1997). The latter provides guanine nucleotide exchange factor (GEF) activity with Rac as target for Sos1 (Scita et al., 1999). In radioactive guanine nucleotide release assays, Sos1 alone can provide GEF activity towards Rac1. This activity is significantly improved in the presence of Eps8 and Abi1, and even more enhanced in the presence of water-soluble PI3,4,5P but not PI4,5P, PI5P or PI3P (Innocenti et al., 2003).

In principle, a signaling pathway can be envisioned as follows: upon external ligand binding, a receptor tyrosine kinase can activate PI3K associated with WRC

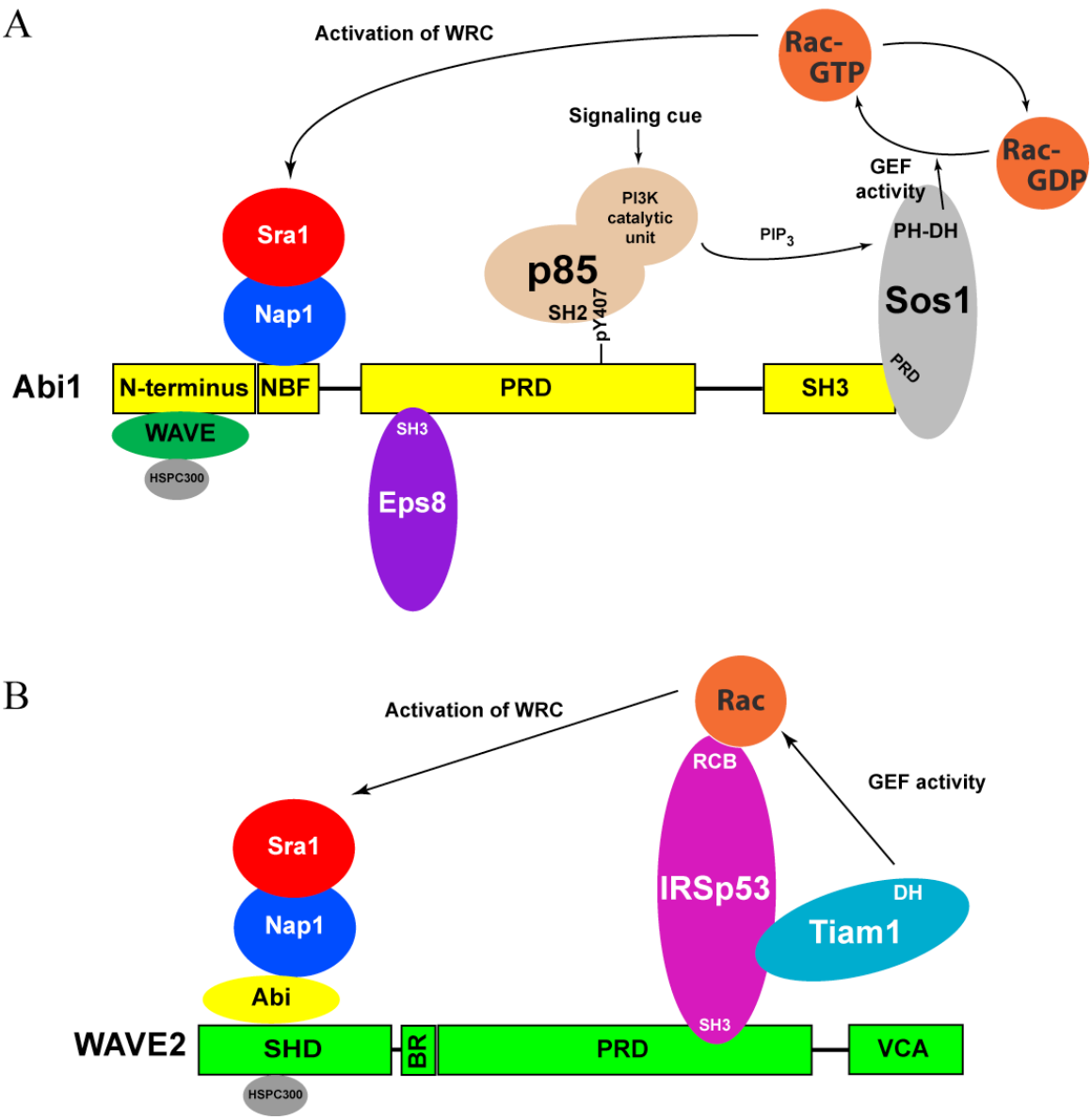

Figure 1.5: potential scaffolding functions of Abi1 and WAVE2

(A) Abi1 can bind Eps8, p85 subunit of PI3K and Sos1. PI3K catalytic subunit can generate PIP_3, which enhances the GEF activity of Sos1 (toward Rac) by binding to its PH domain. GTP loaded Rac can then bind Sra1 and activate WRC. (B) WAVE can bind IRSp53, which recruits Rac and its GEF, Tiam1. Activated Rac can then bind Sra1 and activate WRC. Proteins are not drawn to scale.

through Abi1. The phosphoinositide PIP_3 generated by PI3K then interacts with Sos1, which is also associated with WRC through Abi1. Sos1 activates Rac that will bind to Sra and activate WRC. For such a pathway to work, Abi1 has to be phosphorylated on Tyr407 for PI3K to bind to it. Although we do not know which kinase targets this tyrosine in Abi1, we recognize here the potential for integration of two signaling pathways, one leading to the activation of the unknown kinase targeting Tyr407 in Abi, the other leading to PI3K activation. It is also important to note that PIP_3 has been reported to bind WAVE (Oikawa et al., 2004). As PIP_3 is membrane bound, a large localized concentration of it can effectively cluster WRC (already activated by the potential pathway I just described). Once more, clustering (or oligomerization) of active WASP/WAVE proteins could cause hyper-potentiation toward Arp2/3 (Padrick et al., 2008). Therefore, this pathway can work on both branches of the hierarchical regulation model of WAVE (see chapter IV for description of this model).

Rac can be recruited to WRC through yet another set of interactions centered around the insulin receptor substrate IRSp53 and WAVE2 (Fig. 1.5B). IRSp53 has an SH3 domain that binds WAVE2, but not WAVE1 or WAVE3, as evidenced by immunoprecipitation from endogenous sources or by pull-down with purified components (Miki et al., 2000). The N-terminus of IRSp53 (RCB domain) binds Rac (Miki et al., 2000), however full length IRSp53 does not bind Rac unless WAVE2 is simultaneously bound to it (Miki and Takenawa, 2002). WAVE2 disrupts an IRSp53 intra-molecular interaction between RCB and the C-terminus that prevents Rac binding to RCB otherwise. IRSp53 also recruits Tiam1, a Rac GEF, to the complex (Connolly et al., 2005), presenting another scaffold upon which Rac can be activated in the vicinity of Sra,

its target protein. Although IRSp53 and WAVE2, visualized by immunostaining, co-localized to lamellipodia tips (Abou-Kheir et al., 2008; Nakagawa et al., 2003), Recruitment of Tiam1 and activation of Rac were essential for WAVE2 activation in response to stimulus (Abou-Kheir et al., 2008). In summary, both Abi1 and WAVE2 recruit a host of proteins to WRC, and the ultimate purpose of their interactions appears to be activating Rac within the same scaffold that includes WRC.

On the other hand, WAVE1 binds a protein that deactivated Rac. The WAVE associated RacGAP protein, or WRP, was identified by tandem MS/MS as a protein that co-immunoprecipitates with WAVE1 from rat brain extracts (Soderling et al., 2002). Purified WRP SH3 domain and WAVE1 or WAVE1 PRD co-immunoprecipitate, and the Rho GAP domain of WRP do function as a GAP for Rac, as assessed by ^{32}P-GTP hydrolysis assay. This suggests that WAVE1 can terminate Rac signaling/activation by recruiting WRP into the complex. WAVE1 also binds the cAMP dependent protein kinase A, or PKA, but WAVE2 and WAVE3 do not. The interaction has been mapped to the RII domain of PKA and residues 500 to 520 in the VCA domain of WAVE1 (Westphal et al., 2000). Those residues overlap with actin binding site on VCA. In fact, actin and PKA RII are mutually exclusive for binding to WAVE1*. The physiological and biochemical significance of WRP and PKA interaction with WAVE1 is not established yet. Sra and PIR121 have been reported to bind FMRP as explained earlier (Schenck et al., 2001). Again, the relevance of this interaction for the function of FMRP or WRC is not understood.

It is not clear if all these various complexes/pathways described above occur simultaneously on a given WRC (or in a given sub-cellular compartment), or if they are

distinct pathways that have different functions, and are used in different locations, circumstances.

1.4. Transgenic models of WRC

Through Arp2/3 complex, WRC controls new actin filaments formation and enables cells to migrate and undergo proper morphogenesis. Knock-out and mutation of WRC components in different animal model or cells lines result in defects most related to the loss of the cell's ability to migrate, form synapses or establish new contacts.

1.4.1. In different cell lines

A large body of experiments has been performed on WRC in different cell lines to uncover the cellular functions that WRC controls. But perhaps the most significant result from a number of publications is the discovery that Sra, Nap, Abi, HSPC300 and WAVE protein levels are tightly regulated together. If the expression of any of those proteins is knocked-down by RNAi, the expression of the rest of them is also reduced to barely detectable levels. This has been repeatedly observed in cells (Innocenti et al., 2005; Kunda et al., 2003; Nolz et al., 2006; Rogers et al., 2003; Steffen et al., 2004; Wang et al., 2007), as well as in animals (Bogdan et al., 2004; Qurashi et al., 2007; Schenck et al., 2004). If the proteasome is inhibited, the decrease in protein levels described above is eliminated (Kunda et al., 2003). This suggests that WRC components amounts are regulated at the degradation level rather than transcriptional or translational levels. The loss of one leads to destabilization and consequent degradation of the others. The WRC integrity and function as one unit, as well as the stability interdependence of WRC

components, should be considered when examining experiments where only one WRC component is overexpressed or knocked-down. The requirement for specific domains and the effect of specific mutations is best addressed by modification of the endogenous gene rather than ectopic gene expression or gene knock-down.

WAVE has already been established as an Arp2/3 complex activator (Blanchoin et al., 2000; Machesky and Insall, 1998; Machesky et al., 1999; Panchal et al., 2003). Most of the new actin filaments are generated at the sites of new cellular protrusions like lamellipodia, filopodia and pseudopodia. WRC requirement for these protrusions has been extensively studied. Immunostaining revealed the localization of WRC proteins along the membrane at the leading edge of lamellipodia. This has been observed for WAVE in rat embryonic fibroblasts (Nakagawa et al., 2001), mouse melanoma B16F1 cells (Hahne et al., 2001; Kurisu et al., 2005; Nakagawa et al., 2003), Drosophila S2R+ cells (Kunda et al., 2003), mouse skeletal muscle C2C12 cells (Kawamura et al., 2004), NIH 3T3 cells (Oikawa et al., 2004), mouse embryonic fibroblasts (Yamazaki et al., 2005), human MDA-MB-231 adenocarcinoma cells (Sossey-Alaoui et al., 2005), human fibrosarcoma HT1080 cells (Huang et al., 2006), for Sra in mouse melanoma cells B16F1 cells and swiss 3T3 fibroblasts (Steffen et al., 2004), for Nap in mouse melanoma cells B16F1 cells and swiss 3T3 fibroblasts (Steffen et al., 2004), Hela cells (Innocenti et al., 2005), embryonic mouse neuroepithelial cells (Yokota et al., 2007), and for Abi in mouse melanoma B16F1 cells (Stradal et al., 2001), Hela cells (Innocenti et al., 2005; Innocenti et al., 2004), and jurkat T-cells (Zipfel et al., 2006).

Consistent with WRC localization at lamellipodia leading edge and its ability to activate Arp/23 complex, knock-down of any protein in WRC leads to mislocalization of

the partner WRC proteins and failure to generate lamellipodia, along with the loss of spreading and migration potential. This has been observed for WAVE in Drosophila S2R+ cells (Kunda et al., 2003), mouse skeletal muscle C2C12 cells (Kawamura et al., 2004), mouse melanoma B16F1 cells (Kurisu et al., 2005), mouse embryonic fibroblasts (Yamazaki et al., 2005), human MDA-MB-231 adenocarcinoma cells (Sossey-Alaoui et al., 2005), for Sra in Drosophila S2R+ cells (Kunda et al., 2003), mouse melanoma B16F1 cells (Steffen et al., 2004), for Nap in Drosophila S2R+ cells (Kunda et al., 2003), mouse melanoma B16F1 cells (Steffen et al., 2004), Hela cells (Innocenti et al., 2005), embryonic mouse neuroepithelial cells (Yokota et al., 2007), for Abi in Drosophila S2R+ cells (Kunda et al., 2003), Hela cells (Innocenti et al., 2005), and for HSPC300 in 293T cells (Derivery et al., 2008).

In addition to its essential role in controlling formation of protrusions and cellular migration, WRC has been implicated in T cell activation. Antigen presenting cells (APCs) bind to T cell receptors (TCRs) and an immunological synapse (IS) is formed at the site of contact. Actin polymerizes at the IS and T cells are activated as a result. Activation includes TCR clustering, mature synapse formation by the extension of T cell lamellipodia around the APC, interleukin-2 (IL-2) production and T cell proliferation [reviewed in (Billadeau et al., 2007)]. When WAVE and Abi are knocked-down by RNAi (Nolz et al., 2006; Zipfel et al., 2006), actin does not polymerize at the IS and lamellipodia fail to extend from T cells in response to APC contact. IL-2 is not produced, and TCRs do not cluster as well. In short, T cells are not activated in the absence of WRC. Other immune system cells, like macrophages (Kheir et al., 2005) and neutrophils

(Weiner et al., 2006), also fail to migrate in response to physiological chemo-attractants if WRC is disrupted.

1.4.2. In different animal models

1.4.2.1. In mice

Abi2 knock-out mice exhibited reduction in eye size and problems in learning and memory exercises (Grove et al., 2004). Further examination revealed aberrant eye development. The migrating secondary lens fibers did not orient properly, causing the formation of a convex lens instead of a concave one. In the central nervous system (CNS), more than nine neuro-anatomical abnormalities were detected, all linked to cellular orientation, shape and migration. For example, dendritic spines were less mushroom-like and more stubby-like in shape and their overall density decreased compared to dendritic spines from wild type mice.

Abi2 knock-out mice were nonetheless viable, possibly due to redundancy in Abi1, Abi2 and Abi3 roles in most developmental stages. On the other hand, Nap1 knock-out mice die during early embryonic development (Rakeman and Anderson, 2006). In cells extracted from the embryos, WAVE1 levels were over 10 fold less than in equivalent cells extracted from wild type embryos. These cells failed to polarize and form lamellipodia. Abi1, Sra1, WAVE1 and Nap1 could all be detected at the leading edges of migrating cells from wild type embryos, but not from equivalent cells from Nap1 knock-out embryos. Mouse embryos evolve from a single-cell layer into three germ layers through the gastrulation process. All tissues differentiate from those three germs layers. (Tam and Behringer, 1997). In Nap1 knock-out embryos, cells movement

into the three layers fails, resulting in a mass of disorganized mesenchymal cells (Rakeman and Anderson, 2006). These observations confirm the important role WRC plays in regulating actin cytoskeletal dynamics.

WAVE1 is predominantly expressed in the brain (Suetsugu et al., 1999). Consistent with that profile, WAVE1 knock-out mice exhibit defects related to the central nervous system. These mice are smaller in size than wild type animals, and they survive for only 21-26 days after birth (Dahl et al., 2003). An examination of their different organs, including kidney, lungs, skeletal muscle, liver and small intestine tissues, revealed no abnormalities. The only defects were observed in the development of the CNS. The brain was underdeveloped, and the cerebral cortex in particular was shorter than normal, leaving large portions of the midbrain uncovered. Similar to spine morphology in Abi2 knock-out mice, hippocampal and cortex neurons also had stubbier dendritic spines and reduced spine density, and neurite growth cone dynamics was severely disrupted (Soderling et al., 2007). Behavioral impairment is also observed, as WAVE1 knock-out mice have reduced alertness and anxiety levels, and they have delayed learning and memory deficits (Soderling et al., 2007; Soderling et al., 2003).

Knocking-out WAVE2 proved lethal in mice in early embryonic stages. Embryos were hemorrhagic and died in 10 days during mid-gestation (Yamazaki et al., 2003; Yan et al., 2003). Although vasculogenesis (the formation of new blood vessels from angioblast cells following their migration and differentiation) was largely normal, endothelial cells were unable to produce branching from existing vessels during angiogenesis (the formation of new blood vessels from pre-existing ones through sprouting of the endothelial cells). Primary MEF harvested from these embryos were

slow to grow. They showed reduced formation of circular ruffles, and they lost the ability to extend lamellipodia in a resting state and in a PDGF stimulated state. Rescuing the cells with WAVE2 expressing retrovirus restored both extensions formation and responsiveness to PDGF (Yan et al., 2003). In actin assembly assays, activation of Arp2/3 is not observed when using extracts of cells from wild type embryos. The addition of Rac to the extract activates Arp2/3 in those assays. Stimulation by Rac is lost with extracts of cells from WAVE2 knock-out mice, but it is restored if mice are rescued by WAVE2 retrovirus before extract preparation (Yan et al., 2003). Again, these results corroborate an essential role for WAVE and its complex in mediating lamellipodia formation in a signaling pathway downstream of Rac.

1.4.2.2. In fruit flies

In mice (and humans), more than one paralogue of each WRC component exists, with different tissue distribution. This may explain why the phenotypes of the different knock-outs are not similar. In the fruit fly *Drosophila melanogaster*, there is only one paralogue of each WRC component. Not surprisingly, null mutation or organ targeted RNAi mediated knock-down in genes of dSra, dNap, dAbi, dWAVE and dHSPC all result in almost identical defects. In early embryonic stages, WRC proteins are expressed in all cells, but in later stages they are detected predominantly in the CNS (Hummel et al., 2000; Qurashi et al., 2007; Schenck et al., 2003; Schenck et al., 2004; Zallen et al., 2002). The neuropile of the CNS is composed of axons arranged in two parallel bundles with several perpendicular crossings. This morphology is completely disrupted when expression of dHSPC (Qurashi et al., 2007), dSra (Bogdan et al., 2004; Schenck et al., 2003; Schenck et al., 2004), dNap (Schenck et al., 2004) or dWAVE (Schenck et al.,

2004; Zallen et al., 2002) is blocked, which suggests a failing in axonal guidance and targeting.

Synaptogenesis at the neuromuscular junctions is also affected by knock-down or null mutations in WRC proteins. In the mutant flies, the synapses at the neuromuscular junctions are smaller in size, while the synaptic boutons are bulged and have at least two-fold more terminal buds than in wild type (Bogdan et al., 2004; Qurashi et al., 2007; Schenck et al., 2004). The fly body is covered with bristles that act as sensory organs. Bristles are normally straight structures. However, most bristles show a very distinct bent phenotype when dSra, dNap (Bogdan et al., 2004), dWAVE (Zallen et al., 2002) or dHSPC (Qurashi et al., 2007) are mutated. But when dAbi is deleted, bristles do not form (Bogdan et al., 2005), an effect also observed when dWASP is knocked-out (Zallen et al., 2002).

1.5. Potentiation of WASP family proteins through dimerization

WASP VCA activity is controlled by an auto-inhibitory mechanism in which the GBD domain binds internally to the VCA and inhibits its binding to Arp2/3 complex (Kim et al., 2000). Cdc42 activates WASP by binding to the GBD and allosterically releasing the VCA from the auto-inhibited structure (Abdul-Manan et al., 1999; Kim et al., 2000). WASP can be activated by a number of proteins besides Cdc42. The allosteric activation (by Cdc42) model has been extended to other activators too, although this assertion has never been examined experimentally. The largest group of WASP activators contains the SH3 domain. The binding of SH3 to the PRD region of WASP is required for the ability of the SH3 containing protein to activate WASP. Those activators

include Nck, Grb2, Toca-1, Abi, WISH, endophilin and cortactin (Carlier et al., 2000; Fukuoka et al., 2001; Ho et al., 2004; Innocenti et al., 2005; Kowalski et al., 2005; Otsuki et al., 2003; Rohatgi et al., 2001)

What this group of activators have in common is the multivalency potential, or the potential to bind more than one WASP molecule. Such potential is acquired from the constitutive homo-dimerization of some activators through their BAR domain, like Toca-1 and endophilin (Takano et al., 2008; Wang et al., 2008; Weissenhorn, 2005), or from the presence of two or more SH3 domains per protein, like the Grb2 and Nck adapter proteins. When natural multivalency does not apply, as for Abi, activation of WASP has been observed using SH3 domains purified as GST fusions; GST is a dimer with sub-nanomolar affinity, conferring artificial multivalency to the SH3 domains. In fact, a variety of SH3 domains can activate WASP as dimeric GST-fusions or as part of multivalent proteins, but are largely inactive as individual or monomeric domains (Carlier et al., 2000; Fukuoka et al., 2001; Ho et al., 2004; Innocenti et al., 2005; Kowalski et al., 2005; Otsuki et al., 2003; Padrick et al., 2008; Rohatgi et al., 2001).

There are yet other WASP activators that do not have SH3 domains, but whose activation mechanism still requires some sort of multivalency. For example, the Enterohaemorrhagic E.Coli effector protein EspFu activates WASP through a similar allosteric mechanism as Cdc42 (Cheng et al., 2008). EspFu has multiple repeats of a 47 residue peptide. Although a single repeat can release N-WASP autoinhibition, EspFu fragments containing two repeats have significantly greater activity, even when normalized for total repeat concentration (Padrick et al., 2008). Thus, the EspFu repeats act cooperatively to promote actin assembly. Cooperativity does not involve inter-repeat

effects on the affinity of EspFu for N-WASP, since isothermal titration calorimetry measurements show that one repeat and two repeats bind with indistinguishable affinity but 2-fold different stoichiometry to an autoinhibited C-terminal fragment of N-WASP (Padrick et al., 2008). Another example is WASP activation by PIP2. Our lab has demonstrated that PIP2 vesicles of a certain low density will activate WASP, but when PIP2 density is increased, so is WASP activation of Arp2/3 complex (Padrick et al., 2008).

These observations (SH3 containing multivalent proteins, EspFu and membrane clustering by phosphoinositides) support a new model for WASP activation where the mechanism involves dimerizing or oligomerizing VCA containing proteins. This model is supported by our observation that GST-fusions of WAVE, N-WASP and WAVE1 VCAs have much greater activity than their respective VCA monomers (Padrick et al., 2008). This effect is due to dimerization rather than simply attachment to GST, since purified GST:GST-VCA heterodimers have activity similar to the free VCA. The effect is also not specific to GST-mediated dimerization. Chemically crosslinked WASP VCA and the rapamycin-mediated heterodimer of FKBP-VCA and mTOR-VCA show activity comparable to GST-VCA (Padrick et al., 2008).

In the first part of this dissertation (chapters II and III), I will address the question of whether WRC is constitutively active or inhibited, by reconstituting human and drosophila versions of WRC from different sources. I will analyze those complexes for activity towards Arp2/3 complex and demonstrate that WRC is indeed inhibited through intra-complex interaction, and that Rac does activate it. This will reconcile the

conflicting models presented in figure 1.3. In the second part (chapter IV), I will explore the mechanistic principle behind WASP family protein potentiation by dimerization. I will demonstrate that one Arp2/3 complex can bind two tethered VCA domains with at least 100 fold higher affinity than it binds one VCA domain. I will also show that heterodimerization of WASP and WAVE can potentiate the activity of their VCAs. This will lead to the development of a new model of hierarchical regulation of WASP/WAVE proteins.

Chapter Two: WRC Reconstitution

2.1. Expressing WRC components

The WAVE Regulatory Complex contains five proteins: Sra, Nap, Abi, WAVE and HSPC300. Since its discovery, two opposing models have been proposed for the function of this complex (Fig. 1.3). The dissociation model (Eden et al., 2002) postulates that WRC inhibits WAVE activity toward the Arp2/3 complex. The VCA domain of WAVE interacts with an unidentified partner with the complex. Moreover, the complex dissociates into two sub-complexes when activated by Rac-GTP. Sra, Nap and Abi form one sub-complex and WAVE and HSPC300 constitute the second sub-complex. On the other hand, the non-dissociation model (Innocenti et al., 2004) considers WRC a vehicle for cellular localization of WAVE. That is, WAVE VCA is not inhibited within WRC, and proteins interacting with the different WRC components help localize the entire complex, without dissociating it, to sites of lamellipodia formation where Arp2/3 activation by WAVE VCA is required.

The first model was proposed by Eden *et.al.*, who purified WRC from bovine brain. The second model was proposed by Innocenti *et.al.*, who reconstituted their WRC from Sra–Nap and WAVE–Abi sub-complexes, with the addition of HSPC300 in some of their experiments. This difference may be the source of the different inherent activities observed for WRC in the two models. It is possible that Eden *et.al.* missed an essential inhibitory component of the WRC during their identification, and therefore Innocenti et.al. did not account for it during their reconstitution. It is also possible that WRC is indeed a pentameric complex, but the protocol followed by Innocenti *et.al*. did not lead to

the proper folding of the complex, especially since they omitted HSPC300 from most of their preparations.

To fully understand WRC activity, a reconstitution from purified components is essential. Biochemical reconstitution of biological processes or systems has a fundamental importance in cell biological research. It represents the strongest means of demonstrating that all necessary components of a process have been identified, and that these are fully sufficient. In order to reconstitute a biological system, we need to be able to express and purify its components. However, we and other labs have encountered problems with the expression of most WRC components. Shae Padrick and I have tested expression in bacteria, yeast and insect cell systems.

In bacteria, using the BL21 strain of *E. coli*, HSPC300 is the only protein that expresses and purifies as an intact protein. However, it aggregates into large assemblies, probably bigger than 10 units per aggregate. That problem is prevalent whether HSPC300 was untagged, or N-terminally tagged with MBP, GST or His_6-Ubiquitin. GST or His_6 tagged Abi2 expresses poorly and yields heavily degraded product. WAVE1 has the same degradation and low yield problems as Abi2. Nap1 and Pir121, with various tags, do not express.

For expression in yeast, I opted to use the *Pichia pastoris* X33 wild type strain. Expression in X33 requires the generation of stable recombinant strains, where the gene of interest replaces, through recombination, the alcohol oxidase gene (AOX). As the alcohol levels in a culture dictate AOX expression, I can induce expression in the system by adding alcohol. I generated recombinant X33 strains containing the human Sra1 or

PIR121 genes, the drosophila Sra or the *C.elegans* Sra. I tested the strains for expression of the recombinant proteins in a shaker setting without success.

Next, I decided to test expression in a fermentor setting. Growing *Pichia pastoris* in a fermentor provides a number of advantages. The yeast cultures typically take few days. Lots of foam is generated that can isolate the culture from ambient air, making it hard for the culture to access oxygen. In a fermentor, I can control foaming and I can sparge oxygen-enriched air directly into the culture. The result is better culture breathing and a higher density culture can be reached (up to 350 g of wet cell pellet per liter of growth). A fermentor also allows me to maintain temperature and pH at the desired values. Finally, I can keep a continuous flow of methanol into the culture to maintain high induction levels. Combined, those effects may increase the yield of a given protein by 10~50 fold.

Unfortunately, I did not get a different result using the fermentor instead of the shaker for the X33-HsSra1 recombinant strain. I did not test the remaining strains in the fermentor because of a breakthrough in the insect cell expression system. Shae Padrick had succeeded in expressing Nap1 in insect cells using the baculovirus system, but Sra1 still did not express. In parallel to my trials with the yeast system, I was exploring a solution for expression in insect cells, based on a newly described promoter sequence (Sano et al., 2002). The sequence, termed L21, contains twenty-one DNA nucleotides found immediately upstream of the translation start codon (leader sequence) of the lobster tropomyosin cDNA. L21 was found to be responsible for the unusually high expression levels of the lobster tropomyosin in insect cells. Upon further examination, a multiple sequence alignment revealed common elements between L21 and two other known

promoters. The first half of L21 contains seven contingent nucleotides also found in the polyhedrin promoter (common in insects) sequence. The second half of L21 contains 8 contingent nucleotides also found in the vertebrate Kozak consensus sequence (Sano et al., 2002).

L21 was reported to produce as much as seven fold increase in the protein expression levels when used in the baculovirus based Sf9 insect cell expression system. To take advantage of the L21 promoter, I engineered two new plasmid series, based on Invitrogen's pFastBac series. The first series, termed pAV5, provides an N-terminal His_6 tag sequence, a TEV protease recognition sequence before the multiple cloning site (MCS) and has L21 sequence inserted between the polyhedrin promoter and the start codon. The second series, termed pAV3, is similar to pAV5 but provides an N-terminal GST instead of His_6 tag (see pAV3 and pAV5 vector maps in appendix I).

I cloned Sra1, Nap1, Abi2 and WAVE1 into pAV5 vectors, and HSPC300 into pAV3 vector. The ultimate goal was to produce a WRC that has His_6 tags on all proteins, except HSPC300, which would have a GST tag. The dual tagging strategy should help in the initial purification of the complex and in separating components that did not integrate into the complex. However, the immediate target was to express all five proteins individually using Sf9 cells. From the clones of WRC components, I generated bacmids that I transfected into Sf9 cells to produce the corresponding baculoviruses. Sf9 cells were infected with individual baculoviruses for all five WRC components, and the result was visualized by coomassie staining of an SDS-PAGE gel run of the cell extracts (Fig. 2.1A). With the L21 promoter, Sra1, Nap1 and HSPC300 express to relatively high levels and the corresponding bands can be clearly detected on the gel. Abi2 expresses

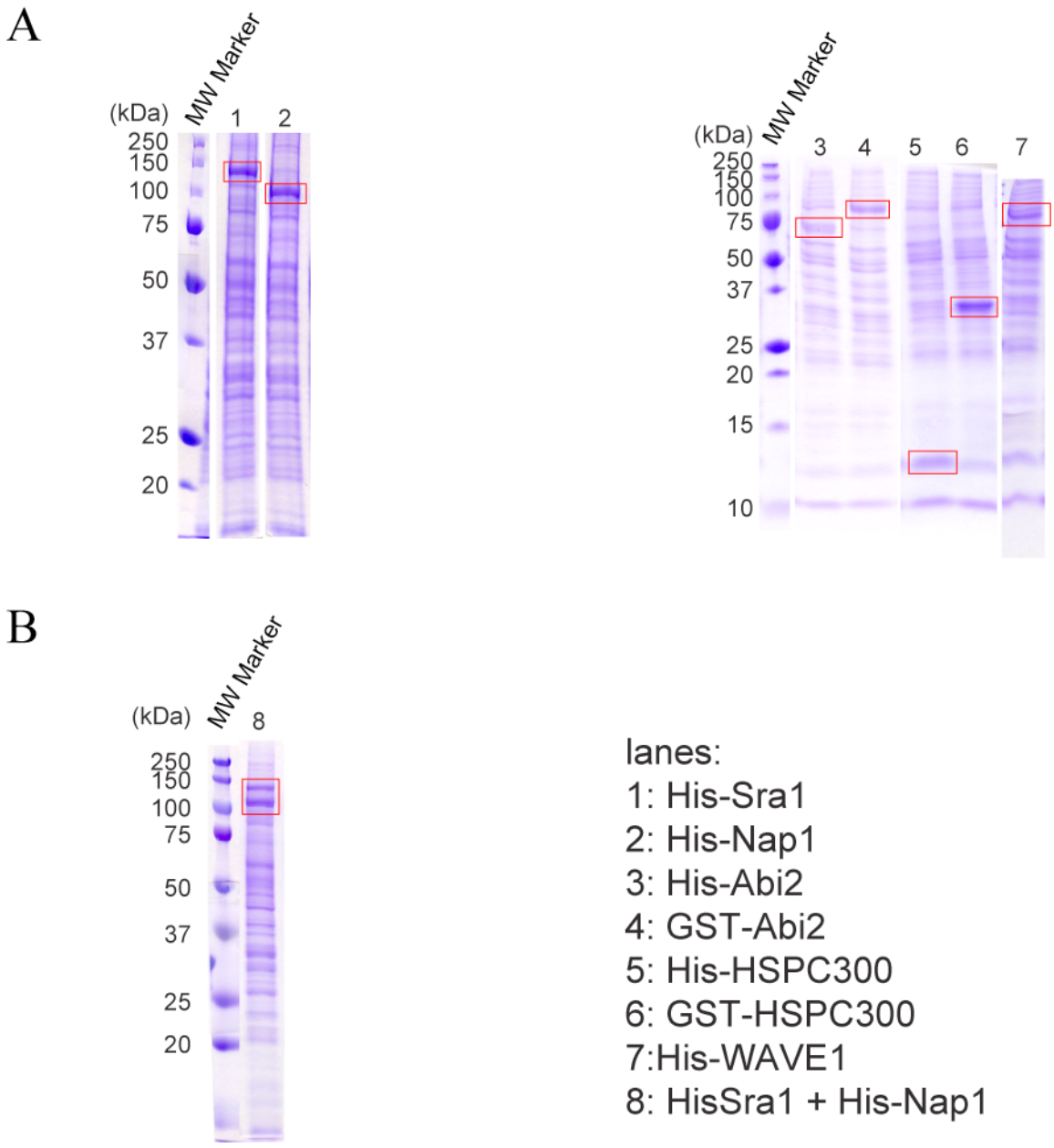

Figure 2.1: L21 driven WRC proteins expression

Commassie stained SDS-PAGE gels for lysates of Sf9 cells infected with (A) His_6-Sra1, His_6-Nap1, His_6-Abi2, GST-Abi2, His_6-HSPC300, GST-HSPC300 or His_6-WAVE1 baculoviruses or (B) co-infected with His_6-Sra1 and His_6-Nap1 baculoviruses.

with less intensity, and WAVE1 expression is the least visible but still detectable. Thus, the insertion of L21 promoter sequence helped solve the expression problems of Sra1, Abi2 and WAVE1, although to a variable degree of success. WAVE1 has a long PRD. This might confer an inherent instability and vulnerability to degradation, or it might cause poor translation, which could explain WAVE1 low levels of expression (see below).

2.2. WRC purification and quality

To reconstitute WRC, I considered two options. I could purify Sra1, Nap1, WAVE1, Abi2 and HSPC300 individually, and then attempt to reform the complex by mixing the components. Alternatively, I could co-infect Sf9 with the five viruses corresponding to the five components, allow the complex to form inside the cells and try to purify it as whole. I was encouraged to follow the co-infection method because I had previously succeeded in expressing and purifying the Sra1-Nap1 heterodimer using co-infection (Fig. 2.1B) (see section 2.3.1. for details on this sub-complex). Also, Shae Padrick has demonstrated that the N-termini of Abi and WAVE are poorly behaved individually, and that HSPC300 is a large aggregate. However when co-expressed in bacteria, these components form a stable trimeric complex.

The main problem with the co-infection approach is that I cannot verify that each insect cell has been actually infected with all five viruses. In fact, it is in most likelihood that each cell is infected with one of the 31 different combinations of one to five virus mixtures possible. Purifying WRC from all the different complexes generated using this method may prove difficult, but the double tagging strategy (His_6, GST) should help

clearing away the majority of sub-complexes that might form and be part of the proteins in the cell lysate.

Each WRC preparation was purified from 3.2 L of Sf9 cell culture co-infected with Sra1, Nap1, WAVE1, Abi2 and HSPC300 viruses and harvested 60 hours post infection. The large volume is necessary to offset the very low yield from Sf9, since I cannot detect the five bands corresponding to the five components by coomassie staining an SDS-PAGE gel run of the cell lysate. After lysis and clarification of cell debris by centrifugation, WRC was purified from the cell lysate using, NiNTA affinity resin (His_6 tag binding), followed by Glutathione Sepharose 4B resin (GS4B, GST tag binding). All tags were removed by TEV protease digestion (Fig. 2.2). In principal, the back-to-back affinity steps should yield a relatively clean complex. In practice, the aggregation of the excess HSPC300 and of some unincorporated sub-complexes, result in a WRC solution mixed with a number of contaminants.

To further purify WRC, I initially used a Source15Q anion exchange column, followed by a Superose6 size exclusion column. Those additional steps yielded a solution that showed only five protein bands on a coomassie stained gel. In addition, the chromatogram of the size exclusion column had only one peak that was almost symmetrical. I had originally concluded from these observations that I had purified a pure WRC. However, when I assayed the complex using the actin assembly assay (explained on page 59), I found that each of the first seven WRC preparations had a different activity: some were active, some were not, and some had variable degrees of activity. I suspected that WRC was actually contaminated with sub-complexes that include WAVE1.

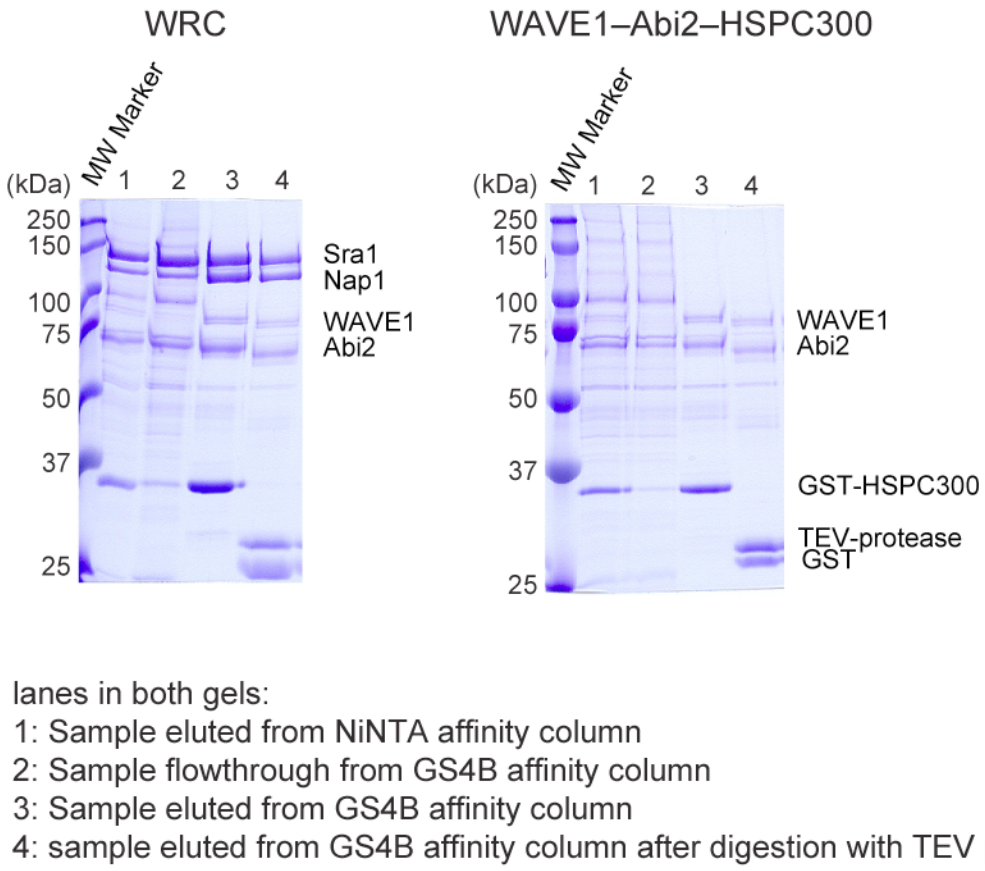

Figure 2.2: NiNTA and GS4B affinity purification steps

Coomassie blue stained 10%SDS-PAGE gel for WRC (left) and 15% SDS-PAGE gel for WAVE1–Abi2–HSPC300 heterotimer. Each complex was expressed in SF9 cells by co-infection of the constituting baculoviruses and incubation for 60 hours. The cell pellet was lysed with one freeze/thaw cycle and cleared by centrifugation at 20,000 rpm. The supernatant was incubated with NiNTA beads, washed then eluted (lane 1). The eluate was incubated with GS4B resin, washed (lane 2) then eluted (lane 3). TEV protease was added to the eluate to cleave the N-terminal tags (lane 4). Untagged HSPC300 is 9 kDa and does not appear in the gel.

To explore this possibility I made two modifications to the purification protocol. First, I used a shallow salt gradient (Δ 35% in 35 CV) over the Source15Q column. What was a single peak containing WRC separates into three peaks (Fig. 2.3A-red chromatogram). Only the first peak has all five WRC proteins (Fig. 2.3B). Surprisingly, the other two peaks contain Sra1, Nap1and Abi2 but not WAVE1. To understand where a WAVE1 containing contaminant elutes on Source15Q, I purified a WAVE1–Abi2–HSPC300 sub-complex following identical steps as for WRC (Fig. 2.2 and 2.3-green chromatogram). This exercise clearly demonstrated that non-incorporated WAVE1 and Abi2–WAVE1 sub-complexes elute at the same salt concentration as WRC on the Source15Q column (Fig. 2.3 green vs. red chromatograms).

To separate WRC from the WAVE1 containing contaminants uncovered by modifying the anion exchange step, I introduced a second modification to the purification protocol: I added a Source15S cation exchange column (Fig 2.4A) after the Source15Q column. After several trials and errors, I discovered that WRC, but not the contaminants remaining after the Source15Q column, would bind the Source15S column if I load the sample at a conductivity of ~6.2 mS/cm (Fig 2.4B,C). At a higher conductivity WRC will not bind to the column. At a lower conductivity, the contaminants will bind and their elution peak will overlap with WRC peak. The chromatogram of the final Superose6 size exclusion column shows a symmetrical WRC peak (Fig 2.5A), an indication of the high uniformity of the solution. The coomassie stained SDS-PAGE gel of the peak from Superose6 column shows a pure complex with five bands (Fig 2.5B). The actin assembly assay results became consistent from preparation to preparation when WRC was purified following the modified protocol.

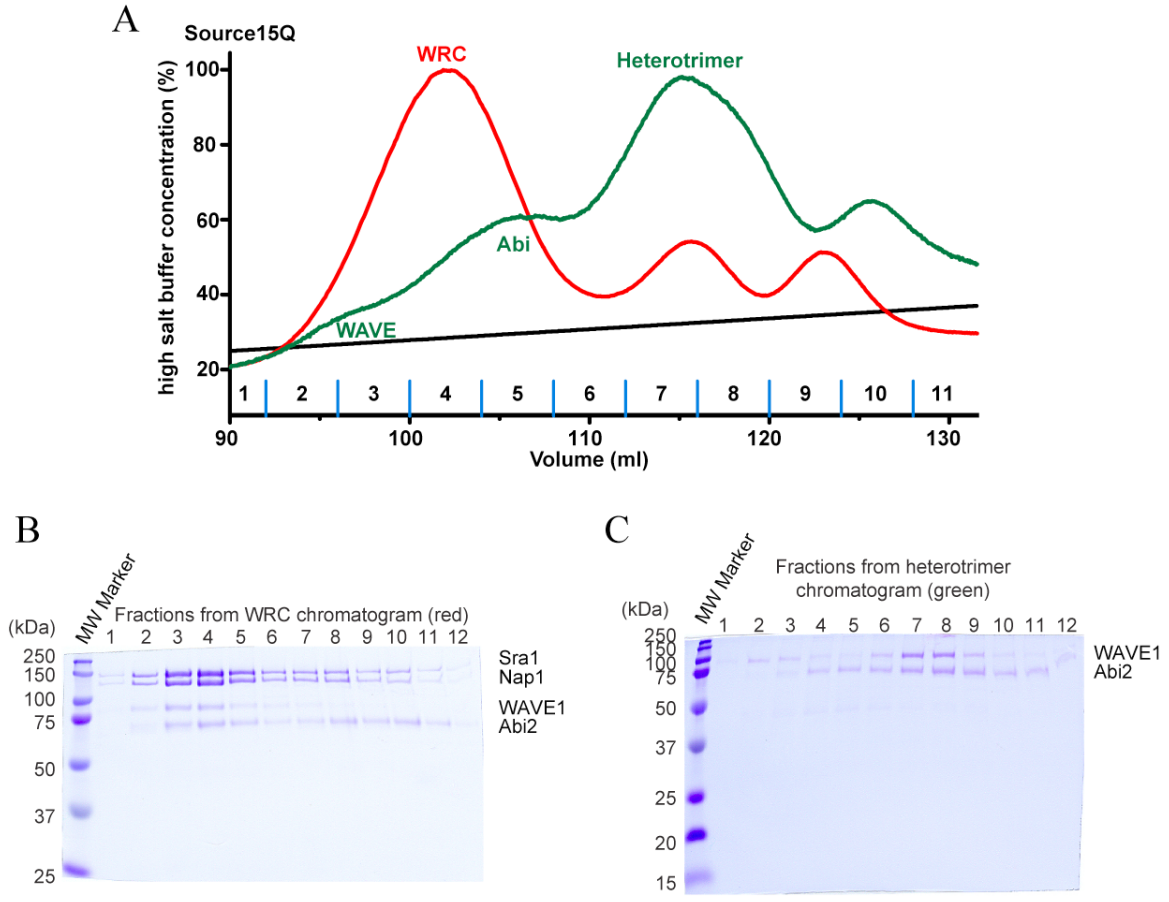

Figure 2.3: anion exchange chromatography separates WRC from some contaminants

(A) Source15Q Chromatograms of WRC (red) and the heterotrimer (green) ran under the same conditions. Althought WRC and the heterotrimer elute at different salt concentrations, unincorporated WAVE and Abi contaminants overlap with WRC. (B,C) Coomassie stained 10% (B) and 15% (C) SDS-PAGE gels for the fractions collected from the Source15Q run of WRC (B) and the heterotimer (C).

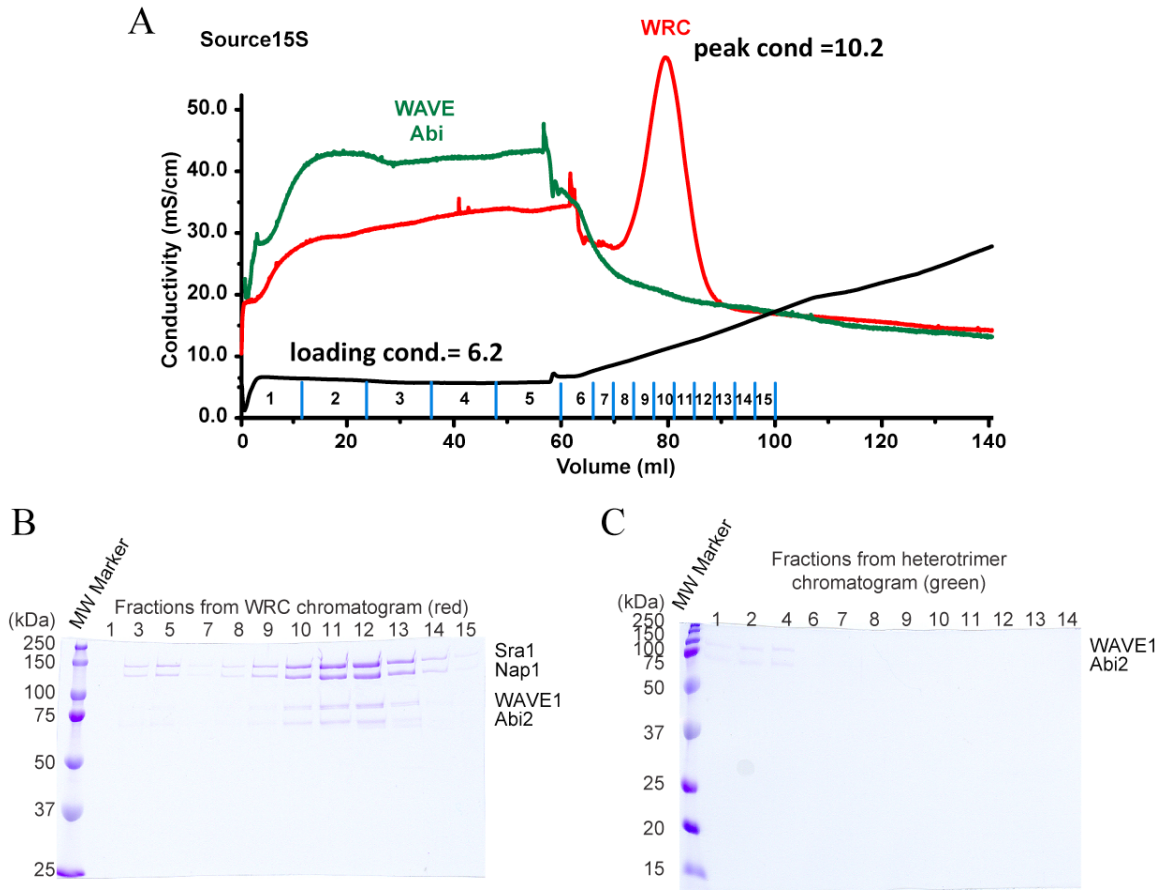

Figure 2.4: cation exchange chromatography separates WRC from other contaminants

(A) Source15S Chromatograms of WRC (red) and the heterotrimer (green). Fractions 3-4-5 from the Source15Q run (Fig 2.3) were pooled and injected onto the Source15S column. If loaded at the appropriate salt concentration, WRC peak from Source15Q step can be separated from its contaminants. (B,C) Coomassie stained 10% (B) and 15% (C) SDS-PAGE gels for the fractions collected from the Source15S run of WRC (B) and the heterotimer (C). Fractions 1 to 6 correspond to the flowthrough during injection of each solution.

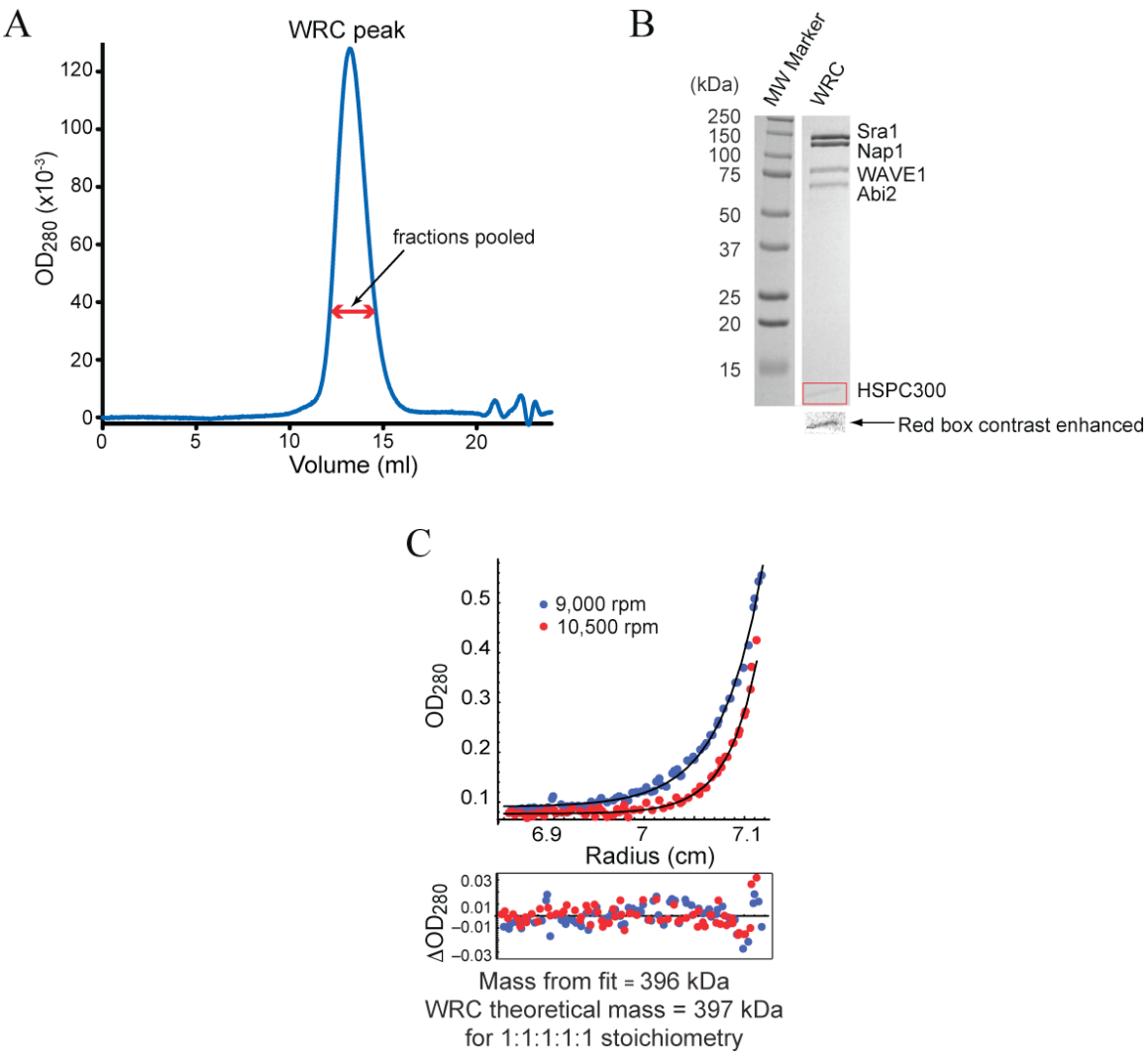

Figure 2.5: WRC is a heteropentamer

(A) Superose6 size exclusion chromatogram of WRC. Fractions 10 to 13 from the Source15S run were pooled and injected over the Superose6 column. OD_{280}: optical density at 280 nm. (B) Coomassie stained 8%-20% SDS-PAGE gel of WRC post size exclusion chromatography. (C) Equilibrium ultracentrifugation absorbance traces for WRC with fits and residuals at 9,000 and 10,500 rpm.

It is important to note here that the contaminants that caused the variability in the actin assembly assays are made from some of the five WRC proteins. A simple coomassie stained gel cannot identify these as contaminants of WRC. It is also surprising that the size exclusion chromatograms for WRC, before and after the two major modifications to the purification protocol, look very similar. That suggests that the contaminants elute with a similar profile as WRC, and sample heterogeneity cannot be concluded from that. This made it especially hard to identify the contaminants. In fact, the variability in the results of the actin assembly assay was the only reason I suspected that the original purification protocol does not produce pure and homogeneous WRC.

Starting from 3.2 L of Sf9 culture, I can purify about 1 ml of WRC at a concentration of 2.5~3 μM, or 6.2~7.5 mg. This yield is at least 10 fold higher than any previously reported (Derivery et al., 2009; Eden et al., 2002; Innocenti et al., 2004). Throughout the purification, all solutions contained 20% glycerol. WRC tends to precipitate when glycerol concentration drops below 10%. Purified WRC solution remains clear with no visible signs of precipitation up to at least four days after the final purification column. After two weeks, cloudiness is visible to the naked eye. As I explain in chapter IV, precipitation of WRC activates the complex because of the effect of aggregation on the potentiation of VCA. All assays reported in this dissertation where WRC was used have been performed within two days after purification.

The stoichiometry of WRC proteins has been considered to be one copy each, but the measurement has been indirect so far. In the only study addressing this issue, the molecular weight of WRC was estimated to be 320 kDa based on its elution volume on a size exclusion column (Eden et al., 2002). The authors calculated that to be very similar

to the theoretical molecular weight of WRC counting one copy of each unit. However, they did not include Abi in their calculation because they did not realize initially that Abi is part of the complex. Although they corrected Abi's omission in a note added in proof, they did not revisit their molecular weight estimates. Having succeeded in purifying high quality WRC, I was in a good position to answer the question of stoichiometry. Shae Padrick and I performed equilibrium ultracentrifugation, following the absorbance of the complex at λ=280 nm (Fig 2.5C). The absorbance profiles at 9,000 rpm and 10,500 rpm were fitted using SEDNTERP and SEDPHAT software. The calculated molecular weight is 396 kDa +/-20 kDa. The theoretical molecular weight of WRC is 397 kDa, considering one copy for each component, an almost perfect match with the calculated weight from the fit. The only caveat is HSPC300, with its molecular weight of 9 kDa. This is smaller than the error in calculation. We cannot determine the exact stoichiometry of HSPC300 from this experiment. However, Shae Padrick, in unpublished work, showed that HSPC300 forms a heterotrimer with the N-termini of WAVE1 and Abi2. Based on that, we believe that HSPC300 has only one copy in WRC, same as Sra1, Nap1, WAVE1 and Abi2.

2.3. Different complexes and sub-complexes produced

Full length WRC was not the only complex generated in this study. To fully understand WRC activity, I needed a number of complexes and sub-complexes that can help explain the interaction between WRC components. I reconstituted three sub-complexes and six truncated complexes either fully from baculovirus based insect cell expression, or from a mixed source of Sf9 and BL21 *E.coli*.

2.3.1. Sub-complexes

One common theme among several studies on WRC components is that Sra1 and Nap1 are pulled down together through immuno-precipitation (Kitamura et al., 1996; Kitamura et al., 1997; Kobayashi et al., 1998; Weiner et al., 2006). Innocenti *et.al.* were able to purify Sra1–Nap1 as a complex from 293T cells (Innocenti et al., 2004). Based on these data, I postulated that WRC could be split into two sub-complexes, Sra1–Nap1 and WAVE1–Abi2–HSPC300. I used the L21 based baculovirus system to co-infect Sf9 with Sra1 and Nap1 viruses. This strategy allowed co-expression of both proteins (Fig. 2.1B). I was able to purify the sub-complex using NiNTA affinity column, followed by Source15Q anion exchange column and Superose6 size exclusion column. If needed, the His_6 tag on both proteins could be removed through cleavage by TEV protease (Fig. 2.6A) before the anion exchange step, which clears away both the tags and TEV protease. The final gel filtration peak is near symmetrical, indicating high uniformity of the solution (Fig. 2.6B).

To determine whether Sra1–Nap1 sub-complex aggregates or self associates, I calculated the stoichiometry using multi-angel static light scattering (MALS). The molecular weight of the His_6 tagged sub-complex is 289.5 kDa, indicating a 1:1 stoichiometry (the theoretical molecular weight is 287.3 kDa) (Fig. 2.6C). The molecular weight of the untagged sub-complex is 277.8 kDa, again showing 1:1 stoichiometry (the theoretical molecular weight is 278.6 kDa) (Fig. 2.6D). Thus, Sra1–Nap1 sub-complex is a heterodimer. This heterodimer is not stable: it easily precipitates if I try to concentrate it by centrifugation. It also forms a thin film on top of the solution within 2-3 days. I observe heavy precipitation within two days if stored at room temperature, and within

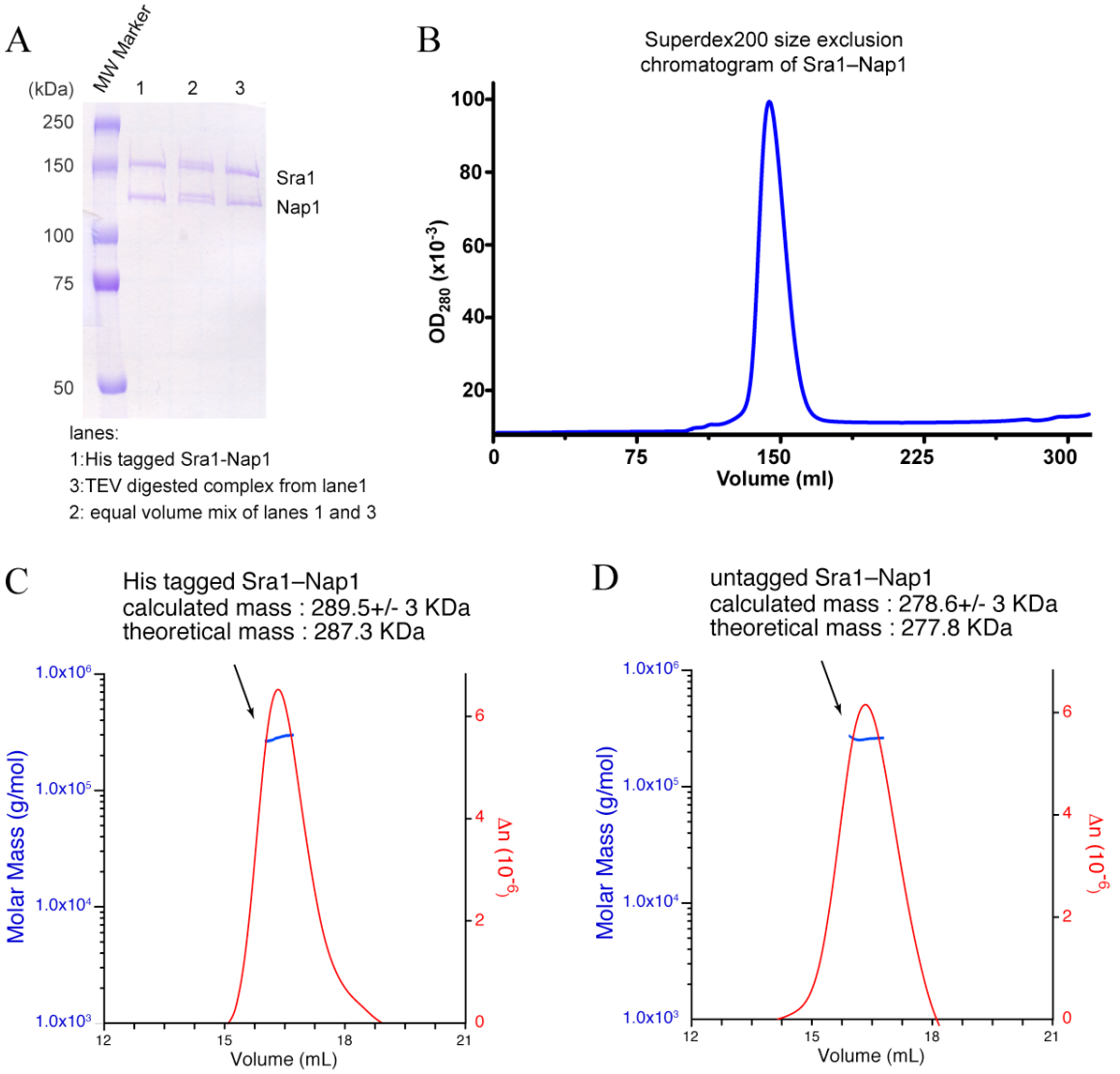

Figure 2.4: Sra1–Nap1 is a heterodimer

(A) Coomassie stained 10% SDS-PAGE gel showing the Sra1–Nap1 heterodimer before and after removal of the His_6 tag from both proteins. (B) Superdex200 size exclusion chromatogram for Sra1–Nap1 (C,D) MALS molecular weight measurement of Sra1-Nap1 heterodimer before (C) and after (D) removal of the His_6 tag from both proteins.

two weeks if stored at 4°C. Remarkably, if NBF is added to Sra1–Nap1, the heterodimer stabilizes. It can remain in solution for at least a month without visible precipitation and it can be concentrated by centrifugation.

The remaining three proteins from WRC are WAVE1, Abi2 and HSPC300. Co-infection of Sf9 with the corresponding baculoviruses yields a trimeric sub-complex. When run on a size exclusion column, two peaks contain the trimer, one in the void volume and one in the included volume. A re-injection of the latter within 12 hrs results again in a void volume peak and included volume peak. This demonstrates that the WAVE1–Abi2–HSCP300 is not a stable sub-complex, and that it aggregates over time. Similar to Sra1–Nap1 heterodimer, this trimer precipitates upon concentration by centrifugation. The yield was very low, which prevented the use of MALS to determine stoichiometry, and analytical ultracentrifugation could not be used because of the aggregation problem.

In unpublished work, Shae Padrick established the interacting domains among WAVE1, Abi2 and HSPC300. WAVE1 (aa 1-178), Abi2 (aa 1-158) and HSPC300 form a heterotrimeric sub-complex. The WAVE1 and Abi2 N-terminal sections and HSPC300 can be purified from bacterial cultures as MBP fusion proteins. The three components can then generate the aforementioned sub-complex when mixed with a detergent. However, when the MBP tags are removed, this sub-complex precipitates. Since the NBF fragment of Abi2 is part of it, mixing this sub-complex with the Sra1–Nap1 heterodimer stabilizes both, similarly to the stability I get when adding NBF only to the heterodimer: the formed complex is stable in solution and can be concentrated by centrifugation.

2.3.2. Truncated complexes

One reason for the low expression of Abi2 and WAVE1 baculoviruses could be that both proteins contain a PRD, a long sequence (> 200 aa) highly enriched in proline residues. Our lab has always had problems expressing WASP and WAVE proteins with PRDs, and found with WASP and N-WASP that removal of the PRD increases bacterial expression a lot. I generated L21 based baculoviruses for WAVE1 where the PRD domain was replaced by GGS_6 linker and a PreScission protease cleavage site (called WAVE1ΔP-PreS), and for Abi2 lacking the PRD and the C-terminal SH3 domains (Abi2 (aa1-158)). Again using co-infection of Sf9 with the corresponding baculoviruses, I expressed two new truncated complexes. The first, named WRC-PreS, is similar to WRC except that WAVE1 is replaced by WAVE1ΔP-PreS. The second, named MiniWRC-PreS, is similar to WRC-PreS except that Abi2 is replaced by Abi2 (aa1-158). Complex components are summarized in Table 2.1 and Figure. 2.7 shows their schematic cartoons. The reason for integrating a PreScission protease cleavage site between SHD and VCA in WAVE1ΔP-PreS will be explained later in this chapter.

I can purify both WRC-PreS and MiniWRC-PreS with a protocol similar to the one followed for WRC purification. WRC-PreS has a yield twice as high as WRC, and MiniWRC-PreS yield is even better, at least four times as high as WRC. VCA can be cleaved from both complexes using PreScission protease (Fig. 2.8A,B). I can reconstitute the MiniWRC-PreS from baculovirus infected Sf9 cells, as described above. Alternatively, I can reconstitute it from a mixed source of two sub-complexes. The first one, the Sra1–Nap1 heterodimer, is purified from Sf9 as described above. The second, a WAVE1ΔP-PreS–Abi2 (aa1-158)–HSPC300 sub-complex, is reconstituted from

	WRC	WRC-PreS	MiniWRC-PreS	MiniWRCΔVCA
Sra1	+	+	+	+
Nap1	+	+	+	+
WAVE1	+			
WAVEΔP-PreS		+	+	
WAVE1(aa 1-178)				+
Abi2	+	+		
Abi2 (aa 1-158)			+	+
HSPC300	+	+	+	+

	dWRC	dWRC-PreS
dSra	+	+
dNap	+	+
dAbi	+	+
dWAVEΔP	+	
dWAVEΔP-PreS		+
dHSPC	+	+

Table 2.1: protein components of the different complexes

WAVEΔP-PreS is WAVE1 (aa 1-208)-GGSGGSGGS-LEVLFQGP-GGSGGSGGS-WAVE1 (aa 484-559), and dWAVEΔP-PreS is dWAVE (aa1-222)-GGSGGSGGS-LEVLFQGP-GGSGGSGGS-dWAVE (aa 532-613), where LEVLFQGP is the PreScission protease cleavage site.

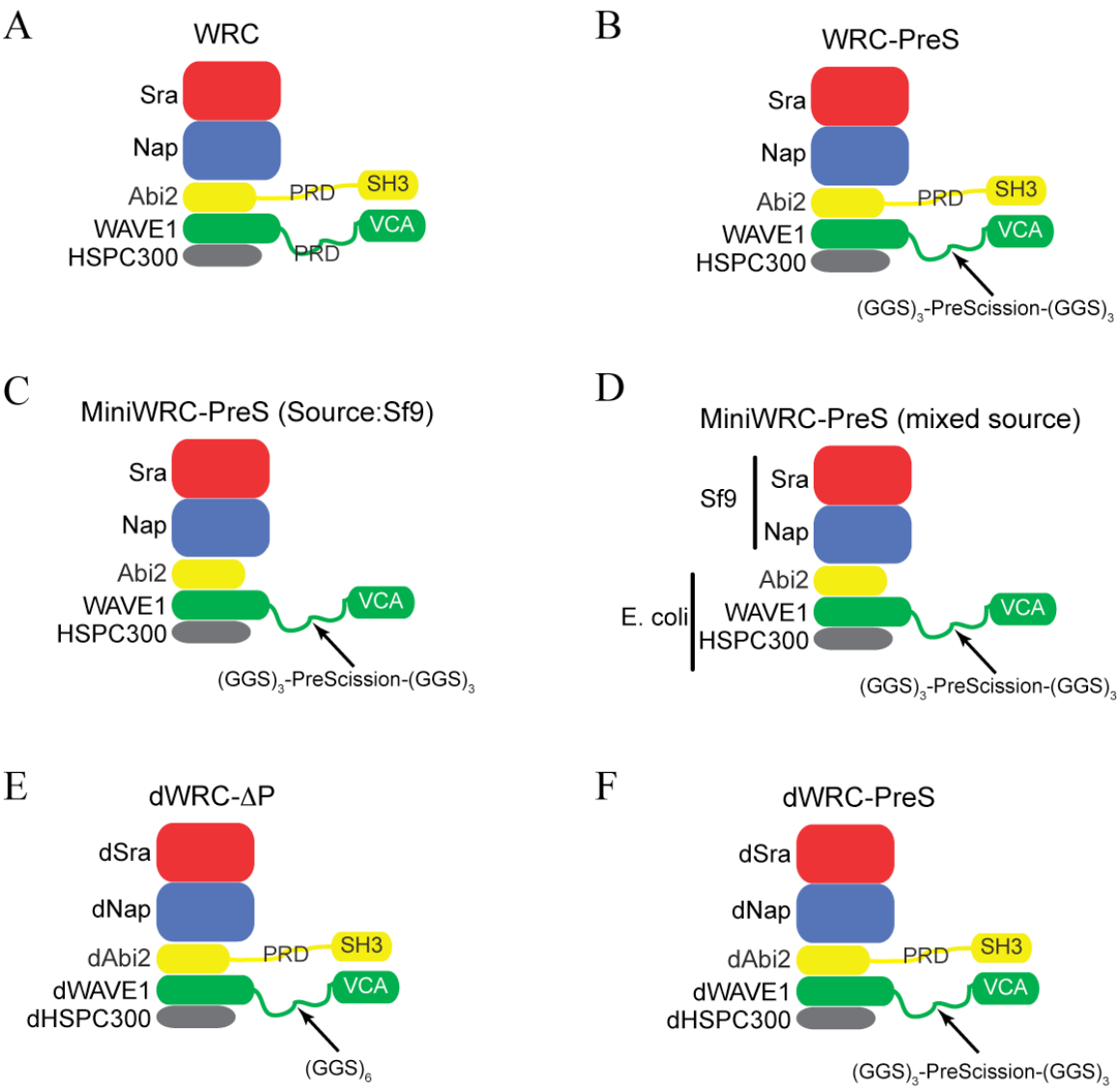

Figure 2.7: Cartoon presentation of the different complexes

Cartoons presenting the protein constructs constituting (A) WRC, (B) WRC-PreS, (C) MiniWRC-PreS purified from Sf9, (D) miniWRC-PreS purified from both Sf9 and E.coli, (E) dWRC-ΔP and (F) dWRC-PreS

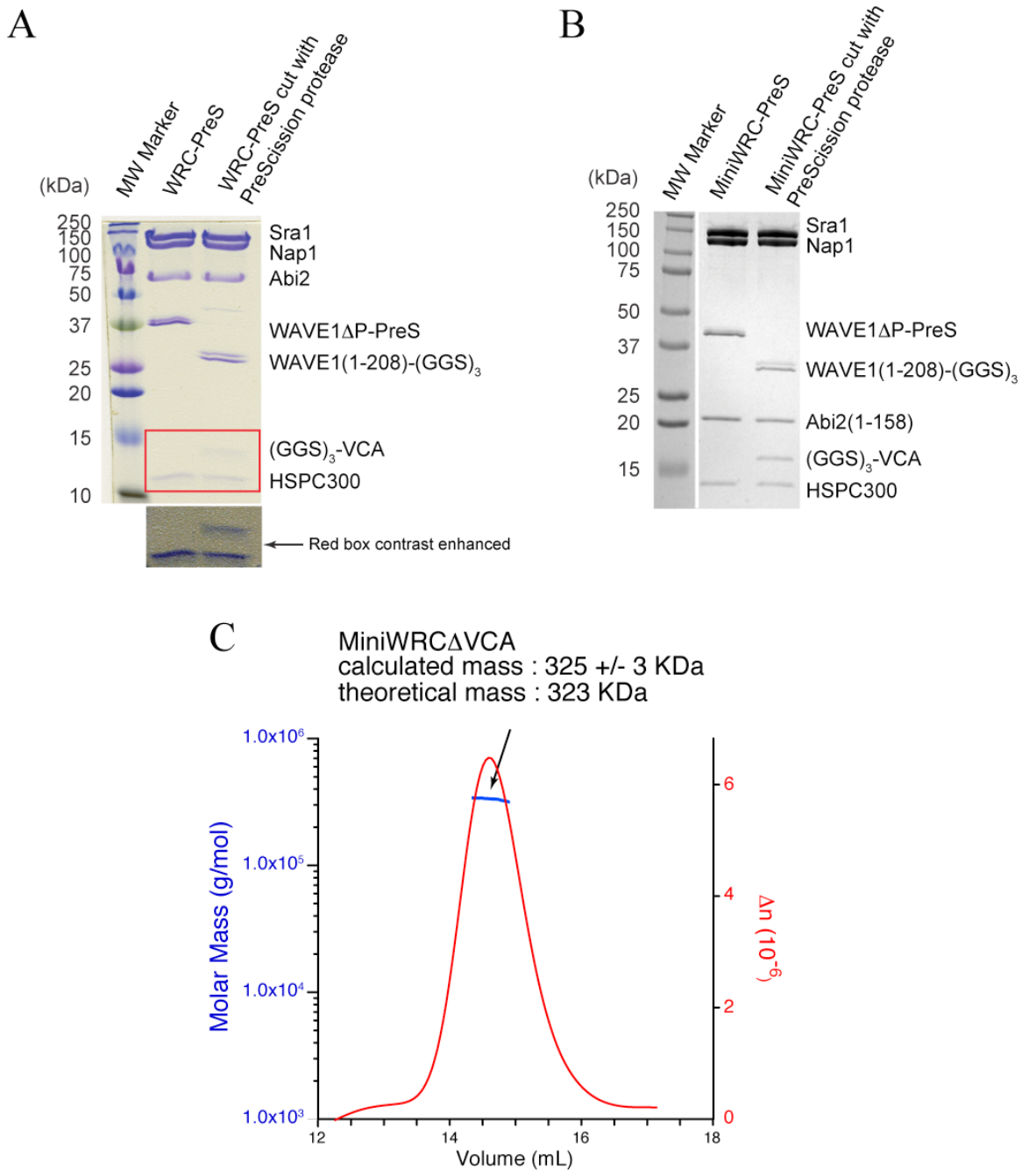

Figure 2.8: Truncated WRC complexes

Coomassie stained gradient SDS-PAGE gels of WRC-PreS (A) and MiniWRC-PreS (B) before and after digestion with PreScission protease. (C) MALS molecular weight measurement of MiniWRCΔVCA.

individual components expressed in BL21 *E. coli*. WAVE1ΔP-PreS, Abi2 (aa1-158) and HSPC300 are expressed as MBP tagged proteins. They are purified using Amylose resin, then they are mixed in equal ratios in the presence of 1% NP-40 detergent. The mixture is incubated overnight and purified over a Source15Q column. The resulting complex is mixed with Sra1–Nap1 to reconsitute the mixed source MiniWRC-PreS.

Also from a mixed source, and similarly to MiniWRC-PreS in the previous section, I can form a complex from the Sf9 cells derived Sra1–Nap1 heterodimer and the BL21 derived WAVE1 (aa 1-178)–Abi2 (aa 1-158)– HSPC300 heterotrimer. This complex is called MiniWRCΔVCA (Table 2.1). To verify that the PRD deletions did not fundamentally change WRC integrity, I used MALS to calculate the molecular weight of MiniWRCΔVCA. The calculated mass is 325 kDa, and the theoretical mass is 323 kDa (Fig. 2.8C). This demonstrated that the stoichiometry remains 1:1 for all components. Further functional testing (see next section) provided additional proof that the truncated complexes behave like WRC.

I also used L21 based vectors to generate baculoviruses for the Drosophila orthologues of WRC components, dSra, dNAP, dAbi, dWAVE and dHSPC. Several dWAVE baculoviruses failed to express the protein in Sf9. To overcome this problem, and following on the effectiveness of PRD deletion in increasing the yield of WAVE1, I generated baculoviruses for a dWAVEΔP and a dWAVEΔP-PreS. dWAVEΔP is a dWAVE where the PRD is replaced by GGS_6. Co-infection with the remaining four dWRC components allowed the reconstitution of dWRCΔP complex. dWAVEΔP-PreS is dWAVE where the PRD has been replaced by GGS_6 and a PreScission protease

cleavage site. This protein allowed the reconstitution of dWRC-PreS complex. Table 2.1 and figure 2.7 summarize the constituents of all the truncated complexes.

2.4. WRC activity

The pyrene actin assembly assay is the standard assay used to study the activity of actin nucleators and their activators like the VCA containing WASP family. This assay is greatly detailed in the journal Methods in Enzymology (Mullins and Machesky, 2000). It is based on the fluorescence of pyrene, a small fluorophore that can be conjugated to actin. When pyrene-actin incorporates into the growing actin filament, pyrene fluorescence increases by as much as 20 fold, theoretically. In practice, a 5 to 10 fold increase in fluorescence intensity is rather the norm. By monitoring fluorescence increase, we directly measure the elongation kinetics of actin filaments. This provides an indirect measure of nuclei formation and of the ability of NPFs (like WAVE) to activate nucleator (like Arp2/3 complex).

When using the Arp2/3 complex as nucleator, a polymerization curve has three phases. In the initial phase, the lag or nucleation phase, the increase in fluorescence will be very slow because elongation depends on the spontaneous nucleation of G-actin. Once few filaments form, VCA bound Arp2/3 can bind to those filaments, completing Arp2/3 activation requirements. New filaments quickly start elongating from Arp2/3 complex, and the elongation rate increases relatively to the concentration of activated Arp2/3 units. This is the elongation or growth phase. Filaments grow until the concentration of G-actin reaches the critical concentration for barbed end growth, 100 nM. At this stage, the steady state or equilibrium phase, filaments stop growing and the

fluorescence of the system in principle stabilizes at a certain value. In practice, and depending on the fluorometer setup, the steady state fluorescence can decrease slowly because of photobleaching..

2.4.1. WRC

The activity of WRC has to be tested against that of the free VCA domain of WAVE1 to determine its level. In actin assembly assays that include the Apr2/3 complex, the addition of the WAVE1 VCA domain, in increasing concentrations, produces shorter lag phase and increased elongation rates, both of which characterize activation of the Arp2/3 complex (Fig. 2.9A). Another measurement of Arp2/3 activation is the number of barbed ends generated at any given NPF concentration. This number can be calculated based on data extracted from the polymerization curves, including the maximum slope, the initial and final fluorescence values (Leung et al., 2006). 500 nM VCA can generate six times more barbed ends than actin and Arp2/3 complex alone (Fig 2.9B). The addition of the WRC complex to actin and Arp2/3 complex, at similar concentrations to VCA, do not produce any noticeable difference in the shape of the polymerization curves (Fig. 2.9A) or in the number of barbed ends generated (Fig. 2.9B). In other words, WRC do not activate the Arp2/3 complex.

2.4.2. Sra1–Nap1, WAVE1–Abi2–HSPC300 and WAVE1 VCA

As stated earlier, WRC can be thought of as two sub-complexes, an Sra1–Nap1 heterodimer and a WAVE1–Abi2–HSPC300 heterotrimer. The heterotrimer contains the activity-bearing domain (VCA). In a study to identify the minimal inhibitory components of WRC, I measured the activity of the heterotrimer in the actin assembly

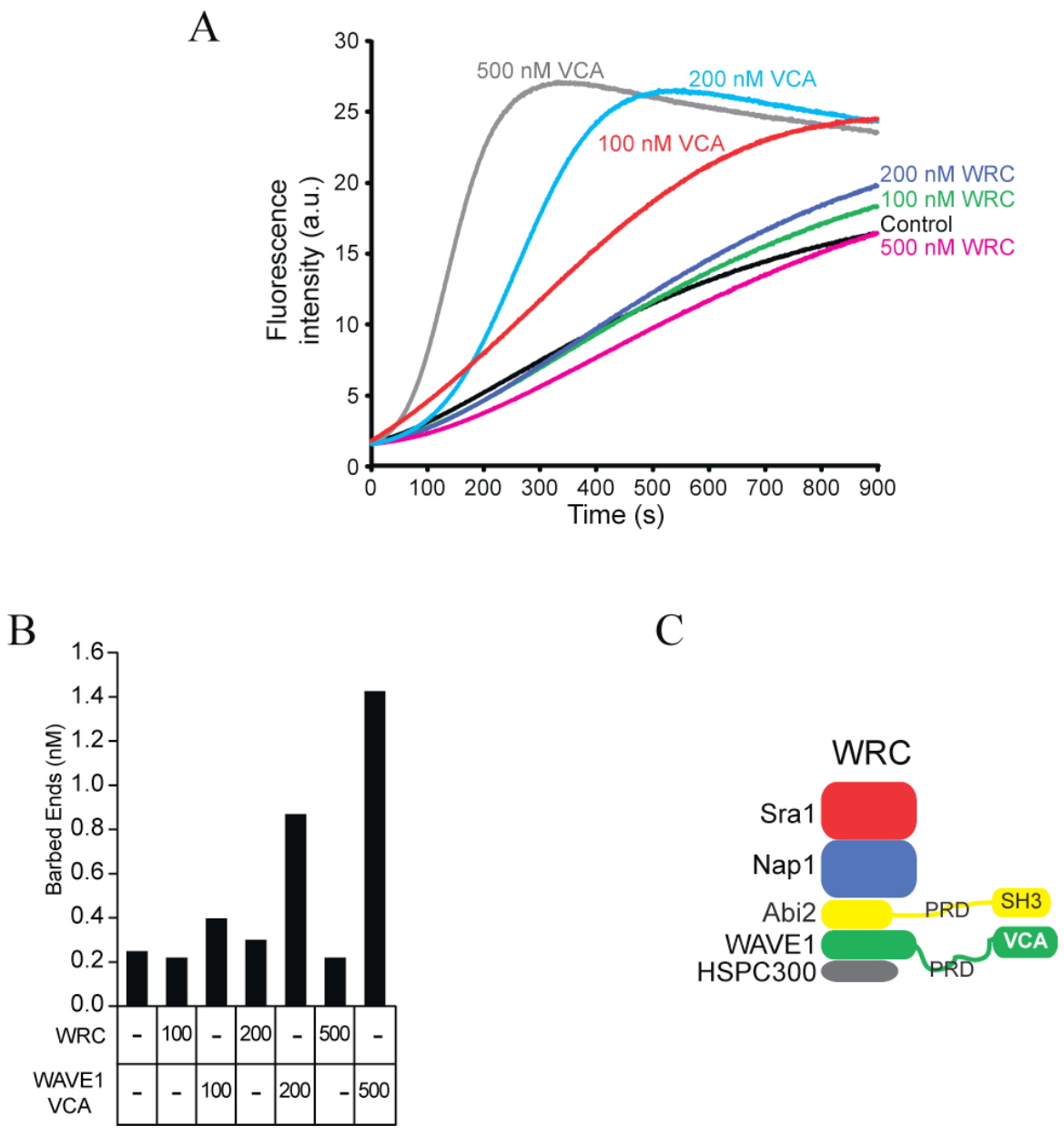

Figure 2.9: WRC is inactive

(A) Actin assembly assay performed with actin (4 μM) and Arp2/3 (10 nM) alone (control), or in the presence of 100, 200 or 500 nM of WRC or WAVE1 VCA. (B) Bar chart presenting the barbed ends generated by each assay condition in (A). (C) Cartoon presentation of WRC, the complex used in the assays in (A).

assay. At 100 nM, the heterotrimer greatly activates the Arp2/3 complex (Fig. 2.10A), far more potently than 100 nM VCA alone (e.g. see Fig. 2.9A). As mentioned earlier, the heterotrimer tends to aggregate over time. Correspondingly, older heterotrimer solution exhibits even higher activity toward Arp2/3. This hyperactivity is probably caused be the inherent aggregated state of the heterotrimer. Such aggregation would create oligomers of VCA, a species that is a very potent Arp2/3 activator, as explained in the last section of chapter one. However, oligomerization would not lead to potentiation if the VCA were not already active. The experimental results are consistent with variable degrees of aggregation of an intrinsically active VCA. Therefore, the WAVE1-Abi2-HSPC300 heterotrimer is active.

Since WRC is inhibited, the Sra1–Nap1 heterodimer must contain, at least partially, an inhibitory function towards the VCA domain. The heterodimer might directly bind and inhibit VCA. Alternatively, it might bind the heterotrimer and allosterically cause a change in it that results in the inhibition of VCA. To test whether Sra1–Nap1 inhibits the activity of WAVE1–Abi2–HSPC300, the heterodimer was titrated into the heterotrimer, where the concentration of the heterodimer was increase gradually up to ten-fold above the heterotrimer concentration (Fig. 2.10A). Equal concentrations of heterodimer and heterotrimer (as is found in WRC) did not result in the inhibition of the heterotrimer. However, with the gradual increase of the heterodimer concentration, the activity of the heterotrimer decreased until reaching control levels. Accordingly, the Sra1–Nap1 heterodimer is capable of inhibiting WAVE1–Abi2–HSPC300.

In WRC, all components are present with one copy each. Why then an equimolar mix of Sra1–Nap1 and WAVE1–Abi2–HSPC300 is not inhibited? Two pieces of data

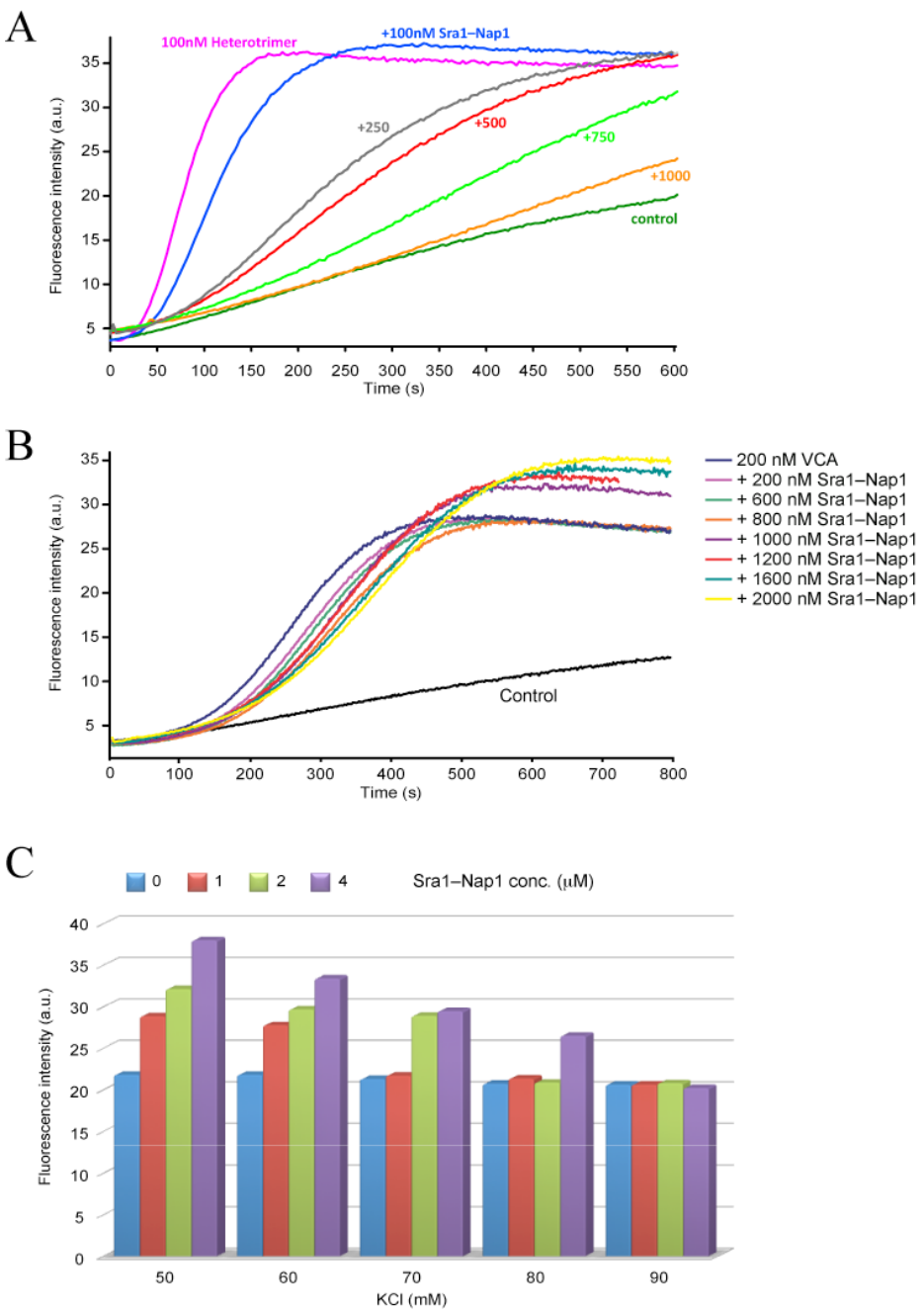

Figure 2.10: Sra1–Nap1 heterodimer contains inhibitory element.

Actin assembly assays performed with actin (4 μM) and Arp2/3 (10 nM) alone (control), or with increasing concentrations of Sra1–Nap1 in the presence of a 100 nM of WAVE1–Abi2–HSPC300 heterotrimer (A) or 200 nM VCA (B). (C) Fluorescence intensity (averaged over 120 seconds) of 4 μM polymerized actin in the presence of indicated Sra1–Nap1 concentrations at different salt concentrations

might help explain this data. I have noticed that the age of the heterotrimer affects the degree of inhibition. Older heterotrimer, which is largely an aggregate, is less inhibited by the heterodimer than a freshly purified heterotrimer, which has less aggregation than an old heterotrimer. Da Jia, a post-doctoral fellow in our lab, also observed that a solution of heterodimer and heterotrimer incubated for few hours has less activity than a similar solution assayed immediately after mixing. These observations suggest that the inhibition in this particular experiment is affected by the slow kinetics of assembly and disassembly of the heterotrimer aggregate.

To test whether the Sra1–Nap1 sub-complex inhibits VCA by direct interaction, a titration of the heterodimer against a fixed concentration (200 nM) of VCA was performed using the actin assembly assay. Contrary to the result obtained with the two WRC sub-complexes, ten-fold heterodimer to VCA ratio did not result in total inhibition of VCA (Fig. 2.10B). Increasing concentrations of the heterodimer did gradually decrease VCA activity, but the level of inhibition remained low. This result is best explained by a low affinity of the VCA domain *in trans* to the Sra1–Nap1 heterodimer. Additional interactions between heterodimer and heterotrimer should in principal enhance this affinity, such that the VCA domain *in cis* binds more tightly to the heterodimer.

One intriguing result presented itself from the previous experiment: the steady state fluorescence levels of pyrene-actin filaments increased proportionally to the concentration of Sra1–Nap1 heterodimer added to each experiment. One explanation would be that the heterodimer binds to the filaments, further shielding the pyrene fluorophore from quenching elements in solution and therefore increasing its quantum

yield. To verify this hypothesis, actin was polymerized overnight to reach equilibrium state (i.e. ADP-filaments), and the fluorescence level was measured in the presence of increasing concentrations of Sra1-Nap1 (Fig. 2.10C). Initially, the measurements were made in the actin assembly assay buffer, which contains 50 mM KCl. As expected, the higher the heterodimer concentration was, the higher the fluorescence level of F-actin was. However, this effect was less pronounced when the assay was repeated using buffers that have higher salt concentrations. At 90 mM KCl, the effect was totally abolished regardless of the heterodimer concentration. The dependence of fluorescence increase upon heterodimer binding on low salt conditions, and therefore low conductivity, could suggest that the interaction of F-actin and the heterodimer might simply be a non-specific one caused by low conductivity. At this point, it is not clear if that is the case, or if this interaction might in fact have some physiological relevance.

2.4.3. WRC-PreS and MiniWRC-PreS

The development of the "PreScission complexes" had two motivations. First, WRC inhibition could be explained by proteolytic degradation of the C-terminus of VCA during purification. A deletion of as little as three amino acids from the C-terminus of VCA renders it inactive toward the Arp2/3 complex (Sanjay Panchal, unpublished observation). If I can cleave VCA from WRC after purification and demonstrate that it can still activate Arp2/3, then I can firmly conclude that the inactivity of WRC toward the Arp2/3 complex is caused by genuine inhibitory interactions within WRC, rather than proteolytic degradation.

Second, the fact that a 1:1 ratio of heterodimer to VCA is sufficient for full inhibition within WRC (Fig. 2.9A) but not *in trans* (Fig. 2.10B) suggests that the affinity

of VCA for the heterodimer is greatly increased in the context of WRC. We already know that the NBF fragment of Abi2 binds Nap1 with high affinity (Shae Padrick, unpublished observation). This interaction physically links the VCA domain in WAVE1 to the heterodimer through the heterotrimer. Such interaction should increase effectively the affinity of VCA (in the context of the heterotrimer) for the heterodimer. Again, if I can cleave VCA from WRC, I would severe the "bridge" between VCA and the heterodimer, resulting in a low affinity binding of the two and probably activation of VCA.

I performed actin assembly assays using 100, 200 and 400 nM of WRC-PreS (Fig. 2.11A) and MiniWRC-PreS purified from Sf9 cells (Fig. 2.12A) or from insect-bacteria mixed source (Fig. 2.12B). All truncated complexes show no change (or very little) in the lag phase and the polymerization rate when compared to the control. Barbed ends calculations for WRC-PreS (Fig. 2.11B), Sf9 sourced MiniWRC-PreS (Fig. 2.12A, C) and mixed sourced MiniWRC-PreS (Fig. 2.12B, C) also show little or no difference from the control. These results indicate that these "PreScission complexes" are inactive toward the Arp2/3 complex.

The same concentrations of these complexes were treated with the PreScission protease and the actin assembly assay repeated. At all concentrations and for all complexes, the lag phase is shorter, the polymerization rate increases and the barbed ends concentration increases by as much as six-fold over control at the highest concentration of PreScission treated complexes (Figs. 2.11, 2.12). Those results indicate that VCA, once severed from the complex, is active toward the Arp2/3 complex.

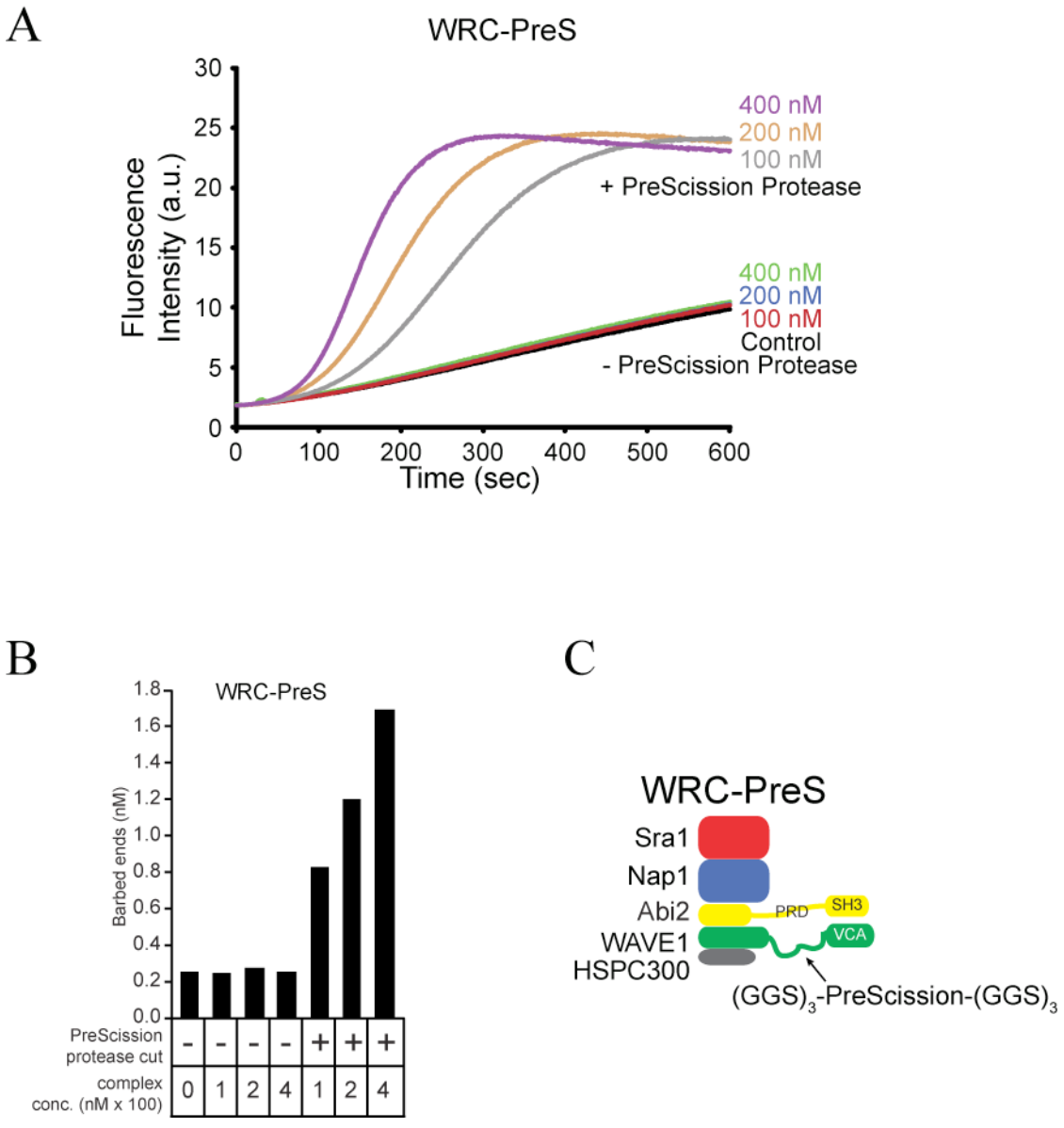

Figure 2.11: WRC-PreS is inhibited

(A) Actin assembly assay performed with actin (4 μM) and Arp2/3 (10 nM) alone (control), or in the presence of 100, 200 or 400 nM of WRC-PreS before or after digestion with PreScission protease. (B) Bar chart presenting the barbed ends generated by each assay condition in (A). (C) Cartoon representing the complex used in this assay, WRC-PreS.

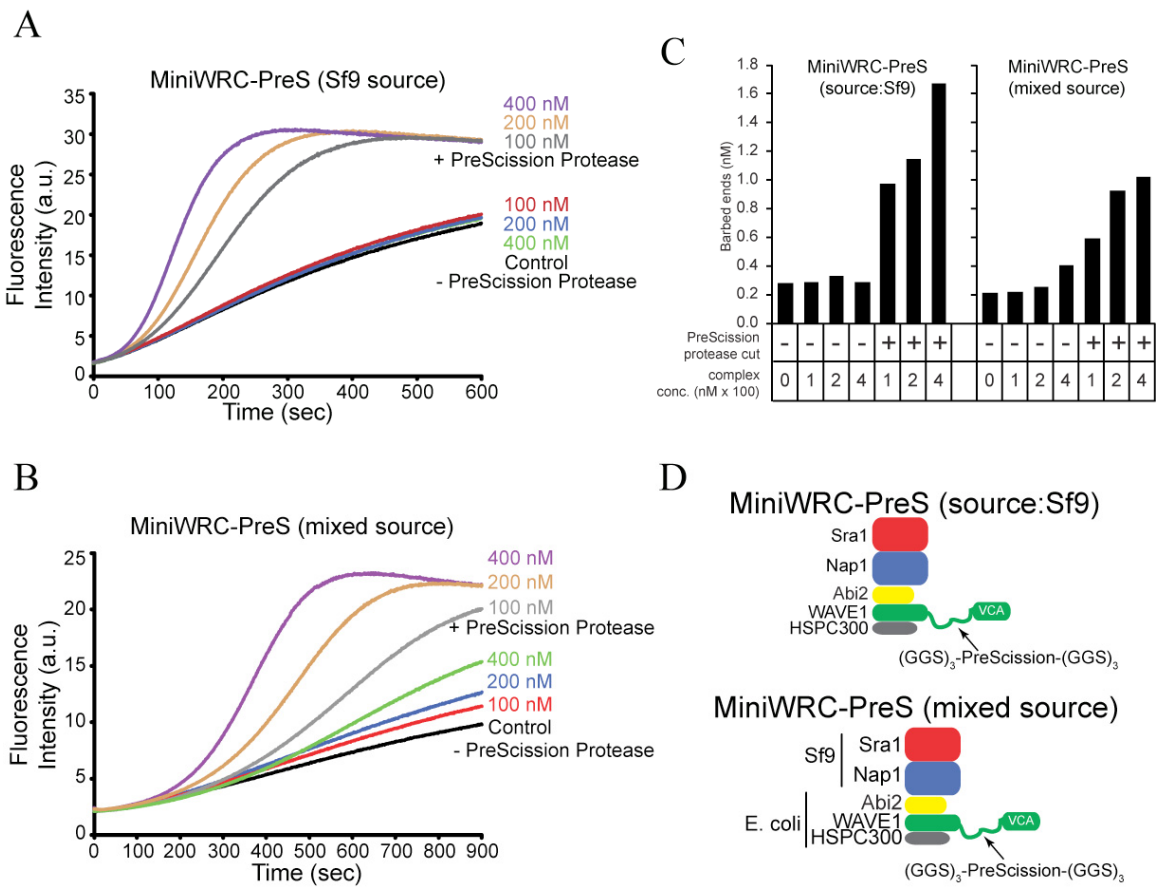

Figure 2.12: MiniWRC-PreS is inhibited

Actin assembly assay performed with actin (4 μM) and Arp2/3 (10 nM) alone (control), or in the presence of 100, 200 or 400 nM of MiniWRC-PreS purified from Sf9 (A) or from mixed source (B), before or after digestion with PreScission protease. (C) Bar chart presenting the barbed ends generated by each assay condition in (A) and (B). (D) Cartoon representing the complexes used in this assay, MiniWRC-PreS.

Data gathered using the "PreScission complexes" demonstrate three points. First, the VCA in these complexes is intact, since it can activate the Arp2/3 complex once cut from WAVE1 using PreScission protease. Therefore, the inactivity of WRC results from an intra-complex inhibition mechanism and not from artifactual proteolytic degradation of VCA. Second, the interaction between VCA and the Sra1–Nap1 heterodimer is indeed of low affinity and cannot by itself drive the inhibition mechanism. This is consistent with the inability of the Sra1–Nap1 to inhibit VCA (Fig. 2.10B). In this sense, the bridge between VCA and the heterodimer, provided by the WAVE1–Abi2–HSPC300 heterotrimer (at least partially through NBF binding to heterodimer), is an integral component of the inhibitory mechanism. Third, the PRDs of WAVE1 and Abi2 and the SH3 domain of Abi2 are not important for the main WRC inhibitory mechanism, since their deletion did not affect the inhibition state of the complex.

2.4.5 dWRCΔP and dWRC-PreS

A primary goal of this dissertation is to establish the activity state of the WRC. In order to do this, I felt that I needed not only the human complex, but also a completely different one from another organism. Similarity between the two would strengthen any argument appreciably. To demonstrate that inhibition observed in the human WRC and MiniWRC-PreS is a main characteristic of WRCs, I turned to the Drosophila WRC, or dWRC, because the fruit fly has only one paralogue of each component, that is, there is only one dWRC version. I compared the activity of dWRCΔP to that of dVCA in the actin assembly assay (Fig. 2.13A). At three different concentrations, dVCA exhibits increasing activation of the Arp2/3 complex, while actin polymerization remains at control levels when dWRCΔP is used. The dWRC-PreS complex also does not stimulate

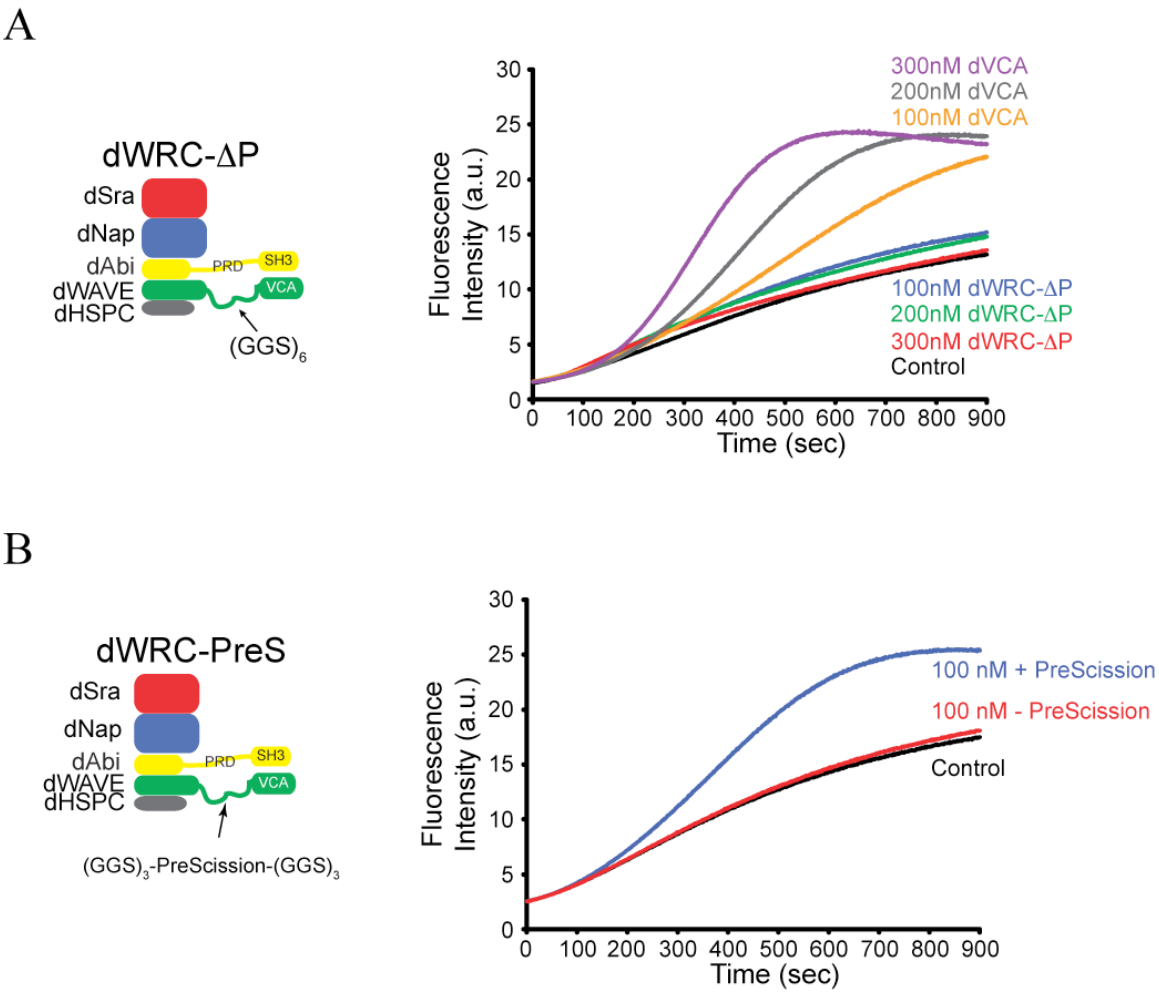

Figure 2.13: dWRC is inhibited

Actin assembly assay performed with actin (4 μM) and Arp2/3 (10 nM) alone (control), or in the presence of 100, 200 or 300 nM of dWRC-DP or dVCA (A) or 100 nM dWRC-PreS before or after digestion with PreScission protease (B). Cartoons on the left represent the complexes used in each assay.

polymerization beyond control levels (Fig. 2.13B). However, when dVCA is released from dWRC-PreS using PreScission protease, it activates the Arp2/3 complex to a level similar to that achieved using the same concentration (100 nM) of free dVCA (Fig. 2.13A, B). These data demonstrate that the Drosophila WRC is inhibited, and that dVCA also requires a link to the core of the complex for effective inhibition. I believe this establishes the generality of WRC function.

2.5. Summary

To resolve the differences between two opposing models of WRC function, I decided to purify WRC and a number of sub-complexes and truncated complexes. I was able to overcome the problem of Sra, Nap, Abi and WAVE expression through the use of a lobster derived promoter sequence, L21, in baculovirus based Sf9 insect cells expression systems. Through co-infection of the five viruses encoding the five components of WRC, I was able to express the complex, as well as an Sra1–Nap1 heterodimeric sub-complex and a WAVE1–Abi2–HSPC300 heterotrimer sub-complex. Also, a number of human and Drosophila complexes where generated where the PRD of WAVE or Abi or both was deleted and a PreScission protease cleavage site was introduced between the N-terminus of WAVE and the VCA domain.

I have optimized a protocol to purify a WRC complex of high quality and purity. I measured the stoichiometry of the components and found it to be one copy of each component. In activity assays, WRC is inhibited, while the WAVE1–Abi2–HSPC300 heterotrimer is active. Consistent with that, the Sra1–Nap1 heterodimer inhibits the heterotrimer and free VCA. However, VCA inhibition is weak, which implies that VCA-

heterodimer interaction is weak and other interactions within the WRC complex are required for full inhibition. WRC-PreS and MiniWRC-PreS, the two truncated complexes with the PreScission protease cleavage site, are also inhibited, and the release of VCA through PreScission digestion results in Arp2/3 activation. Drosophila versions of the complex, dWRCΔP and dWRC-PreS, are also inhibited and PreScission digestion results in active dVCA. Collectively, these data definitively establish that WRC is inhibited through intra-complex interactions.

Chapter III: Insights Into WRC Biochemistry

3.1. WRC activation by Rac1 GTPase

The small Rho family GTPase Rac1 can bind to the WRC through its interaction with Sra1 (Kobayashi et al., 1998). Several studies suggested that WAVE is a downstream effector of Rac1 signaling. When I started this work, it was not known whether Rac1 activates WRC, as the dissociation model suggests (Eden et al., 2002), or it simply localizes the complex to required sites without affecting its activity, as the non-dissociation model proposes (Innocenti et al., 2004) (Fig. 1.3). Another discord related to the role of Rac1 is whether the binding to Rac1 causes WRC to dissociate into two sub-complexes or not. Having purified WRC and demonstrated that it is inhibited, I had the proper materials to address these issues.

I performed actin assembly assays using 100 nM WRC, which does not activate the Arp2/3 complex above control levels (Fig. 3.1A, B). The addition of 5 μM inactive Rac1-GDP barely changes the polymerization rate or the number of barbed ends generated. But when the active Rac1-GMPPNP (GMPPNP is a GTP analog) is added to the assay at increasing concentrations, the polymerization rate and barbed ends concentration increase (Fig. 3.1A, B). Surprisingly, these increases are not proportional to the concentration of Rac1-GMPPNP. At 2.5 μM Rac1-GMPPNP, the barbed ends generated are about 1.2X control levels, indicating almost no activation of WRC. But at 5 μM Rac1-GMPPNP, at least 3X control levels of barbed ends are produced, and at 7.5 μM Rac1-GMPPNP, almost 5.5X control levels of barbed ends are produced. This

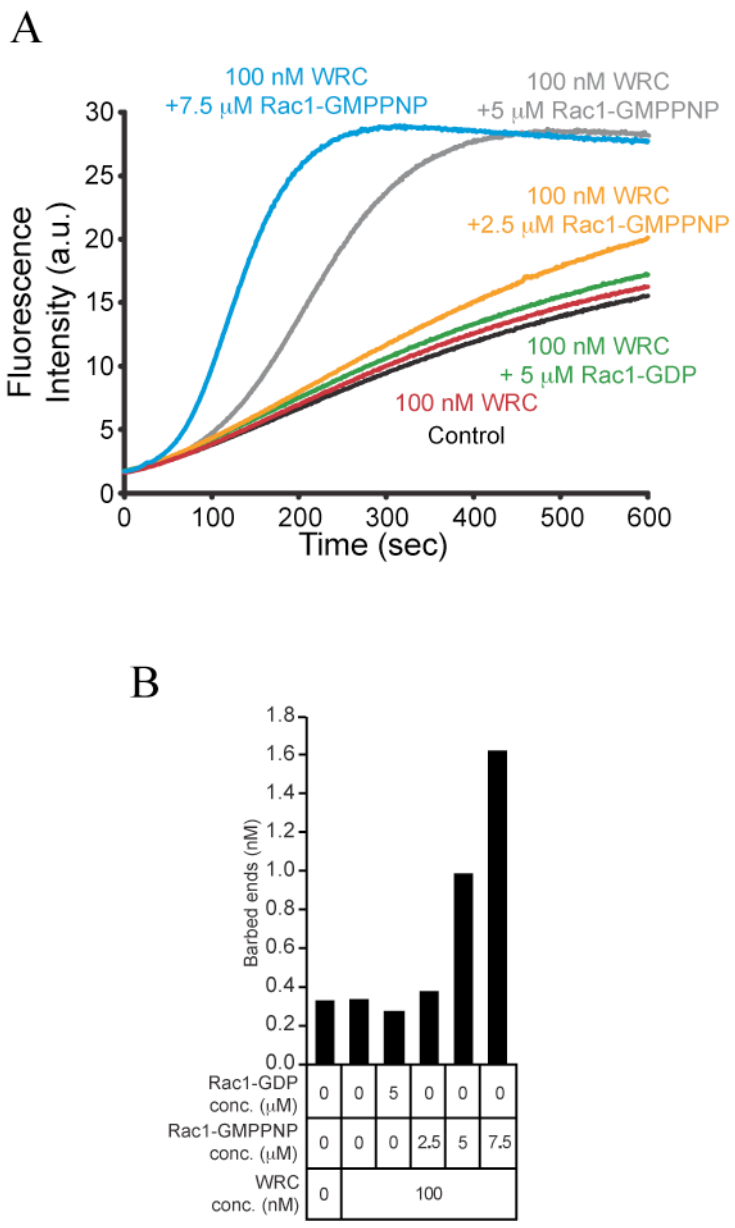

Figure 3.1: Rac1 activates WRC

(A) Actin assembly assay performed with actin (4 μM) and Arp2/3 (10 nM) alone (control), or in the presence of 100 nM WRC. Rac1 was added at the indicated concentrations. (B) Bar chart presenting the barbed ends generated by each assay condition in (A)

clearly indicates activation of WRC by Rac1 in a nucleotide dependent fashion. However the non-linearity of the activity level relative to Rac1 concentration indicates cooperativity between Rac1 molecules in activating WRC. In cells, Rac1 is membrane bound, and aggregation in membrane patches could result in high local concentrations of Rac1. Additionally, other proteins interacting with WRC might modulate the complex and increase its affinity for Rac1 *in vivo*.

To determine if WRC dissociates upon binding to Rac1, pull-down assays were also performed using GST-Rac1 as bait immobilized on GS4B resin. The preys were the Sra1–Nap1 heterodimer, the WAVE1 (aa 1-178)–Abi2 (aa 1-158)–HSPC300 heterotrimer and the MiniWRCΔVCA complex. Baoyu Chen, a post-doctoral fellow in our lab, performed the assays (Fig. 3.2). Rac1-GDP fails to pull-down any complex from solution. Rac1-GMPPNP pulls-down Sra1–Nap1 and MiniWRCΔVCA, but not WAVE1 (aa 1-178)–Abi2 (aa 1-158)–HSPC300. This result clearly indicates that Rac1 binds, in a nucleotide dependent manner, the Sra1-Nap1 heterodimer sub-complex, and this binding does not result in the dissociation of WRC in two sub-complexes.

3.2. VCA phosphorylation

3.2.1 VCA expressed in Sf9 cells is phosphorylated

The possibility that WRC inhibition resulted from VCA proteolytic degradation during purification led to the development of WRC-PreS and MiniWRC-PreS. To prove that VCA was intact, I used two methods. First, I performed the actin assembly assays with these complexes before and after digestion with PreScission protease, as shown in

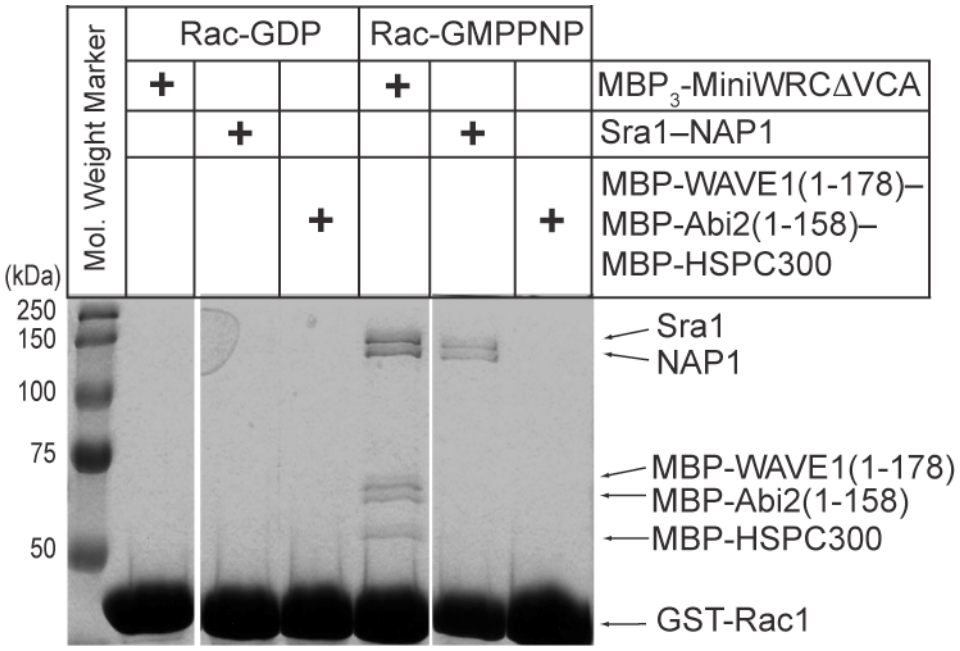

Figure 3.2: Rac1 binding does not dissociate WRC

Coomassie stained SDS-PAGE gel for eluates of pull-down assays. GDP or GMPPNP loaded GST-Rac1 was immobilized on GS4B beads and incubated with Sra1–Nap1, MBP_3-WAVE1(1-178)–Abi2(1-158)–HSPC300 or MBP_3-MiniWRCΔVCA. Each mixture was washed with buffer , then eluted from the beads.

chapter II. Second, I analyzed the absolute molecular weight of the proteins constituting MiniWRC-PreS using mass spectrometry. The protein chemistry technology center on campus performed the mass spectrometry measurements. Not all proteins were detectable by this method, but proteins below 36 kDa, like WAVE1ΔP-PreS, Abi2 (aa 1-158), VCA and HSPC300, gave good signals and their molecular weight was determined with a ± 1~3 Da error. If VCA is not degraded, then its measured molecular weight should match its theoretical one after digestion of the complex with PreScission.

The analysis of the MiniWRC-PreS complex produced in Sf9 cells showed that Abi2 (aa 1-158) and HSPC300 has an identical measured and theoretical molecular weights within error (Table. 3.1). They are intact, and PreScission protease digestion of MiniWRC-PreS does not modify their molecular weight. Surprisingly, WAVE1ΔP-PreS is heavier by 320 Da (Table. 3.1), indicating that the protein had been subject to some sort of post-translational modification (PTM). A phosphorylation adds 80 Da to the molecular weight of a protein. In principal, 320 Da could correspond to 4 phosphorylated residues in WAVE1ΔP-PreS. After digestion with PreScission protease, the two products, Nt-WAVE and VCA are also heavier, Nt-WAVE by 80 Da and VCA by 240 Da.(Table. 3.1). Again, this could mean Nt-WAVE is phosphorylated on one residue while VCA is phosphorylated on 3 residues.

When the MiniWRC-PreS complex produced from mixed sources (Sf9 and Bacteria) was analogously analyzed by mass spectrometry before and after PreScission protease digestion, all proteins returned a measured mass identical to their theoretical mass within error (Table. 3.1). In part, this result confirms that VCA is not degraded, and therefore inactivity is caused by inhibition. It also suggests that some PTM is added to

MiniWRC-PreS Source and treatment	Protein	Theoretical Mass (Da)	Measured Mass (Da)	Mass Difference	Candidate PTM
Sf9 cells source					
No treatment	Abi2 (1-158)	19622	19621	1	-
	HSPC300	9276	9278	2	-
	WAVE1ΔP-PreS	35885	36205	320	4X phosphate
PreScission Protease	Nt-WAVE1	26370	26450	80	1X phosphate
	WAVE1-VCA	9532	9773	241	3X phosphate
PreScission Protease + λPPase	WAVE1-VCA	9532	9534	2	-
Mixed source					
No treatment	Abi2 (1-158)	18212	18212	0	-
	HSPC300	9269	9269	0	-
	WAVE1ΔP-PreS	35676	35677	1	-
PreScission Protease	Nt-WAVE1	26160	26162	2	-
	WAVE1-VCA	9533	9533	0	-

Table 3.1: mass determination of some complex proteins

The MiniWRC-Pres complex from both the Sf9 source and the mixed sources was submitted for mass spectrometry analysis without treatment, after digestion with PreScission protease, and for the Sf9 sourced complex, after digestion with PreScission protease and lambda phosphatase λPPase. PTM: post-translational modification.

WAVE1ΔP-PreS generated in insect cells that is not added in bacteria. Again, the most straightforward possibility is phosphorylation.

To test this possibility, I attempted to dephosphorylate the Sf9-produced complex after PreScission protease digestion. Treatment of the PreScission cut complex with λPPase (a dual specificity phosphatase) results in faster migrating VCA on an SDS-PAGE gel. Mass spectrometry analysis showed that VCA now has a measured mass identical to its theoretical mass without any PTM (Table 3.1), indicating successful dephosphorylation by λPPase.

I submitted a PreScission protease digested MiniWRC-PreS complex (Sf9 source) for PTM analysis. Once more, the protein chemistry technology center on campus performed the analysis. After extraction of the proteins from cut gel bands, they digested them with a cocktail of proteases. Then they analyzed the mass of the resulting peptides using tandem mass spectrometry (MS/MS). They compared the results to a corresponding theoretically digested protein sequence to identify the peptides that deviate from their expected mass. The PTM on both Nt-WAVE and VCA was identified as phosphorylation, and the targeted residues were identified. Ironically, Nt-WAVE is phosphorylated on one of the serine residues in the GGS linker that replaced the PRD. I do not consider this phosphorylation to have any effect on Nt-WAVE interactions with Abi2 and HSPC300. VCA phosphorylation sites were mapped to the three serines residues in the acidic region, Ser544, Ser546 and Ser550. These phosphorylations could affect the interaction of VCA with the Arp2/3 complex, changing its activation.

3.2.2. VCA phosphorylation enhances its activation of Arp2/3

The difference in the VCA phosphorylation based on its source actually translates into a small but noticeable difference in the actin assembly assay. After PreScission protease digestion, the unmodified VCA (produced in bacteria as part of WAVE1ΔP-PreS) is 70% to 80% as active as the phosphorylated VCA (produced in Sf9 as part of WAVE1ΔP-PreS) (compare barbed ends produced by equal concentrations of the two digested complexes in Fig. 2.12C Sf9 vs mixed source).

To verify if the difference in activation by MiniWRC-PreS from the two different sources emanates from VCA phosphorylation in insect cells, I performed actin assembly assays for the PreScission cut MiniWRC-PreS produced in Sf9 cells, with and without dephosphorylation by λPPase. The activity of VCA drops by about 15% to 20% upon dephosphorylation (Fig. 3.3). These data demonstrate that VCA phosphorylation can modulate the activity of WRC by increasing its activation potential toward the Arp2/3 complex. This enhancement may be the result of an increased affinity of the phospho-VCA to Arp2/3, as has been suggested for WAVE2 VCA (Nakanishi et al., 2007).

3.3. Mapping of VCA interaction with Sra1–Nap1 by NMR

3.3.1. HSQC line broadening as a tool

The Sra1-Nap1 heterodimer is able to slightly inhibit WAVE1 VCA (Fig. 2.10B), although saturation of the inhibition is not achieved with the concentrations used in the assay. This suggests that the affinity of VCA for Sra1–Nap1 is low, probably in the micromolar range. The VCA domain is close to 10 kDa in weight, while the Sra1–Nap1.

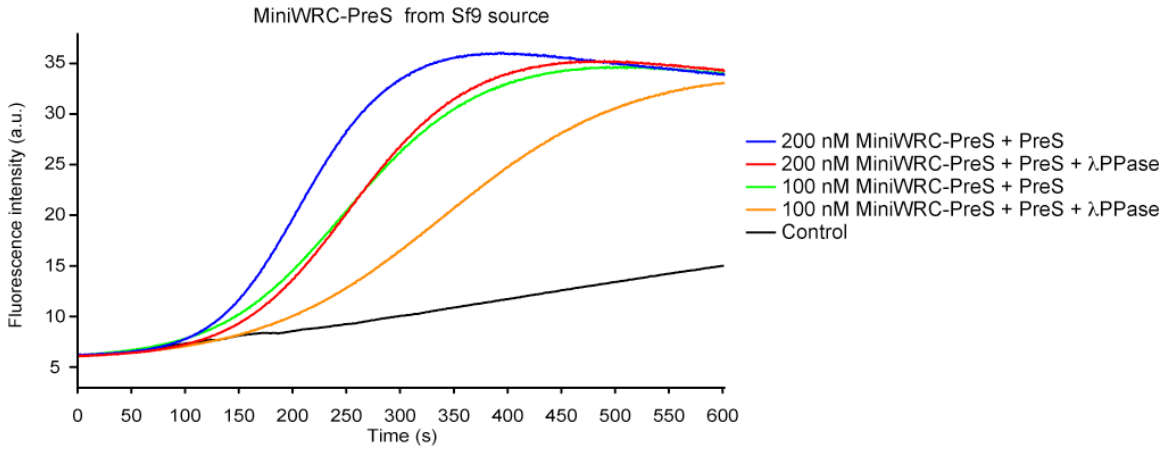

Figure 3.3: phosphorylation slightly increases VCA activity

Actin assembly assay performed with actin (4 μM) and Arp2/3 (10 nM) alone (control), or in the presence of 100 or 200 nM of PreScission digested MiniWRC-PreS with or without treatment with λPPase.

heterodimer is close to 290 kDa in weight. This difference in molecular weight, together with the expected low affinity, constitutes an ideal system for characterization using nuclear magnetic resonance (NMR) line broadening measurements.

Micromolar affinities often correlate with an intermediate NMR chemical-exchange regime. In this regime, resonances of the VCA that undergo large changes in chemical shift (for example, through direct contacts or acquisition of structure) and/or become immobilized upon binding of VCA to Sra1–Nap1 will be broadened in the presence of sub-stoichiometric quantities of Sra1–Nap1 (Matsuo et al., 1999). As broadening arises from a combination of chemical-exchange effects (between bound and free forms) and increased transverse relaxation in the complex (Matsuo et al., 1999), resonances that do not change chemical shift on binding, or that correspond to highly mobile residues in the complex, will remain sharp. Line broadening can thus be used to map approximately the Sra1–Nap1 binding site on VCA. By monitoring the changes, upon addition of the heterodimer, in the intensity of the peaks in a heteronuclear single quantum coherence (HSQC) spectrum of the ^{15}N-labeled VCA, we can determine which section(s) of the VCA domain binds Sra1–Nap1. We may be able then to conclude an inhibitory mechanism. The concept of the line broadening experiment is illustrated in Figure 3.4. This experimental approach was successful in the study of the interaction between the VCA domain and the Arp2/3 complex (Panchal et al., 2003)

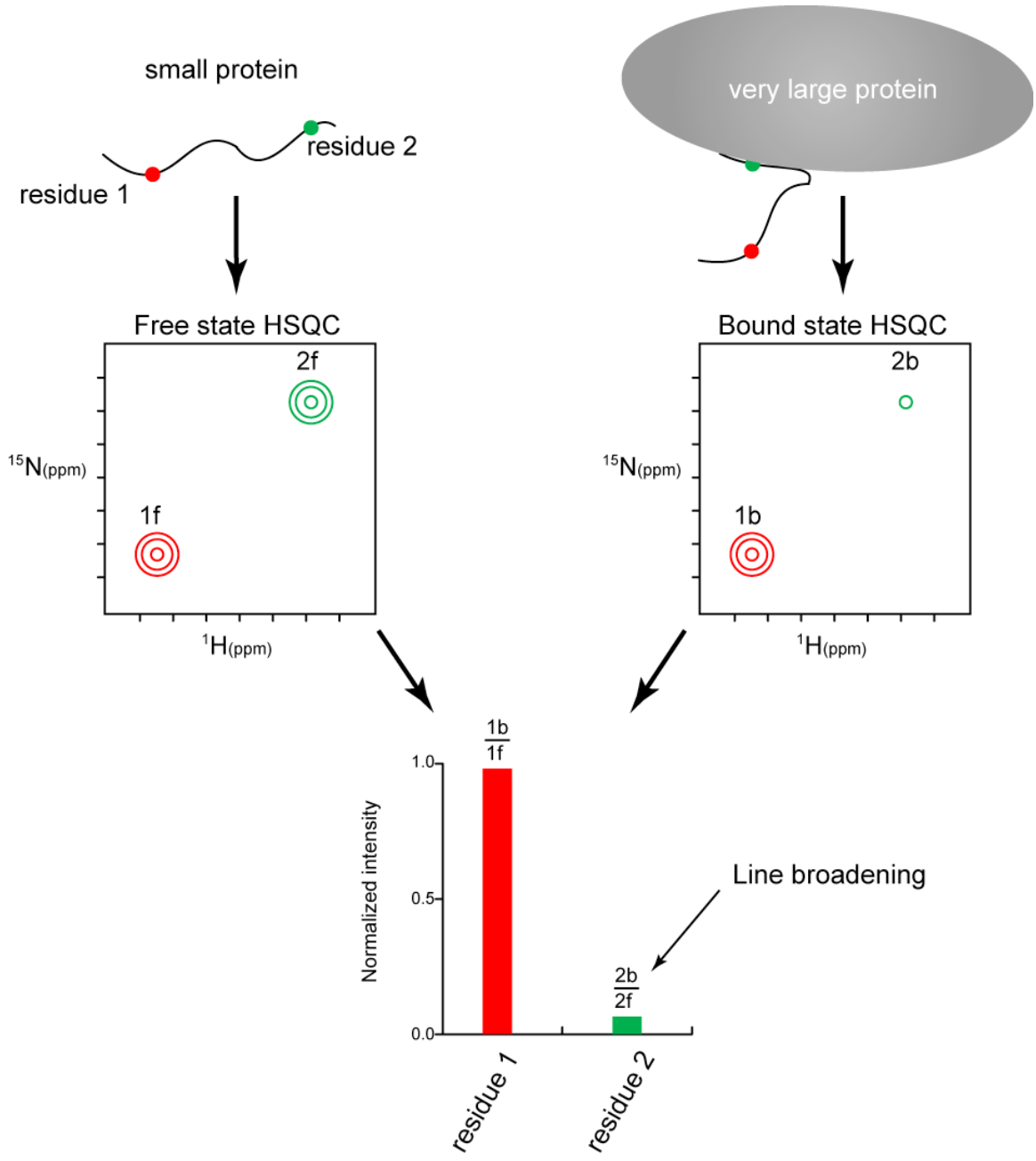

Figure 3.4: NMR Line broadening explained

Diagram explanation of the HSQC NMR line broadening detection. The bigger the protein is, the faster its relaxation rate is and the lower the intensity of corresponding peaks will be. If a small and unstructured protein is bound to a large protein, the bound section will behave like a large protein (weaker signal). The free section largely retains its mobility and its signal intensity.

3.3.2. Analysis of the VCA-Sra1–Nap1 interaction using line broadening

Peak assignment is essential for the analysis of any NMR spectrum. The spectrum of WAVE1 VCA has already been assigned for a previous study (Panchal et al., 2003). However, the mixture of VCA and Sra1–Nap1 precipitated in the buffer condition used for the acquisition of the spectrum in the earlier study. So I had to change the buffer, mainly increasing the pH from 6.8 to 7.4. Although the VCA spectrum changed a little under the new buffer conditions, the pattern of the peaks remained almost identical in the two buffers. By comparison and deduction, I was able to reassign more than 90% of the peaks (Fig. 3.5). The parameters of the HSQC pulse sequence used to acquire this spectrum and all other spectra mentioned below are in Appendix II.

I acquired all HSQC spectra used to study the VCA-Sra1–Nap1 interaction under the same conditions, for the same length of time and using the same VCA concentration. First, I acquired the HSQC spectrum of ^{15}N-labeled VCA (Fig. 3.6A). Then I acquired the spectrum of VCA mixed with a sub-stoichiometric concentration of the Sra1–Nap1 heterodimer (7.5:1 of VCA:Sra1–Nap1) (Fig. 3.6B). By comparing the two spectra, I can see a number of peaks that have reduced intensity or are no longer detectable after addition of the heterodimer. Some of the peaks most affected are circled in red in figure. 3.6B.

Each peak in the VCA spectrum corresponds to the backbone amide of a single residue. I plot the normalized intensities (intensity of the peak when complex is added divided by the intensity in free VCA (Fig. 3.4)) against residue position in the VCA sequence (Fig. 3.7A). This analysis shows a distinctive pattern, where the intensities of

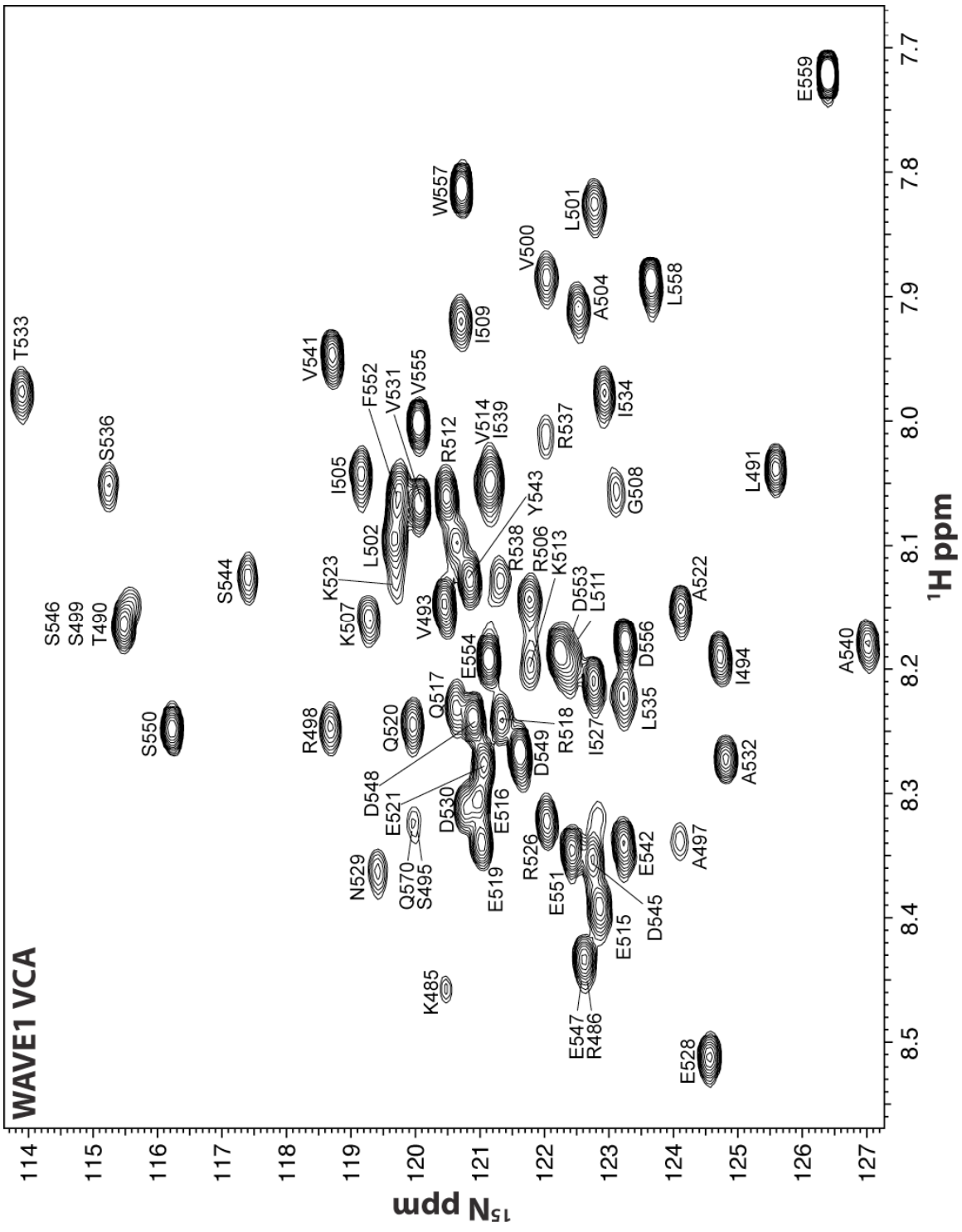

Figure 3.5: WAVE1 VCA ^{15}N-^{1}H HSQC spectrum assignment

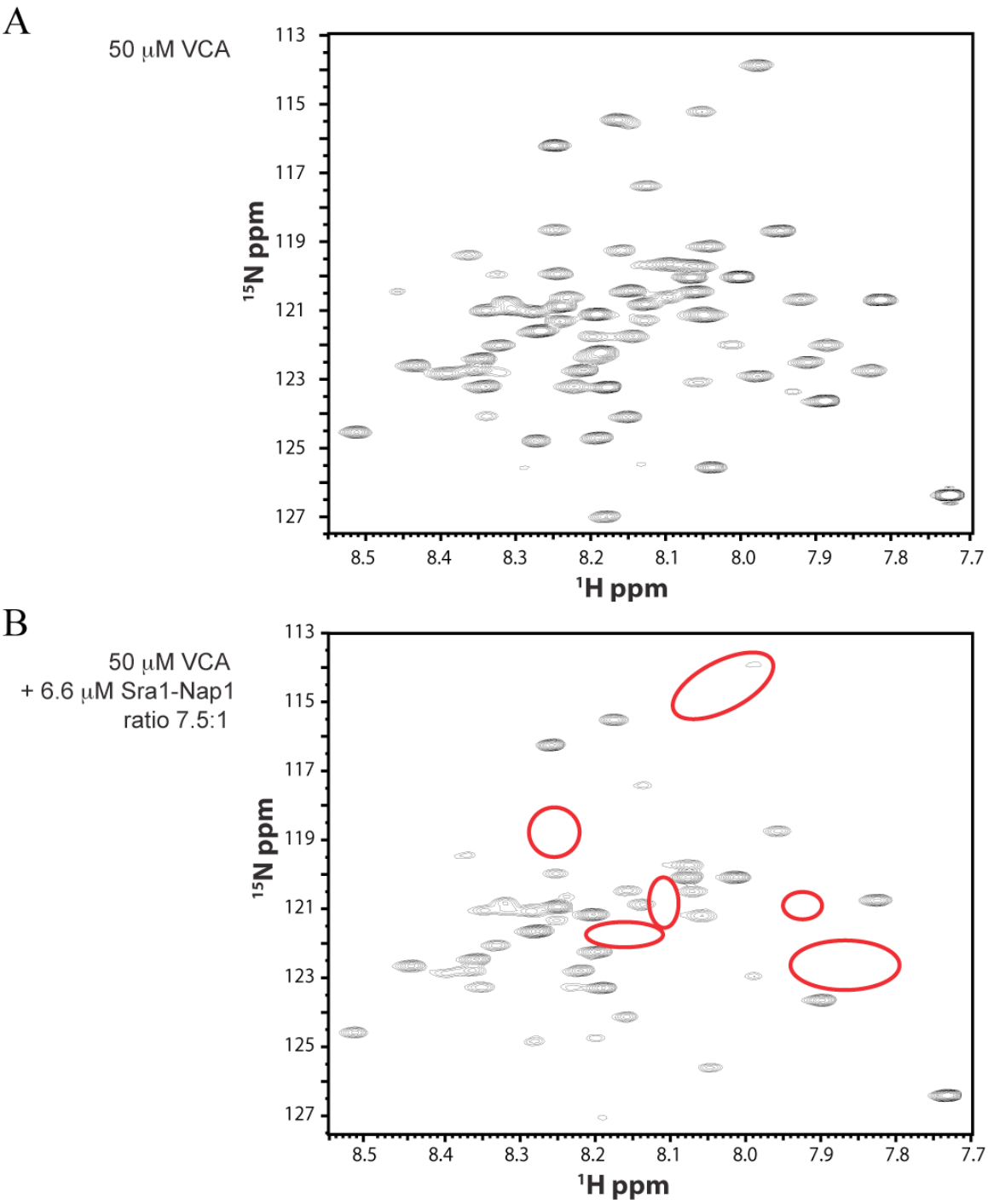

Figure 3.6: Sra1–Nap1 affect HSQC spectrum of VCA

2D 15N-1H HSQC spectrum of WAVE1 VCA (A) and WAVE1 VCA + Sra1–Nap1 heterodimer.

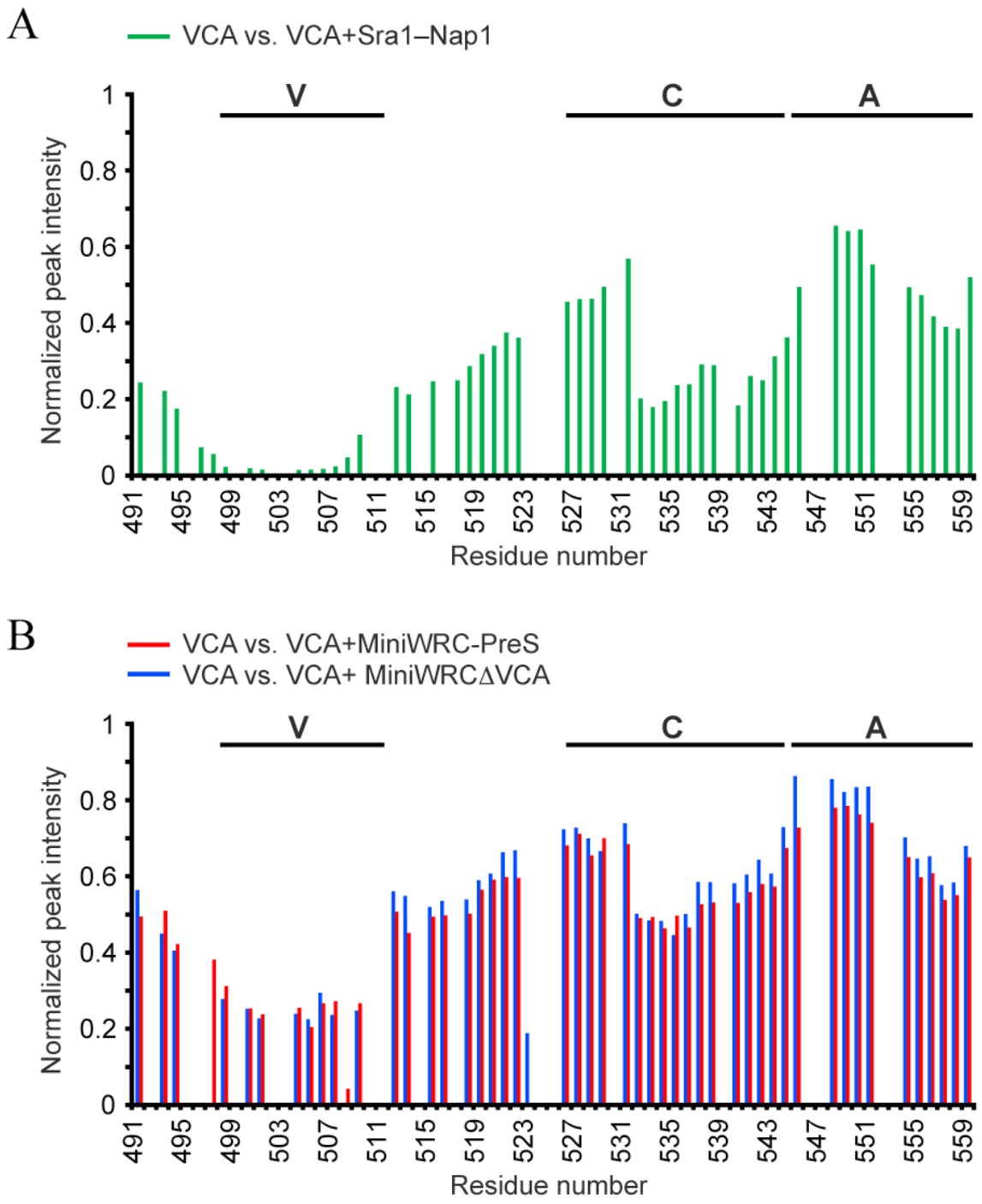

Figure 3.7: V and C segment of VCA are affected by different complexes

Bar chart plots of the normalized peak intensities for the mixtures of 50 μM WAVE1 VCA with 7.5 μM of (A) Sra1–Nap1 heterodimer and (B) MiniWRCΔVCA (blue bars) or MiniWRC-PreS (red bars)

the peaks corresponding to the V and C regions of VCA decrease the most. This suggests that the heterodimer binds preferentially to the V and C regions. A similar analysis was performed on the spectrum of a mixture of ^{15}N-labeled VCA and the MiniWRCΔVCA complex (Fig. 3.7B blue bars). The same profile of peak intensities decrease emerges, although the decrease in some regions is smaller than the one observed with the VCA-heterodimer mixture. Again, this suggests that the VCA interacts with the complex preferentially through its V and C regions.

In these line broadening experiments, competing the ^{15}N-labeled VCA with an excess of unlabeled VCA in a control experiment should regenerate most of the lost intensities. However, WAVE1 VCA aggregates at high concentration, leading to complications that would render the experiment non-interpretable. But I can use another complex in a control experiment. I have shown in chapter II that the MiniWRC-PreS complex is inhibited, and when VCA is released by PreScission protease digestion, it can activate the Arp2/3 complex (Fig. 2.12). Thus, the *in cis* VCA in the MiniWRC-PreS complex is bound to the inhibitory elements and should be able to prevent a free VCA from binding to those elements. Based on that, a mixture of ^{15}N-labeled VCA and MiniWRC-PreS should provide a good control for the line broadening experiment.

Thus, I acquired an HSQC spectrum for the ^{15}N-labeled VCA and MiniWRC-PreS mixture and analyzed the intensity decrease of the VCA peaks (Fig. 3.7B red bars). Once more, the profile of intensity decrease indicates that the V and C region of VCA are still interacting with the complex. In fact, the normalized intensities of the VCA-MiniWRC-PreS mixture and the VCA- MiniWRCΔVCA mixture plotted side-by-side look very similar to each other (Fig. 3.7B). Given that the experiment and its negative

control produce the same result, I cannot conclude that the Sra1–Nap1 heterodimer binds the V and C regions of the VCA domain. At this point, I am not sure how to interpret these data, and my attempt to decipher a WRC inhibitory mechanism by NMR remains inconclusive.

Chapter IV: Hierarchical Regulation of WASP Family Proteins

4.1. Mechanism of VCA potentiation through dimerization

The work on this section was motivated by an observation made by Hui-Chen Cheng, a student in our lab. Using actin assembly assays, she found that a peptide made from two repeats of the EspFu minimal active repeat unit have significantly greater activity than just one repeat. Using ITC, she established that each of the two repeats binds one WASP molecule. One peptide of two repeats has two WASPs bound to it. This is equivalent to dimerizing the VCA domain. In fact, there is a report in the literature of a GST VCA fusion protein (which is dimeric) that is more active than an equal concentration of monomeric VCA (Higgs and Pollard, 2000). Moreover, many reported WASP interacting proteins have a potential for multivalency. Thus, the idea was born that dimerizing WASP may be a regulatory mechanism that is not explored. Various members of our lab have indeed demonstrated that when VCA is dimerized through various methods, both artificial (GST tagging, crosslinking, etc…) and natural (binding to multi-SH3 containing proteins, binding to proteins with constitutive dimerization domain, etc…), its activity is greatly increased.

4.1.1. Stoichiometry of Arp2/3-dimeric VCA complex

To understand the basis of VCA potentiation by dimerization, we turned our attention to the development of a mechanistic model. One possibility was that filament barbed end binding by one V region (Co et al., 2007) increased the local F-actin

concentration relative to the second VCA and its bound Arp2/3 complex. However, a GST-VCA mutant impaired in barbed end binding has activity comparable to wild type (Padrick et al., 2008), arguing against this model. Instead we asked whether the nature of the Arp2/3-VCA interaction is changed when VCA is dimeric. Current models of active Arp2/3 invoke only a single VCA binding site in the complex (Chhabra and Higgs, 2007; Goley and Welch, 2006; Pollard, 2007; Stradal and Scita, 2006).

To determine the stoichiometry of the complex between GST-WASP VCA dimers and Arp2/3, I measured the mass of the complex using MALS. The mixture had a 3-fold excess of GST-VCA to Arp2/3, and it was resolved using Superdex 200 size exclusion column before entering the MALS detector (Fig. 4.1). Two species were detected, with calculated molecular weights of 80 kDa and 302 kDa. This is consistent with a GST-WASP VCA dimer (theoretical mass = 73.9 kDa) and a 2:1 complex of GST-WASP VCA and Arp2/3 (theoretical mass = 294 kDa). The data clearly do not support the presence of a 2:2 complex of GST-WASP VCA and Arp2/3 (theoretical mass = 518 kDa). Sedimentation velocity ultracentrifugation analyses performed by Shae Padrick and Chad Brautigam (Padrick et al., 2008) confirmed this finding. Thus, by two independent analytical methods we find that a VCA dimer binds a single Arp2/3 complex.

4.2.2. Affinity of dimeric VCA for Arp2/3 complex

The clearest manifestation of the dimerization effect on VCA activity is the requirement of much smaller concentrations of dimeric VCA to achieve Arp2/3 activation levels similar to higher concentrations of monomeric VCA. A dimeric VCA species binds as one unit to one Arp2/3 complex, as we have shown above.

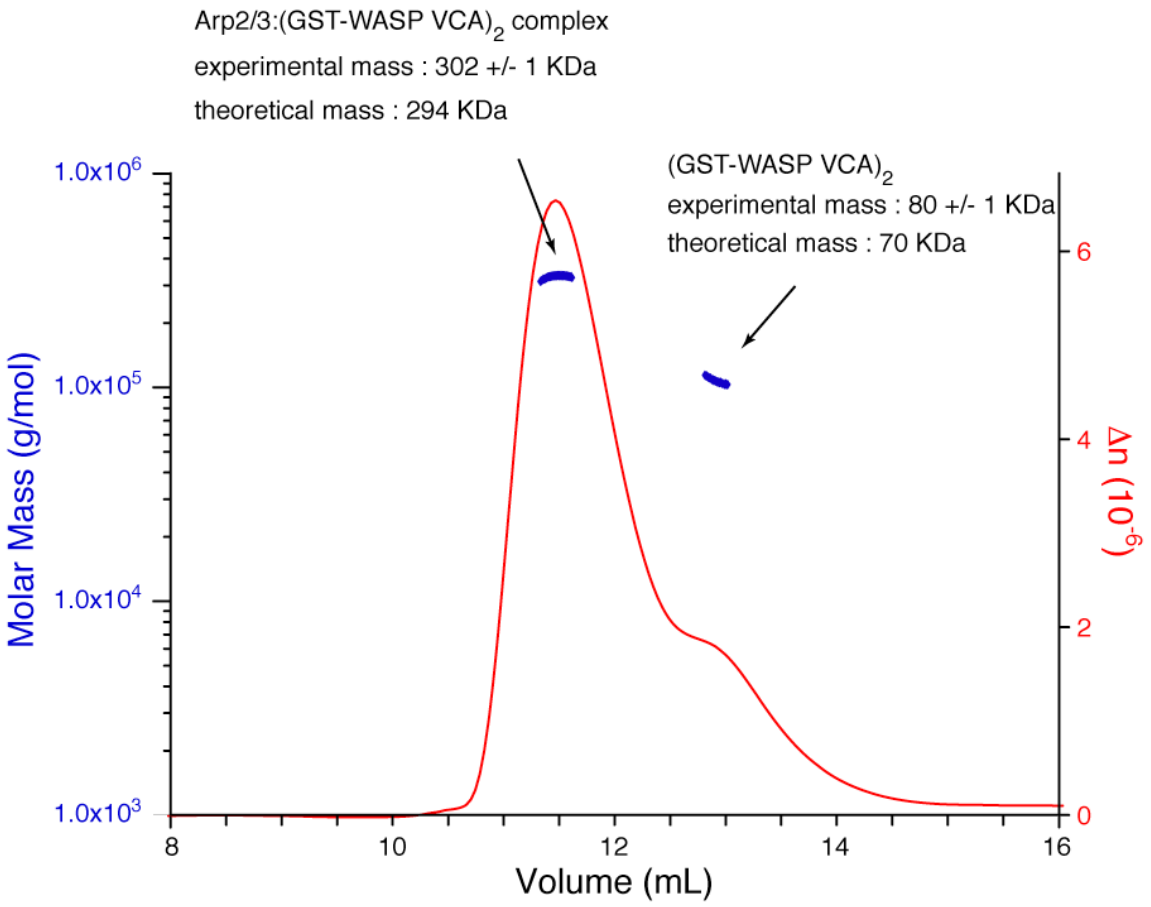

Figure 4.1: A dimer of VCA binds one Arp2/3 complex

MALS molecular weight measurement of Arp2/3 complex in complex with GST-WASP VCA. GST-WASP VCA was 3-fold in excess of Arp2/3. The mix was injected over a size exclusion column attached inline directly to a multi-angel scattering detector and a refracometer. Δn (red chromatogram) is the difference in the refractive index between a reference solution containing buffer only and the sample as it elutes from the column. The blue bars indicate the calculated molecular mass over the volume range (selected peak) the bars cover.

This stoichiometry should, in principal, increase the affinity of VCA for Arp2/3, which would explain the lower concentration requirement for activation. To test this hypothesis, we used a fluorescence competition binding assay to measure the affinities of VCA monomers and GST-VCA dimers for Arp2/3 complex (Marchand et al., 2001). These measurements required a large amount of proteins to be purified simultaneously. Shae Padrick and I handled the purification, while Lynda Dolittle, a senior technician in the lab, acquired the data. Shae Padrick analyzed the data as detailed in Methods. Table 4.1 summarizes the measured affinities.

The affinities of monomers are similar to those reported previously, ranging from 1.6 μM to 4.4 μM for the VCAs of N-WASP and WAVE1, respectively (Marchand et al., 2001; Zalevsky et al., 2001). The dimers all have substantially higher affinity, between 9 nM and 29 nM, when data are fit to a model with 2:1 stoichiometry of GST-VCA to Arp2/3 complex. This corresponds to an increase in affinity of 100, 150 and 180 fold for WASP, WAVE1 and N-WASP, respectively. These findings confirm that dimerization of VCA results in a boost in affinity and therefore a tighter binding between VCA and the Arp2/3 complex.

Increased affinity is also manifest *in vivo*, as confirmed by Soyeon Kim (Padrick et al., 2008). Small amounts of Arp2/3 can be precipitated with Ni^{2+}-affinity resin from HEK293 cells co-expressing His_6-tagged FKBP-VCA and Flag-tagged mTOR-VCA, but dimerization of the VCAs with rapamycin increases the precipitated Arp2/3 by more than three-fold . This effect requires two VCAs in the rapamycin-mediated complex, as His-tagged FKBP precipitates mTOR-VCA but very little Arp2/3 under similar conditions.

Parent protein	K_D (monomer)	K_D (dimer)	Fold difference
N-WASP	1.6 +/- 0.2 μM	9 +/- 2.5 nM	180
WASP	2.6 +/- 0.7 μM	26 +/- 7 nM	100
WAVE1	4.4 +/- 1.8 μM	29 +/- 7 nM	150

Table 4.1: Dimerization increases affinity of VCA to Arp2/3

The dissociation constants for the interaction of Arp2/3 complex with VCA monomers and GST-VCA dimers from N-WASP, WASP and WAVE1. Errors shawn are 1σ confidence intervals from fitting.

4.2. Cooperativity between N-WASP and WAVE1 through heterodimerization

WASP and WAVE proteins often have distinct localization and actin regulatory functions *in vivo*. However, during some processes, including bacterial invasion of eukaryotic host cells, the two sub-families colocalize and appear to control actin assembly cooperatively (Bierne et al., 2005; Unsworth et al., 2004). Such cooperativity may result, in theory, from the formation of a heterodimeric-VCA assembly, where active N-WASP provides one VCA and an activated WRC complex provides the other VCA. The formation of this heterodimeric-VCA assembly could be driven by the binding of the N-WASP PRD to the c-terminal SH3 domain of Abi, a component of WRC. The isolated Abi protein can indeed bind and activate N-WASP through its C-terminal SH3 domain (Innocenti et al., 2005).

Once more, I set out to validate this theory using the actin assembly assay. To mimic an active N-WASP, I used a construct, N-WASP$_{BC*}$ (Fig. 4.2A), that lacks part of the GBD domain. N-WASP$_{BC*}$ is constitutively active. To mimic an activated WRC complex, I used the WAVE1–Abi2–HSPC300 heterotrimer that is also active (Fig. 2.10A). I expected to produce a high potency heterodimeric-VCA complex, as illustrated in Figure 4.2B, aggregation of the heterotrimer over time necessitated doing those experiments with freshly prepared heterotrimer in order to reduce to a minimum the aggregate concentration. Moreover, both the heterotrimer and N-WASP$_{BC*}$ are active under the typical assay conditions (50 mM KCl). In order to increase the dynamics range of the experiment to visualize any hyperactivation effect resulting from their interaction, I increased the salt concentration to 150 mM KCl. At this concentration, monomeric VCA

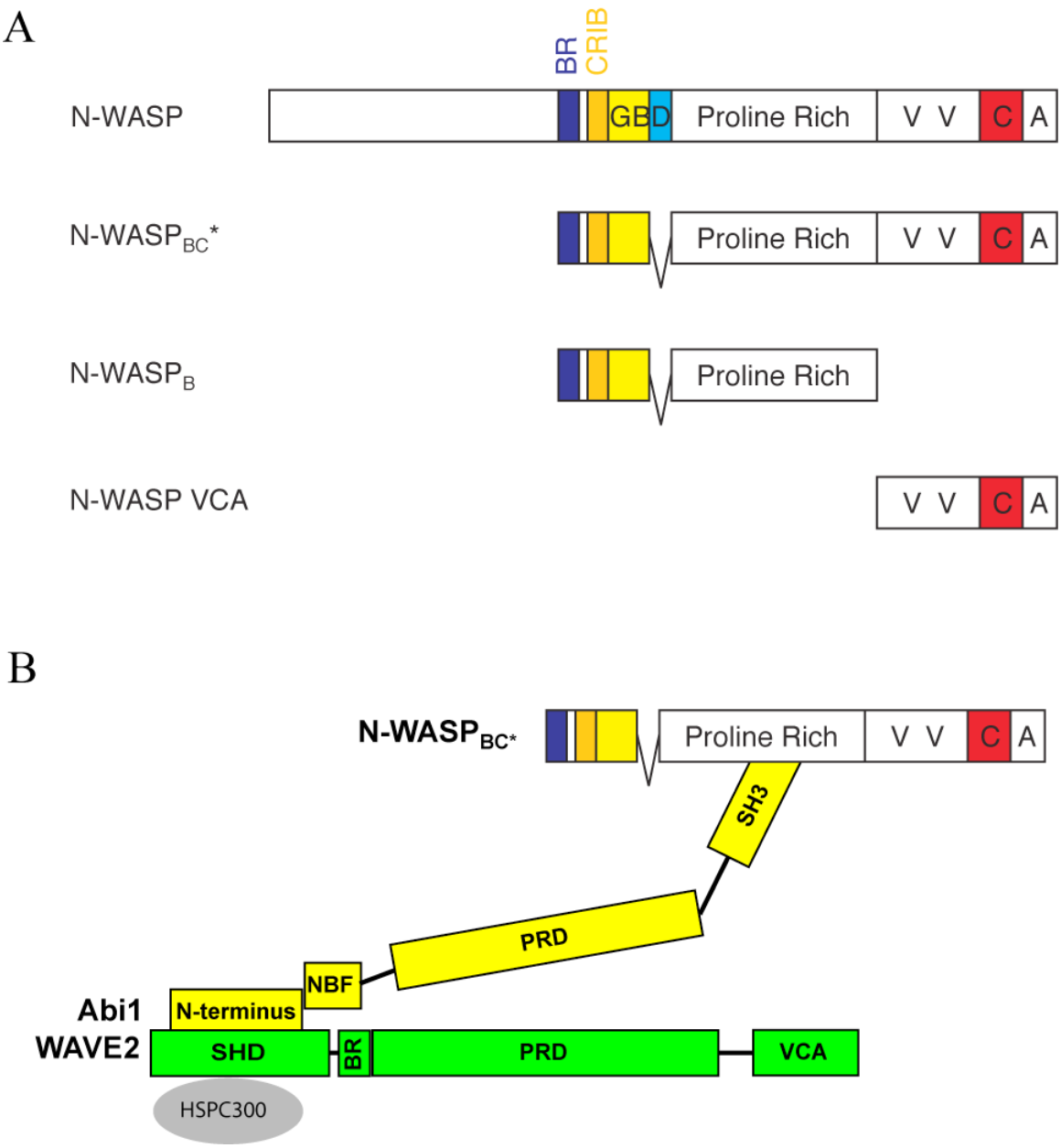

Figure 4.2: A potential Hetero-VCA dimer from WASP and WAVE

(A) Schematic presentation of the two N-WASP constructs used in the hetero-VCA dimer experiments. The yellow, light blue and red layers in N-WASP correspond to the three layers shown in the auto-inhibited structure of WASP in figure 1.2. (B) Since Abi2 SH3 domain can bind PRD in N-WASP, a complex comprising of N-WASP and WAVE1–Abi2–HSPC300 heterotrimer can form, resulting in a hetero-VCA containing complex.

has poor activity toward Arp2/3, and dimerization can still produce hyperactivation (Padrick et al., 2008).

As shown in Figure 4.3, at physiologic salt concentration (150 mM KCl), 100 nM (or 200 nM) heterotrimer and 100 nM (or 200 nM) N-WASP$_{BC}$* have only weak activity individually. However, a mixture of the two reagents is highly active, well beyond 200 nM (or 400 nM) of either alone. This hyperactivation requires binding of trimer to N-WASP$_{BC}$*, since it is not observed for mixtures of heterotrimer with N-WASP VCA or WAVE1 VCA with N-WASP$_{BC}$* (Fig. 4.4A). Hyperactivation also requires the presence of two VCAs in the complex, since it is not observed in a mixture of heterotrimer with a truncated N-WASP lacking the VCA domain (N-WASP$_{B}$) (Fig. 4.4B). Thus, formation of WAVE1:N-WASP heterodimers can produce high-potency activation. This effect may allow integration of signals between the two arms of the WASP family, contributing to the cooperativity between N-WASP and WAVE in the processes described above (Bierne et al., 2005; Unsworth et al., 2004).

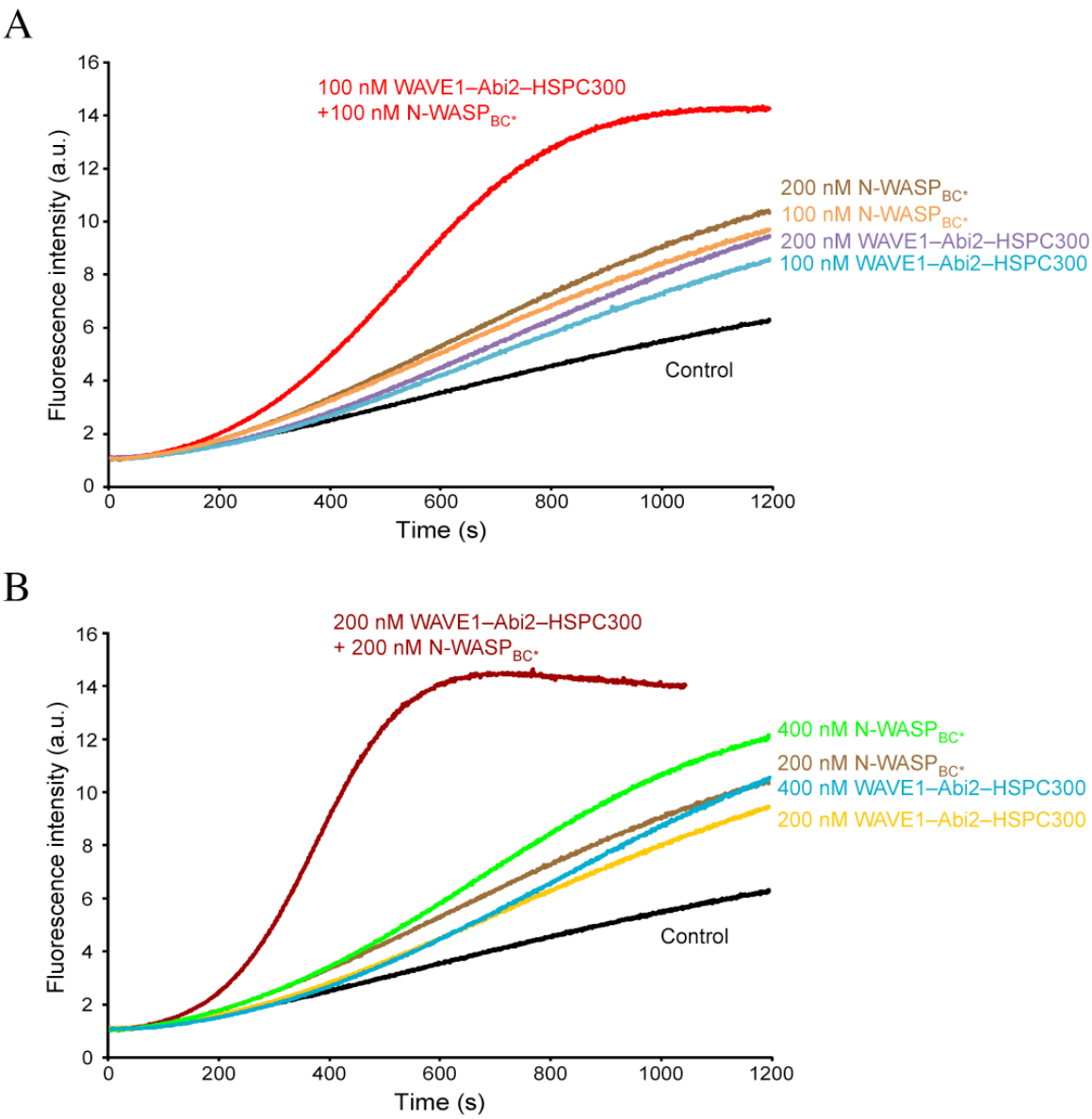

Figure 4.3: A hetero-VCA dimer is hyperactive

Actin assembly assay performed with actin (4 μM) and Arp2/3 (10 nM) alone (control), or with the indicated concentrations of WAVE1–Abi2–HSPC300 and N-WASP$_{BC*}$.

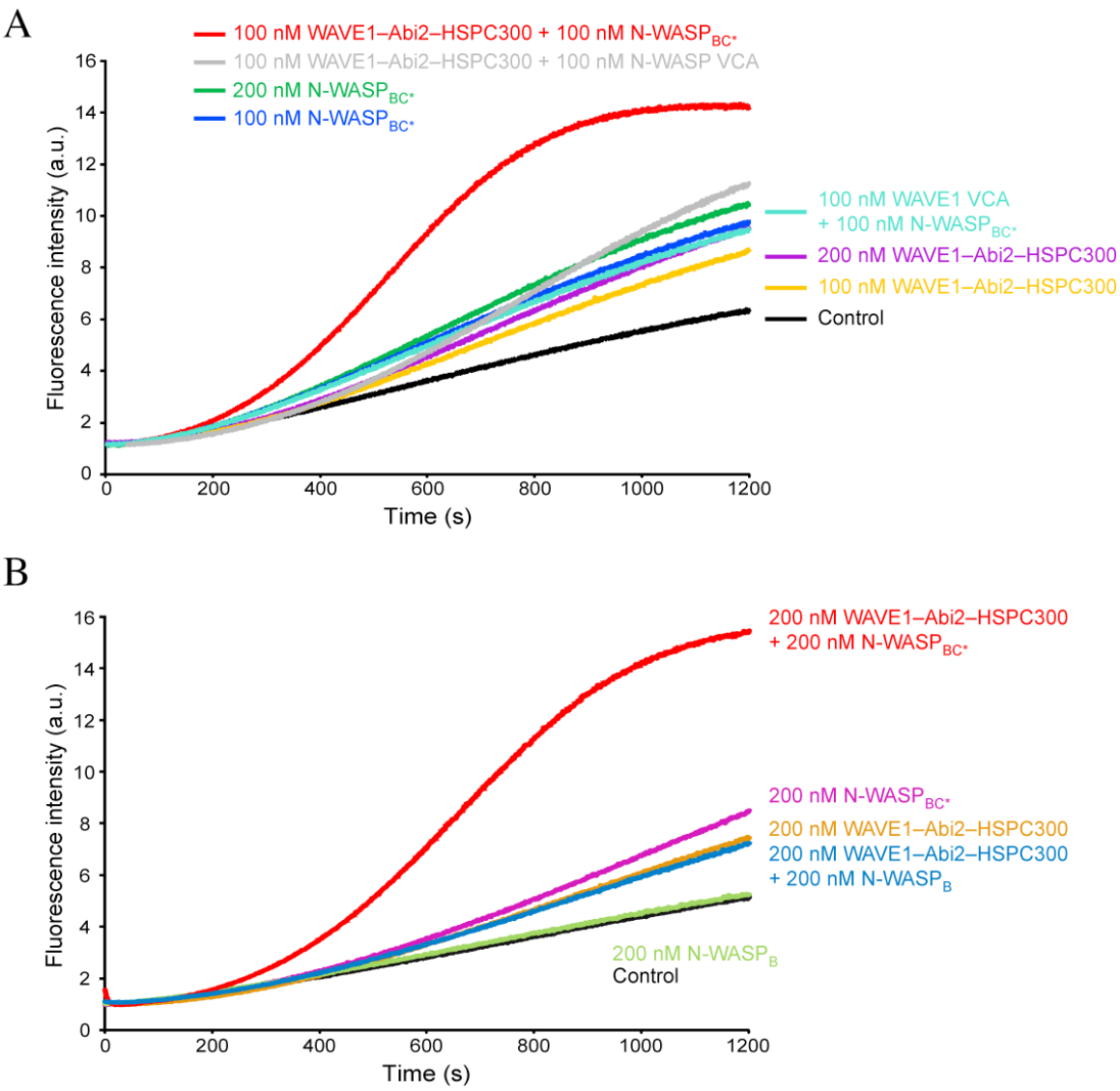

Figure 4.4: Hetero-VCA control assays

Actin assembly assay performed with actin (4 μM) and Arp2/3 (10 nM) alone (control), or with the indicated concentrations of WAVE1–Abi2–HSPC300, N-WASP$_{BC*}$, and (A) N-WASP VCA orWAVE1 VCA or (B) N-WASP$_B$.

Chapter V: Conclusion

5.1. The WAVE Regulatory Complex is inhibited

Remodeling of the actin cytoskeleton is essential for the control of cellular movement (Egea et al., 2006; Evangelista et al., 2003; Pollard and Borisy, 2003; Rafelski and Theriot, 2004). The formation of branched actin filaments depends on the activity of the Arp2/3 complex. Arp2/3 is constitutively inactive, and a number of NPFs can stimulate it to nucleate new actin filaments. The WASP family proteins activate Arp2/3 using their VCA domain (Blanchoin et al., 2000; Machesky and Insall, 1998; Machesky et al., 1999; Panchal et al., 2003). In WASP and N-WASP, the founding members of the family, VCA is regulated through an auto-inhibition mechanism, where VCA binds to GBD (Abdul-Manan et al., 1999; Kim et al., 2000) (Fig 1.2). WAVE, another family member, does not have a GBD, and its VCA is not auto-inhibited. However, WAVE is a part of a five protein complex, WRC, that includes Sra1, Nap1, Abi, WAVE and HSPC300.

The role WRC plays in regulating WAVE activity toward the Arp2/3 complex has been controversial. Two contradictory models have been proposed to explain the function of WRC (Fig. 1.3). The first model indicates that VCA is inhibited within WRC, and to activate it, the complex has to dissociate upon binding to an activator (Eden et al., 2002). The originators of this model used WRC purified from bovine brain in the seminal study that established the existence of WRC. In the second model, VCA is active within an intact WRC, and an activator simply relocalizes WRC to the appropriate intra cellular space where Arp2/3 activation is required (Innocenti et al., 2004). The

originators of this model reconstituted the WRC from two sub-complexes purified from insect cells and mammalian cells and from HSPC300 purified from bacteria.

The main focus of this dissertation was to resolve the contradiction between the two models and to gain insight into the regulatory role of WRC. When I began my work, there were at least two possible sources for the difference between the models. The "inactive WRC" was purified from bovine brain and characterized as containing five components. It was possible that the purification from bovine brain had changed the complex, altering its activity. It was also possible that there is an additional factor necessary for inhibition that remained unidentified in the initial characterization of the purified complex. In that case, the reconstitution work which led to the "active WRC" would have missed such an unknown component. Alternatively, the reconstitution of the "active WRC" may be at fault. Even if all components required for the inhibition of WAVE are purified, mixing them may not necessarily result in the regeneration of the native complex. A folding step, or a crucial assembly step may need some conditions not met by the reconstitution protocol in use.

To examine those possibilities, I reconstituted different versions of WRC. The major problem I faced initially was the inability to express Sra and WAVE in bacteria or insect cell expression systems. That problem stymied much of the biochemical and all structural aspects of research on WRC. I solved this problem by engineering a new set of vectors for baculovirus based expression in insect cells. The new vectors have the L21 sequence, a promoter sequence for the lobster tropomyosin that was reported to enhance expression in insect cells (Sano et al., 2002). The use of L21 based vectors allowed me to express all the proteins constituting WRC in reasonable yield (Fig. 2.1).

I was able to generate WRC by co-infection of Sf9 cultures with the five baculoviruses expressing Sra1, Nap1, WAVE1, Abi2 and HSPC300. I optimized the purification of WRC at several steps. The complex is not stable in buffers containing less than 10% glycerol. Contamination from unincorporated WAVE1 and Abi2 requires precise precautions in ion exchange chromatography (Fig. 2.3, 2.4). The end product is a pure WRC, with a stoichiometry of 1 of each component (Fig. 2.5).

I also generated a number of truncated complexes. Some have a GGS linker that includes a PreScission protease cleavage site to replace WAVE1 PRD. Others also contain a deletion of the Abi2 PRD and SH3 domain. I also made a drosophila complex in which the dWAVE PRD is replaced by the GGS-PreScission site sequence (Fig. 2.7). Moreover, from bacterial cultures, I could generate the N-termini of WAVE and Abi and full length HSPC300. I generated from those constructs a trimeric assembly that binds the Sra–nap1 heterodimer to produce a truncated complex missing VCA.

All of these pentamers are inactive toward Arp2/3 complex in the standard actin assembly assay (Fig. 2.9, 2.11, 2.12. 2.13). These include full length WRC, the truncated complexes and the Drosophila complex. The heterotrimer sub-complex is active, but the heterodimer inhibits its activity (Fig. 2.10). My combined data suggests that WRC is inhibited, and that the core inhibitory function is partially, if not fully, contained in the heterodimer. Digestion of the truncated complexes with PreScission protease activates them (Fig. 2.11, 2.12). That demonstrates that inactivity in WRC is caused by a *bona fide* inhibition, rather than an artifactual proteolysis of the C-terminus of VCA (which would deactivate it). The PreScission experiments also demonstrate that the inhibition requires a physical link between VCA and the rest of the complex, probably to enhance

the poor affinity of VCA to the inhibitory element. This idea is reinforced by the fact that Sra1–Nap1 do not efficiently inhibit free VCA, but inhibits VCA when the latter is part of the WAVE1–Abi2–HSPC300 heterotrimer (Fig. 2.10).

I was able to reconstitute an inhibited WRC from just five proteins and without the addition of any extra factor. I was able to recapitulate WRC function using two sub-complexes with the same total of five proteins. I have also observed the inhibition in a number of truncated human complexes and in the Drosophila complex. I believe all these data point to the fact that WRC is an inhibited heteropentameric complex.

Can I explain why the other reported reconstitution of WRC resulted in the non-dissociation model (Innocenti et al., 2004)? My experience in purifying WRC, as well as several components as individual proteins, helped me uncover a number of properties that can provide an explanation. For example, HSPC300 purifies as a trimer, while WRC contains only one copy of it. HSPC300 forms a heterotrimer with the N-termini of WAVE and Abi, themselves aggregates when purified individually. However, simply mixing the three purified proteins is not enough to create a well-behaved (and thus likely properly assembled) heterotrimer. A detergent must be present in solution to allow the heterotrimer formation, and the association reaction must be allowed to proceed for several days (Shae Padrick, unpublished observations). Most likely, the formation of the heterotrimer involves unfolding of each protein oligomer/aggregate first, and then refolding into the trimer. Innocenti *et.al* mixed purified HSPC300 with a Pir121–Nap1–WAVE2–Abi1 tetramer. I suspect that HSPC300 did not integrate into the complex.

Moreover, Innocenti *et.al* generated WRC by mixing a Pir121–Nap1 sub-complex with a GST-WAVE2–Abi1 sub-complex on glutathione sepharose (and optionally adding

HSPC300), incubating and washing away unbound materials before elution. This method would reject unbound Pir121–Nap1 subcomplex but retain uncomplexed GST-WAVE2–Abi1 material. I have found that various WAVE-containing sub-complexes of the pentamer have very high activity that increases over time due to aggregation. Indeed, I only obtained stable, reproducible activity of our WRC preparations when such sub-complexes were rigorously removed during purification. In addition, GST driven dimerization of WAVE2 should hyperactivate it toward Arp2/3, as I (and my colleagues) have established in the second part of this dissertation. These biochemical properties, plus the constitutive dimerization of GST, suggest that the high activity reported for the previous reconstitution of WRC resulted from contamination of WRC with aggregated, hyperactive sub-complexes, and was wrongly perceived to be the activity of WRC itself.

Another group had also reported purifying an active WRC from rat brain (Kim et al., 2006). Again, I can attribute the activity here to problems in purification and handling of the complex. From the methods section of their paper, that group appears to have frozen their WRC after purification, and then used the frozen stock for all their assays. They also did not appear to use glycerol in their purification or freezing buffers. In my hands, freezing WRC in the absence of glycerol leads to instability and activation of the complex, while freezing in the presence of glycerol conserves the inhibited state of WRC (Fig. 5.1). Therefore, the biochemical data generated by Kim *et.al.* was obtained using faulty material, and is not reliable.

Another point of controversy is the role Rac1 plays in regulating WRC. I observed WRC activation by Rac1, although I had to use relatively high concentrations of the GTPase (Fig. 3.1). As explained earlier, Innocenti *et.al.* probably obtained high

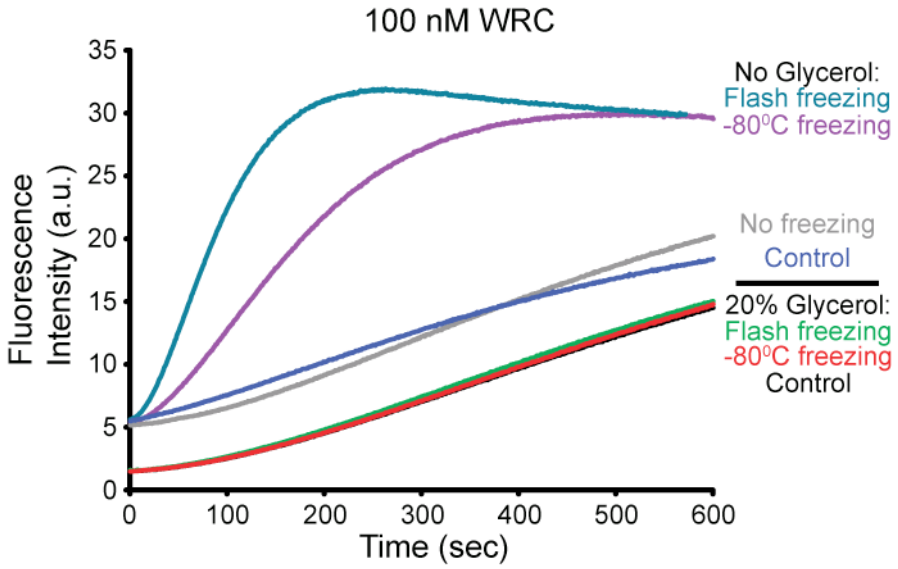

Figure 5.1: Freezing without glycerol activates WRC

Actin assembly assay performed with actin (4 μM) and Arp2/3 (10 nM) alone (control), or in the presence of 100 nM WRC frozen under the listed conditions. Flash freezing is freezing in liquid nitrogen.

levels of activity in their WRC preparation because they had aggregated active contaminants. In their case, it is not possible to distinguish the activity of the contaminants from the activity of Rac1-activated WRC. Thus, it was wrongly concluded that Rac1 does not stimulate further activity of WRC. On the other hand, Eden *et.al.* were able to activate WRC with Rac1, which is consistent with my observation.

I was able to pull-down all five proteins in a truncated WRC complex with immobilized Rac1 without dissociating the complex (Fig. 3.2). I cannot currently explain the reported WRC dissociation upon Rac1 activation (Eden et al., 2002), but note that Rac may bind sub-complexes lacking WAVE with higher affinity than intact WRC, since there would be less resistance to allosteric change in the former.

In my preliminary study on the effect of VCA phosphorylation, I found that VCA purified from insect cells is phosphorylated on three serine residues in the A segment. This phosphorylation increases moderately the activity of VCA toward Arp2/3 complex. More work is needed to fully understand the importance of the different WRC phosphorylations discovered *in vivo* so far.

There are strong mechanistic parallels between the regulation of WASP and WAVE (Fig. 5.2). In WASP, the VCA is inhibited by intramolecular contacts to the GTPase binding domain (GBD). WASP is activated by Cdc42 binding to the GBD, causing release of the VCA (which remains tethered to the GBD). In the WRC, the VCA is inhibited by an intra-complex interaction, perhaps to Sra1 and/or Nap1, since the pentamer is inactive but the WAVE1–Abi2–HSPC300 trimer is active(Padrick et al., 2008). The WRC is activated by Rac1 binding to Sra1, which may release the VCA, but does not cause

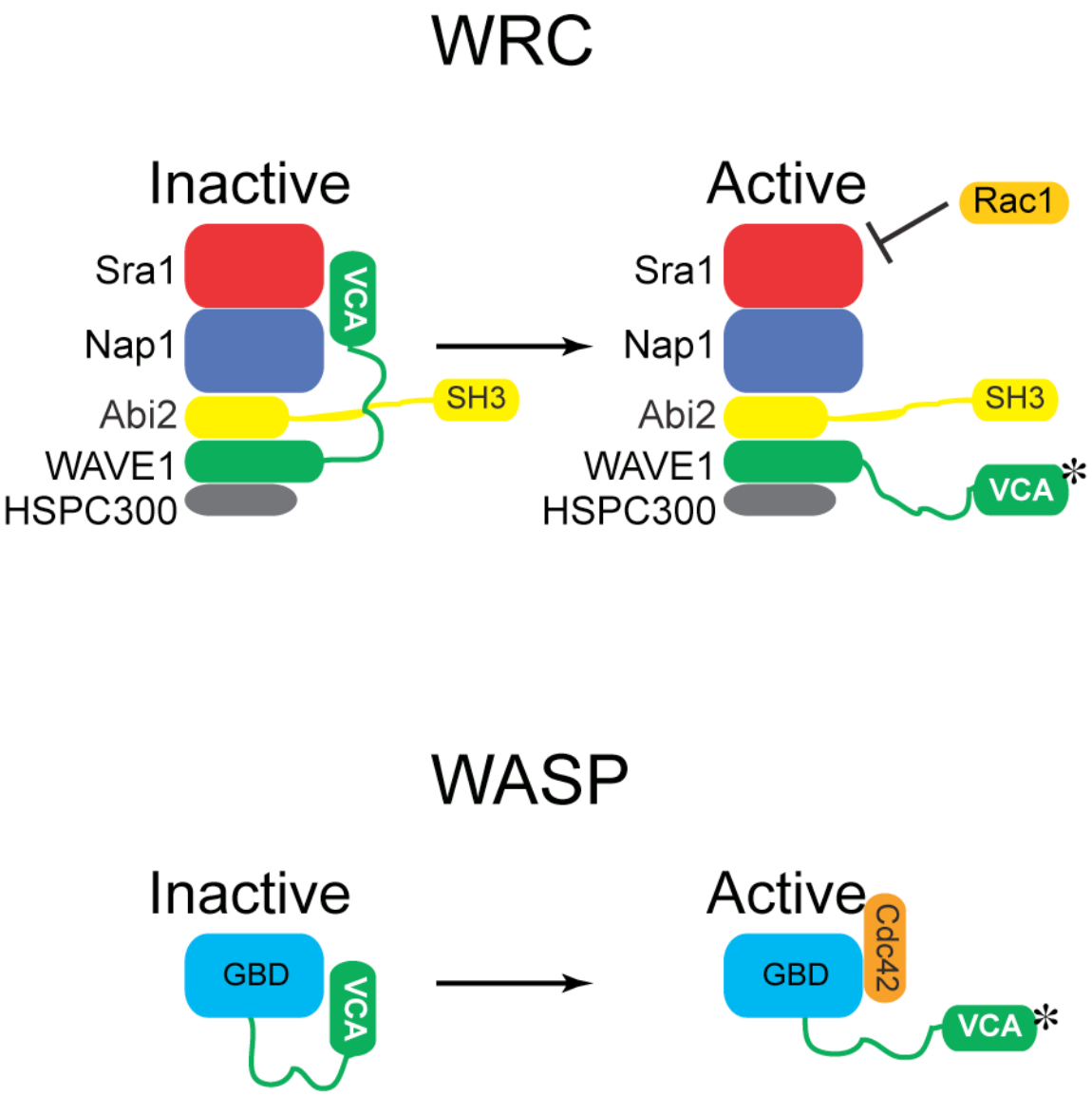

Figure 5.2: Analogous regulatory models for WASP and WAVE

Cartoon presentation of the parallel between the regulatory models for WASP and WAVE. WASP VCA is inhibited by an intra-molecular interaction. WAVE VCA is inhibited by an inter-complex interaction. The Rho GTPase Cdc42 binds the inhibitory element of WASP, GBD, releasing VCA. The Rho GTPase Rac1 binds the inhibitory element of WAVE, Sra1–Nap1, releasing VCA.

dissociation of the complex. Thus, WASP and WAVE proteins are regulated by the same principles, achieved through different molecular details. It remains to be seen whether other WASP family members such as WHAMM, WASH and Bee1 are regulated by analogous or distinct mechanisms.

5.2. Hierarchical regulation of WASP family proteins

The allosteric activation of auto-inhibited WASP has long been the prevalent model for WASP activation. This model has been extensively characterized for the activator Cdc42 (Abdul-Manan et al., 1999; Kim et al., 2000), and extended by default to most WASP activators without strong data supporting such extension. We have discovered that an already fully active WASP, or VCA, can be hyperactivated if it is dimerized (Padrick et al., 2008), indicating the existence of a mechanism distinct from allosteric relief of auto-inhibition. This dimerization, or oligomerization in general, does occur naturally in cells because the largest group of WASP activators has an SH3 domain and possesses the potential for multivalency, i.e. they either contain more than one SH3 domain or they are natural dimers.

I was able to uncover, in close collaboration with my colleagues, the mechanism of WASP hyperactivation. We found that when VCA is dimerized, both VCAs in the same dimer bind to one Arp2/3 complex (Fig. 4.1). One VCA binds the canonical site on Arp2/3, the other VCA binds the cortactin binding site on the complex (cortactin is another activator of Arp2/3, unrelated to WASP) (Padrick et al., 2008). This results in a high affinity interaction between Arp2/3 and dimeric VCA, at least 100 fold stronger than the interaction between Arp2/3 and monomeric VCA (Table 4.1). The increase in

affinity is sufficient to explain the increased actin assembly activity of the dimeric VCA, because saturating concentrations of dimeric and monomeric VCA display identical kinetics of actin assembly and produce identical concentration of filament barbed ends (Padrick et al., 2008).

I have also found that WRC may interact with WASP through the binding of the Abi SH3 domain to the PRD of WASP. Although Abi is not multivalent, WRC obviously has a VCA in WAVE. This interaction can still generate a dimer of VCAs, but it is a heterodimer: one VCA from WASP, the other from WAVE. Such heterodimers produce high-potency activation only when both VCAs are present (Fig. 4.3, 4.4). The signaling networks converging on WASP and WRC can thus reinforce each other through WASP and WAVE cooperativity.

These findings lead to a new, hierarchical model for regulation of WASP/WAVE proteins (Fig. 5.3). In this model, WASP activity is controlled by two mechanistically distinct processes. An inner layer of allostery controls accessibility of the VCA. In WASP, this occurs through auto-inhibitory GBD-VCA interactions. In WAVE, this occurs through inter-subunit interactions in the WRC. For both WASP and WAVE, exposure of the VCA (through presently unknown mechanisms for the latter) produces a monomeric species with micromolar affinity for Arp2/3 complex. In both cases this allosteric layer lies under a second layer of regulation, in which dimerization greatly increases affinity for Arp2/3 complex. Thus, when WASP protein concentrations are low, dimerization can potently enhance activity towards Arp2/3 complex. Dimerization can occur through assembly by multi-valent protein ligands and/or recruitment to high

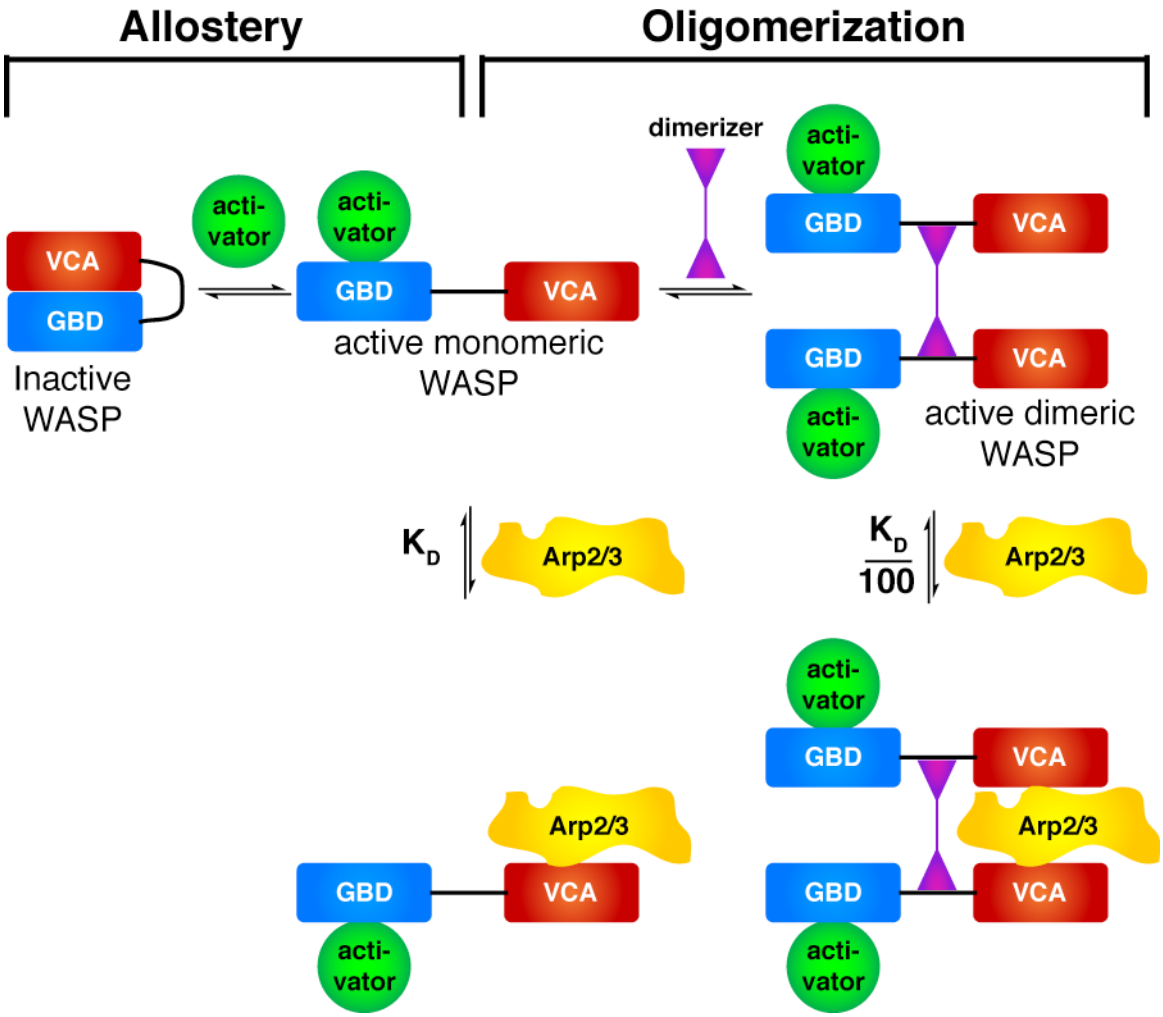

Figure 5.3: A hierarchical model for WASP/WAVE regulation

Cartoon presentation of the two layers of control for WASP family proteins. A first layer of control acts through the allosteric relief of auto-inhibition. This yields active VCA with micromolar affinity to Arp2/3. A second layer of control acts through dimerization of active VCA. That results in a 2:1 complex of VCA and Arp2/3 with nanomolar affinity.

density at membranes. The system is genuinely hierarchical, since dimerization of completely auto-inhibited WASP will not enable Arp2/3 stimulation. For example, the dimeric SH3-containing N-WASP ligand, Toca-1, cannot activate the strongly inhibited N-WASP:WIP complex, except when Cdc42 partially relieves auto-inhibition (Ho et al., 2004). The second layer of regulation provided by dimerization will increase the inherent complexity afforded by the WASP allosteric switch, and introduces a new complexity in signaling networks cooperativity through WASP/WAVE hetero-dimerization.

5.3 Concluding remarks

In this work, I tried to reconcile two opposing models on the function of WRC. I have generated a strong set of evidence that WRC is inhibited. I have discovered a number of biochemical characteristics of the proteins that constitute WRC, which provided reasonable alternative explanations for the apparent WRC activity in some reports in the literature. In order to reach these conclusions, I generated a range of protein and complex reagents. These reagents will be very useful in the biochemical and structural characterization of WRC. So far, almost all the work on WRC proteins has been performed in cells. The only biochemical purifications of the complex (in three published papers) lead to the two contradictory models. The limitation in expression and yield stymied further biochemical studies, that is until I succeeded in overcoming those hurdles.

The data available from all the cell biological studies raise lots of interesting question. It is obvious that phosphorylation of Abi and WAVE plays an important role in modulating WRC activity. As different kinases can modify WRC, we need to know if

some of them enhance activity while others repress it. How do multiple phosphorylations modify WRC behavior? Are there specific WRC ligands required as precursors for phosphorylation, or, for that matter, do any of the phosphorylations create new binding sites for new SH2 domain containing ligands?

A very important question relates to WRC activators. The complex is about 400 kDa, while its only known activator, Rac1, is about 23 kDa. That leaves a lot of interaction surfaces on the complex. Are there other activators as yet undiscovered? Does WRC interact with proteins that function outside of the actin cytoskeleton network in the cell? FMRP has been reported to bind Sra, and the significance of this interaction is still open for speculation. As FMRP controls translation, does its interaction with Sra, and subsequently with WRC, affect the function of any of the two proteins? If that is the case, what would be the consequences of this interaction on two seemingly independent systems in the cell, the actin cytoskeleton and the translation machinery?

Elucidating the role of the different interactions between WRC components and other proteins like IRSp53, Sos1, Eps8, PI3K is also important. The availability of the reagents I developed in this work should help advance the understanding of a lot of this biochemical questions. In addition, an important aspect of WRC regulation can now be tackled, that is, what are the intra-complex interactions that deactivate VCA within WRC. Structural studies, both X-ray crystallography and electron microscopy, are already underway in the Rosen Lab. We hope that we will soon be able to provide more answers surrounding the function of WRC. But the most basic question about WRC, whether it is inhibited or not, is now answered. Explaining the meaning of any work on WRC has to be undertaken in relation to WRC basic status. Now we can do that. With the

publication of this work, a review will probably be published soon, revising the entire database available on WRC in light of its confirmed inhibition status.

Materials and Methods

1. Cloning

All WRC components except human NAP1 and HSPC300 were cloned into pAV5 vectors (N-terminal TEV cleavable His_6 tag, Appendix I). Human NAP1 was cloned into pFASTBacHtC vector (N-terminal TEV cleavable His_6 tag, Appendix I), and HSPC300 was cloned into pAV3 vector (N-terminal TEV cleavable GST tag, Appendix I). The constructs were used to generate baculoviruses used in Sf9 insect cells infections using the Bac-to-Bac system. In addition, WAVE1-PreS (WAVE1 with residues 209-483 replaced by $(GGS)_3$-PreScision protease recognition site-$(GGS)_3$, Abi2 (residues 1-158) and HSPC300 were cloned into a modified pMal-c2 vector (NEB, Tev protease recognition site added after MBP sequence) for expression in *E. coli.*

2. Baculovirus production:

For a detailed step-by step protocol for the generation of bacmids and baculoviruses in Sf9 cells, see appendix III

3. Protein purification

Sf9 cells were co-infected with approximately equal amounts of the viruses expressing the different components for WRC or the desired truncated WRC complex or sub-complex. Cells were harvested 60 hours post infection, resuspended in lysis buffer (LyB: 25 mM Tris pH 8.5, 20 mM imidazole pH 8, 150 mM NaCl, 20% glycerol (w/v), 5 mM βME, protease inhibitors mix) and lysed using one freeze/thaw cycle. All subsequent handling was performed at 4°C.

WRC lysate was cleared by centrifugation (48,000 *g* for 45 min). WRC was adsorbed to NiNTA-agarose (Qiagen, six ml per liter of culture) in batch mode with nutation for 45 min in LyB. Tubes were completely filled with buffer to avoid excess aeration. Beads were washed in column mode three times with three column volumes (CV) of LyB, followed by three times with three CV of NiNTA wash buffer (NiWB: 25 mM Tris pH 8.5, 40 mM imidazole pH 8, 150 mM NaCl, 20% glycerol (w/v), 5 mM βME) and eluted with three times one CV of NiNTA elution buffer (NiEB: 25 mM Tris pH 8.5, 400 mM imidazole pH 8, 150 mM NaCl, 20% glycerol (w/v), 5 mM βME). Combined eluate was adsorbed to glutathione sepharose 4B resin (GE healthcare, three ml per liter of culture) in batch mode with nutation for 30 min in NiEB. Beads were washed in column mode four times with four CV of GS4B wash buffer (GSTWB: 25 mM Tris pH 8.5, 100 mM NaCl, 20% glycerol (w/v), 5 mM βME) and eluted with three times one CV GS4B elution buffer (GSTEB: 100 mM Tris pH 8.5, 100 mM NaCl, 20% glycerol (w/v), 30 mM reduced glutathione, 5 mM βME). Tags were cleaved by overnight incubation with TEV protease without agitation. Digest was diluted with an equal volume of Q1A (25 mM Tris pH 8.5, 20% glycerol (w/v), 5 mM βME), applied to a two ml SOURCE15Q anion exchange column (GE Healthcare) and eluted using a 15 to 50% Q1B (25 mM Tris pH 8.5, 20% glycerol (w/v), 1 M NaCl, 5 mM βME) gradient developed over 35 CV. A shallow gradient at this stage was necessary to resolve WRC from Nap1/Sra1 and WAVE1/Abi2/HSPC300 subcomplexes. Pooled fractions were diluted with two volumes of S1A (20 mM HEPES pH 7, 20% glycerol (w/v), 1 mM DTT), applied to a two ml SOURCE15S cation exchange column (GE Healthcare) and eluted using a 8 to 30% S1B (20 mM HEPES pH 7, 20% glycerol (w/v), 1 M NaCl, 1 mM DTT) gradient developed

over 44 CV. It is important to load the cation exchange column at a relatively high conductivity (about 130 mM NaCl) to prevent WAVE1 containing contaminants from binding to the column, thus separating WRC from free (active) WAVE1. WRC-containing fractions were concentrated using Amicon Ultra, 10000 MWCO (Millipore) and applied to 24 ml Superose6 gel filtration column (GE Healthcare) in 10 mM imdazole pH 7, 20% glycerol (w/v), 100 mM KCl, 1 mM EGTA pH 8, 1 mM $MgCl_2$, 1 mM DTT.

WRC-PreS, MiniWRC-PreS (Sf9 source), dWRC and dWRC-PreS were purified identically to WRC, except that the cation exchange step was unnecessary and omitted.

MiniWRC-PreS (mixed source) was reconstituted from two parts. First, a Nap1/Sra1 heterodimer was coexpressed in Sf9 cells and purified by NiNTA affinity, Source15Q anion exchange and gel filtration chromatographies as above. Second, a WAVE1-PreS/Abi2(residues 1-158)/HSPC300 heterotrimer was generated from bacterially expressed material. The three materials were expressed separately as TEV cleavable MBP fusions in BL21 (DE3) $T1^R$ *E. coli*, in LB (+ 2 g per L glucose). In each case, cells were grown to an OD_{600} of 0.6-0.9 and induced with 1 mM IPTG, for 16 hours at 20˚C. Cells were harvested, resuspended in 20 mM Tris pH 8, 200 mM NaCl, 2 mM EDTA, 2 mM DTT, 1 mM PMSF and frozen. Cells were thawed in cool water and lysed using two passes of a cell disruptor (Avestin EmulsiFlex C5). Lysate was clarified by centrifugation (45,000 *g* for 45 minutes) and applied to a Amylose High Flow (N.E.B.) column in column mode. Column was washed with 2.5 CV of 20 mM Tris pH 8,

200 mM NaCl, 1 mM EDTA, 1 mM DTT, then with 4 CV of 20 mM Tris pH 8, 20 mM NaCl, 1 mM EDTA, 1 mM DTT and eluted with 2.5 CV of 20 mM Tris pH 8, 20 mM NaCl, 1 mM EDTA, 1 mM DTT and 30 mM maltose. Equal concentrations of MBP fusions were mixed with 1% NP-40 and incubated overnight at 4˚C to reconstitute a trimeric assembly. A long incubation and addition of NP-40 detergent were essential for complex formation. Complex was applied to an eight ml SOURCE15Q (equilibrated in Q2A: 20 mM Tris pH 8, 1 mM DTT) and eluted with a 0 to 50% gradient of Q2B (20 mM Tris pH 8, 1 M NaCl, 1 mM DTT) developed in 15 CV. Pooled fractions were concentrated and applied to a 320 ml Superdex200pg gel filtration column (GE Healthcare) and eluted with (20 mM Tris pH 8, 150 mM NaCl, 1 mM DTT). This purified trimer was then mixed with the Nap1/Sra1 dimer, in a 1.2:1 ratio. This mixture was incubated overnight and applied to an amylose column, washed three times with three CV of (20 mM Tris pH 8, 200 mM NaCl, 1 mM EDTA, 1 mM DTT, 20% glycerol (w/v)), then eluted two times with three CV of (20 mM Tris pH 8, 200 mM NaCl, 1 mM EDTA, 1 mM DTT, 20% glycerol (w/v), 30 mM maltose). Eluted complexes were cleaved with TEV protease at 22˚C for six hours and applied to a 320 ml Superdex200pg column in KMEI plus 20% glycerol (w/v). Complete TEV cleavage is required at this point, as cleaved trimer is resolved from MiniWRC-PreS, while uncleaved trimer is not. MBP-WAVE1(residues 1-178)/MBP-Abi2(residues 1-158)/MBP-HSPC300 trimer and its complex with Nap1/Sra1 (MBP_3-MiniWRCΔVCA) were made exactly as above.

Rac1, actin, pyrene-actin, Arp2/3 complex and N-WASP constructs were purified as previously described (Aghazadeh et al., 2000; Padrick et al., 2008).

4. Actin assembly assays

All actin polymerization assays contained 4 μM actin (5% pyrene labeled) and 10 nM Arp2/3 complex in KMEI-G buffer, and were performed as described (Padrick et al., 2008). KMEI-G contains 15% (w/v) glycerol, 50 mM KCl, 1 mM $MgCl_2$, 1 mM EGTA, and 10 mM imidazole (pH 7.0). Barbed ends were calculated as described (Leung et al., 2006), with the exception that the 15% glycerol present to stabilize the WRC materials reduces the barbed end actin on rate (k_{on}) in a diffusion limited fashion (Drenckhahn and Pollard, 1986) which can be corrected for using literature values for the viscosity of glycerol solutions (Cheng, 2008; Segur and Oberstar, 1951). The adjusted K_{on} used in the barbed ends calculation was 7.7205298 $\mu M^{-1}s^{-1}$.

To measure the effect of Sra1–Nap1 on the fluorescence level of F-actin, actin (5% pyrene labeled) was incubated overnight in KMEI-G buffer to allow it to polymerize and reach equilibrium. The heterodimer was added to 4 μM of the polymerized actin and the fluorescence of pyrene was measured for 120 seconds and averaged.

5. Multi-angle light scattering

Arp2/3 complex and GST-WASP VCA were mixed in a 1:3 ratio (i.e. 1:1.5 Arp2/3:VCA dimer). The mixture was injected onto a Superdex200 gel filtration column connected in line to a DAWN EOS light scattering instrument equipped with 18 angle detectors and a 690 nm laser light source and OPTILAB DSP interferometric refractometer (Wyatt Technology Corporation). Data were analyzed using ASTRA software (Wyatt Technology Corporation).

6. Affinity measurements

VCA affinities for Arp2/3 complex were determined by competition against rhodamine-labeled N-WASP VCA (rVCA) (Marchand et al., 2001), which binds Arp2/3 complex with K_D of 73 nM (see Methods in main text). In competition assays, unlabeled VCA competitor was titrated into 10 nM rVCA plus 1 μM Arp2/3 complex in KMEI buffer, and rhodamine fluorescence anisotropy (λ_{EX} = 552 nm, λ_{EM} = 574 nm) was measured. Anisotropy data were fit using equations S1-S6 solved for $r_{observed}$ (terms in equations defined below eq. S6). There are three solutions to the system of equations, only one of which will be valid for any given range of K_D, with a discontinuity occurring at $K_D = K_{D,rV}$. The binding equation was fit using the FindFit algorithm in the NonlinearRegress function of Mathematica 5.2 (Wolfram), optimizing K_D, r_{free} and r_{bound} for the best fit to the data. Errors were estimated using Monte Carlo error analysis; 1000 simulated data sets were used to estimate the 1σ confidence interval, which is the reported error.

Equation S1:
$$K_D = \frac{[Arp2/3][VCA]}{[Arp2/3:VCA]}$$

Equation S2:
$$K_{D,rV} = \frac{[Arp2/3][rVCA]}{[Arp2/3:rVCA]}$$

Equation S3:
$$[VCA]_{total} = [VCA] + [Arp2/3:VCA]$$

Equation S4:
$$[rVCA]_{total} = [rVCA] + [Arp2/3:rVCA]$$

Equation S5:
$$[Arp2/3]_{total} = [Arp2/3] + [Arp2/3:VCA] + [Arp2/3:rVCA]$$

Equation S6:
$$r_{observed} = \frac{r_{free}[rVCA] + r_{bound}[Arp2/3:rVCA]}{[rVCA]_{total}}$$

Terms are defined as follows: $r_{observed}$ is the observed anisotropy, K_D is the affinity of the VCA competitor for Arp2/3, $K_{D,rV}$ is the affinity of the rhodamine labeled WASP VCA for Arp2/3, $[VCA]_{total}$ is the total concentration of competitor VCA in solution, [VCA] is the concentration of competitor VCA not in complex, [Arp2/3:VCA] is the concentration of VCA competitor in complex with Arp2/3, $[rVCA]_{total}$ is the total concentration of all rhodamine labeled VCA in solution, [rVCA] is the concentration of rhodamine labeled VCA not in complex, [Arp2/3:rVCA] is the concentration of rhodamine labeled VCA in complex with Arp2/3, $[Arp2/3]_{total}$ is the total concentration of Arp2/3 in solution and [Arp2/3] is the concentration of Arp2/3 not associated with VCA

7. Equilibrium ultracentrifugation

Equilibrium sedimentation experiments were performed in an XL-I ultracentrifuge (Beckman-Coulter) using sapphire-windowed, six-sectored cells in an An60-Ti rotor. After 22 hours at each speed (9,000, 10,500, 15,000 rpm), an absorbance profile was recorded using absorbance at 280 nm (in KMEI buffer plus 15% glycerol (w/v) at 20˚C). Absorbance profile at 15,000 rpm was used to estimate the baseline. SEDPHAT was used to fit the data from both speeds simultaneously with baseline correction. Protein and buffer parameters were estimated using SEDNTERP (Laue et al., 1992).

8. Pull-down assays

GST-Rac1 is loaded with GDP when purified from bacteria. The protein was loaded with GMPPNP as described (Abdul-Manan et al., 1999). GST pulldown experiments were performed by mixing 400 pmol of GST-Rac1, 40 pmol of different WAVE complexes, and 15 μL glutathione sepharose 4B resin in one ml of pulldown buffer (PB: 20 mM Tris-

HCl pH 8.5, 50 mM NaCl, 2 mM $MgCl_2$, 5% glycerol (w/v) and 5 mM βME). After gentle mixing at 4˚C for 60 min, the resin was sedimented by gravity and washed three times with one mL of PB, followed by elution using 25 μL of PB plus 30 mM reduced glutathione. Eluted proteins were resolved by SDS-PAGE and visualized with Coomassie blue.

9. NMR acquisition

NMR data were collected on Varian Innova spectrometer operating at 800-MHz ^{1}H frequency. All experiments were carried out at 25°C., $^{1}H/^{15}N$ HSQC spectra were acquired on 50 μM ^{15}N labeled WAVE1 VCA in 10 mM HEPES pH 7.5,100 mM KCl, 1 mM $MgCl_2$, 1 mM EGTA, 1 mM DTT and 20% (w/v) deuterated glycerol either alone or in the presence of 7.5 μM of Sra1–Nap1, MiniWRCΔVCA or MiniWRC-PreS.

Appendix I

pAV3a

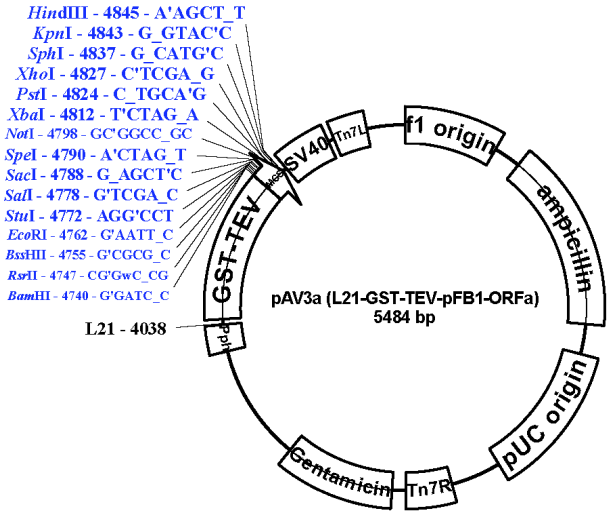


```
                                                          BamHI  RsrII
4701 CATCCTCCAA AATCGGATGA AAACCTGTAT TTTCAGGGCG GATCCCGGTC
     H  P  P  K   S  D  E   N  L  Y   F  Q  G  G   S  R  S
                          TEV cleavage site

        BssHII  EcoRI   StuI     SalI   SacI  SpeI    NotI
4751 CGAAGCGCGC GGAATTCAAA GGCCTACGTC GACGAGCTCA CTAGTCGCGG
      E  A  R   G  I  Q  R   P  T  S   T  S  S   L  V  A  A

               XbaI    PstI    XhoI   SphI  KpnI   HindIII
4801 CCGCTTTCGA ATCTAGAGCC TGCAGTCTCG AGGCATGCGG TACCAAGCTT
       A  F  E   S  R  A   C  S  L  E   A  C  G   T  K  L

4851 GTCGAGAAGT ACTAGAGGAT CATAATCAGC CATACCACAT TTGTAGAGGT
     V  E  K  Y   *
```

In frame restriction enzymes sites: BamHI-BssHII- StuI- NspV- XbaI- XhoI- SphI-KpnI-HindIII

Made by: Ayman Ismail
Constructed from: pFastBac1 (Invitrogen)

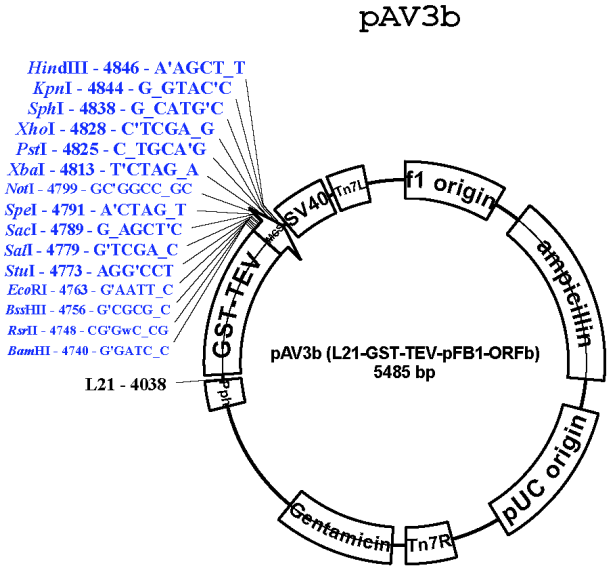


```
                                                          BamHI   RsrII
4701 CATCCTCCAA AATCGGATGA AAACCTGTAT TTTCAGGGCG GATCCACGGT
     H  P  P  K   S  D  E   N  L  Y   F  Q  G  G   S  T  V
                           TEV cleavage site

         BssHII  EcoRI    StuI    SalI   SacI   SpeI   NotI
4751 CCGAAGCGCG CGGAATTCAA AGGCCTACGT CGACGAGCTC ACTAGTCGCG
      R  S  A   R  N  S  K   A  Y  V   D  E  L   T  S  R  G

                  XbaI     PstI   XhoI   SphI  KpnI   HindIII
4801 GCCGCTTTCG AATCTAGAGC CTGCAGTCTC GAGGCATGCG GTACCAAGCT
       R  F  R   I  *
```

In frame restriction enzymes sites: SalI- SacI- SpeI- NotI-PstI

Note1: PstI site is in frame but after a termination sequence, so it can't be used in this vector at the 5' end of your insert. If you need to use it, you'll have to use pAV3a and adjust your 5' primer to accommodate for the frame shift.

Made by: Ayman Ismail
Constructed from: pFastBac1 (Invitrogen)

pAV3c

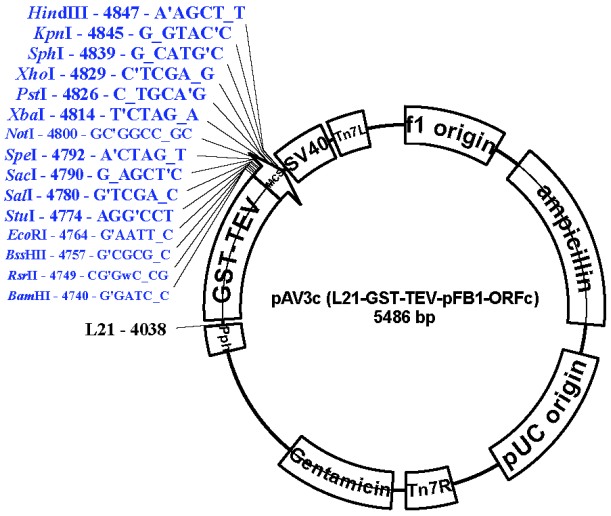


```
                                                        BamHI     RsrII
4701 CATCCTCCAA AATCGGATGA AAACCTGTAT TTTCAGGGCG GATCCACCGG
     H  P  P  K   S  D  E   N  L  Y   F  Q  G  G   S  T  G
                         TEV cleavage site

          BssHII  EcoRI    StuI    SalI   SacI   SpeI   NotI
4751 TCCGAAGCGC GCGGAATTCA AAGGCCTACG TCGACGAGCT CACTAGTCGC
      P  K  R   A  E  F  K   G  L  R   R  R  A   H  *

                  XbaI     PstI   XhoI   SphI   KpnI  HindIII
4801 GGCCGCTTTC GAATCTAGAG CCTGCAGTCT CGAGGCATGC GGTACCAAGC

4851 TTGTCGAGAA GTACTAGAGG ATCATAATCA GCCATACCAC ATTTGTAGAG
```

In frame restriction enzymes sites: RsrII- EcoRI

Made by: Ayman Ismail
Constructed from: pFastBac1 (Invitrogen)

pAV5a

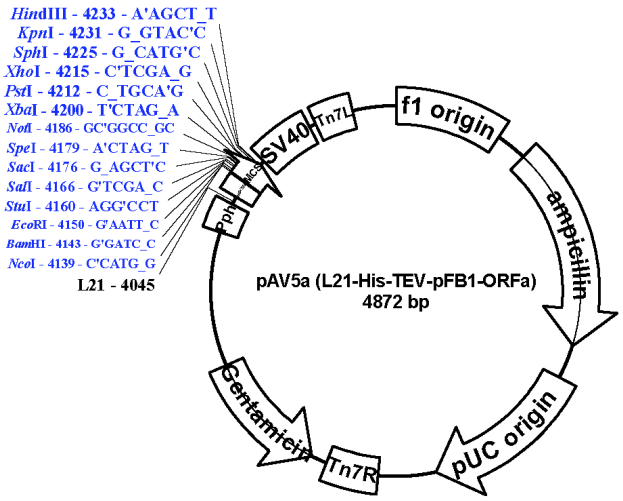


```
4051 TAAAAAACCG CCACCATGTC GTACTACCAT CACCATCACC ATCACGATTA
                    M  S    Y  Y  H    H  H  H  H    H  D  Y
                                      6xHIS tag

                                                 NcoI BamHI  EcoRI
4101 CGATATCCCA ACGACCGAAA ACCTGTATTT TCAGGGCGCC ATGGATCCGG
      D  I  P   T  T  E  N   L  Y  F   Q  G  A   M  D  P  E
                     TEV Cleavage Site

           StuI     SalI   SacI   SpeI   NotI           XbaI
4151 AATTCAAAGG CCTACGTCGA CGAGCTCAAC TAGTGCGGCC GCTTTCGAAT
       F  K  G   L  R  R   R  A  Q  L   V  R  P   L  S  N

           PstI    XhoI   SphI  KpnI   HindIII
4201 CTAGAGCCTG CAGTCTCGAG GCATGCGGTA CCAAGCTTGT CGAGAAGTAC
     L  E  P  A   V  S  R   H  A  V   P  S  L  S   R  S  T

4251 TAGAGGATCA TAATCAGCCA TACCACATTT GTAGAGGTTT TACTTGCTTT
      R  G  S   *
```

In-frame restriction enzymes sites: EcoRI

Note1: NcoI is not in frame with any pAV5 vector, but it's ATG is in frame with all pAV5 vectors. If your gene starts with ATGG, just add CC to your 5'end and your NcoI site is ready. If your gene doesn't start with ATGG, you need to add GG to 5'end after the NcoI site to make your gene in frame

Made by: Ayman Ismail
Constructed from: pFBHTa (Invitrogen)

pAV5b

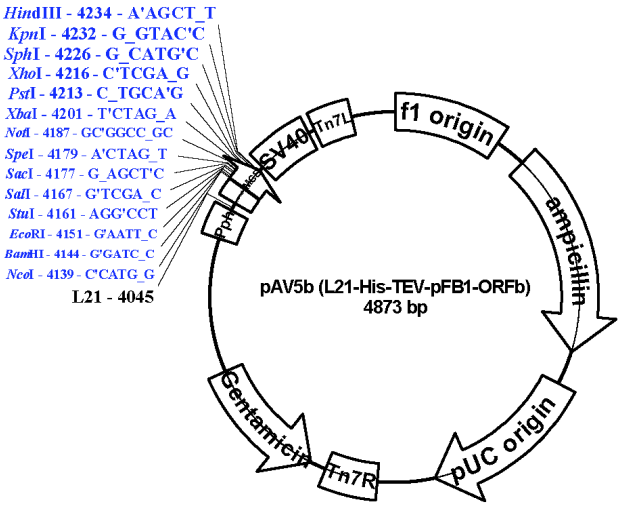


```
4051 TAAAAAACCG CCACCATGTC GTACTACCAT CACCATCACC ATCACGATTA
                    M  S    Y  Y  H    H  H  H  H    H  D  Y
                                      6xHIS tag

                                                  NcoI  BamHI
4101 CGATATCCCA ACGACCGAAA ACCTGTATTT TCAGGGCGCC ATGGGATCCG
      D  I  P    T  T  E  N    L  Y  F    Q  G  A    M  G  S  G
                     TEV Cleavage Site

     EcoRI    StuI      SalI    SacI  SpeI    NotI
4151 GAATTCAAAG GCCTACGTCG ACGAGCTCAC TAGTCGCGGC CGCTTTCGAA
       I  Q  R    P  T  S    T  S  S  L    V  A  A    A  F  E

     XbaI     PstI     XhoI    SphI  KpnI    HindIII
4201 TCTAGAGCCT GCAGTCTCGA GGCATGCGGT ACCAAGCTTG TCGAGAAGTA
     S  R  A  C    S  L  E    A  C  G    T  K  L  V    E  K  Y

4251 CTAGAGGATC ATAATCAGCC ATACCACATT TGTAGAGGTT TTACTTGCTT
      *
```

In-frame restriction enzymes sites: BamHI – StuI – XbaI – XhoI- SphI – KpnI – HindIII

Note1: NcoI is not in frame with any pAV5 vector, but it's ATG is in frame with all pAV5 vectors. If your gene starts with ATGG, just add CC to your 5'end and your NcoI site is ready. If your gene doesn't start with ATGG, you need to add GG to 5'end after the NcoI site to make your gene in frame

Made by: Ayman Ismail
Constructed from: pFBHTb (Invitrogen)

pAV5c

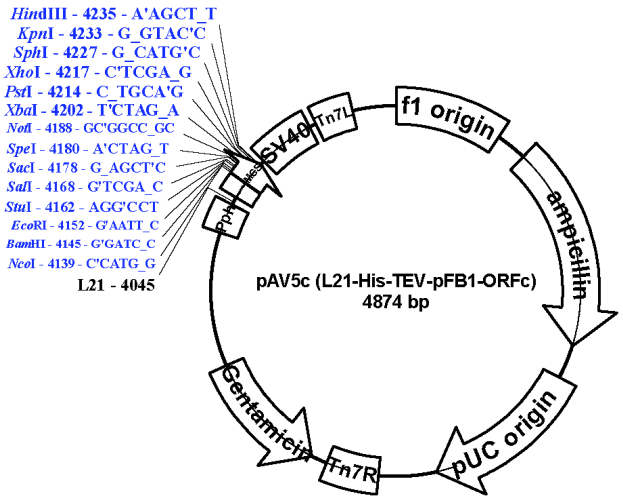


```
4051 TAAAAAACCG CCACCATGTC GTACTACCAT CACCATCACC ATCACGATTA
                    M  S    Y  Y  H    H  H  H  H    H  D  Y
                                      6xHIS tag

                                                  NcoI    BamHI
4101 CGATATCCCA ACGACCGAAA ACCTGTATTT TCAGGGCGCC ATGGGGATCC
      D  I  P    T  T  E  N    L  Y  F    Q  G  A    M  G  I  R
                       TEV Cleavage Site ↑

      EcoRI    StuI      SalI    SacI  SpeI    NotI
4151 GGAATTCAAA GGCCTACGTC GACGAGCTCA CTAGTCGCGG CCGCTTTCGA
       N  S  K    A  Y  V    D  E  L  T    S  R  G    R  F  R

      XbaI     PstI     XhoI    SphI  KpnI    HindIII
4201 ATCTAGAGCC TGCAGTCTCG AGGCATGCGG TACCAAGCTT GTCGAGAAGT
     I  *
```

In-frame restriction enzymes sites: SalI – SacI- SpeI – NotI

Note1: **NcoI is not in frame with any pAV5 vector, but it's ATG is in frame with all pAV5 vectors. If your gene starts with ATGG, just add CC to your 5'end and your NcoI site is ready. If your gene doesn't start with ATGG, you need to add GG to 5'end after the NcoI site to make your gene in frame**

Note2: **PstI site is in frame but after a termination sequence, so it can't be used in this vector at the 5' end of your insert. If you need to use it, you'll have to use pAV5a or pAV5b and adjust your 5' primer to accommodate for the frame shift.**

Made by: Ayman Ismail
Constructed from: pFBHTc (Invitrogen)

Appendix II

All HSQC spectra were acquire on a Varian 800 MHz magnet, equipped with a cold-probe. To acquire HSQC spectra, I used the gNhsqc pulse sequence from the Varian Biopack suite, modified with the following parameters:

Acquisition H1:

sfrq = 800.458
at = 0.109
np = 2048
sw = 9429.5
ss = 16
tpwr = 56
tpwrsf_t = 2460
pwHs = 1062.0
compH = 1.06
pw = calibrated for each sample
dl = 1.500
tof = calibrated for each sample
nt = 120 or 300
ct = 120 or 300
gain = calibrated for each sample

HSQC options:

C13refoc = n
NHonly = y
NH2only = n
T1 = n
T1rho = n
T2 = n
TROSY = n

relaxT = 0

maxrelasT = 0

N15 RF:

Dfrq2 = 81.119

Dof 2 = 2510

pwN = 36

pwN1v1 = 59

compN = 0.99

JNH = 93.0

calN = 1.00

dpwr2 = 45

dm2 = nny

dm2 = ccg

15N dimension:

sw1 = 1216.8

ni = 80

phase = arrayed

f1180 = n

Gradients:

mag_flg = n

gstab = 0.000400

gzcal = 0.002000

gt1 = 0.00200

gzlvl1 = 13000

gt2 = 0.000200

gzlvl2 = 13200

gt3 = 0.001000

gzlvl3 = 15000

Sample:

solvent = D2O

temp = 26

Channel 2:

dfrq = 201.297

dn = C13

dpwr = 0

dof = 4619.1

dm = nnn

dmm = ccp

Channel 3:

dfrq2 = 81.119

dn2 = N15

dpwr2 = 45

dof2 = 2509.8

dm2 = nny

dmm2 = ccg

dmf2 = 5840

dseq2 = wurst40N

dres2 = 1.0

Gradients:

gzlvl1 = 13000

gzlvl2 = 13200

gt1 = 0.00200

gzlvl0 = 1000

gt0 = 0.00200

gzlvl3 = 15000

gt3 = 0.00100

gzlvl4 = 8000

gt4 = 0.00100

gzlvl5 = 2000

gt5 = 0.00050

gzlvl6 = 3000

Appendix III

I. Transformation

A) LB plate (1 liter)

LB	25g
Agar	15g
Water	up to 1L

- Autoclave @121^{o}C for 35 min with a stirring magnet rod inside the solution
- After autoclaving put on a stirring plate (medium speed, don't let air bubbles get trapped in solution)
- When solution cools down to about 50^{o}C, add following

Gentamicin	10mg/L
Kanamycin	50mg/L
Tetracycline	10mg/L

-Mix for 1 minute and poor into plates (20ml/plate)
-Let Plates cool-down to room temperature before storing them upside-down at 4^{o}C

* Before using plates, add the following and spread them on plate surface

IPTG	20µl/plate of a 1M stock solution
Bluo-gal	10µl/plate of a 200mg/ml stock solution

B) Transformation
Use DH10Bac competent cells

1. Thaw competent cells on ice and transfer 20µl to new microtube for each transformation
2. Add 1 µl of plasmid (with your insert) to the 20µl DH10Bac, mix gently and incubate on ice for 30 min
3. Heat shock in 42^{o}C water bath for 60-90 sec
4. Cool on ice for 5 min
5. Add 1ml SOC medium and mix gently and transfer to 14 ml round bottom culture tube
6. Incubate in Shaking incubator for 4 hrs at 37^{o}C
7. Spin cells down for 10 min (3500 rpm, 4^{o}C)
8. Discard SN, put leave 40 to 100µl to resuspend cells
9. Spread 10 µl of suspended cells onto 1 plate and the rest on another plate
10. Incubate plates at 37^{o}C for 48 hrs (white and blue colonies will appear on the plates

II. Bacmid preparation

It is advised to prepare 3 bacmid preps per gene of interest
-for each bacmid prep you need

14 ml round bottom culture tube	
LB medium	3ml per tube
Kanamycin	50µg/ml LB
Gentamicin	7µg/ml LB
Tetracycline	10µg/ml LB

Inoculate 1 white colony per tube and incubate in Shaking incubator for 16 hrs at 37^{o}C

The protocol to prepare the bacmid from these cultures is in two parts

Part I:
for this part we use the Promega wizard Plus SV miniprep kit to produce the cleared lysate. The protocol of the kit for this step is the following (from Promega technical bulletin TB225):

1. Harvest 1.5ml (high-copy-number plasmid) or 10ml (low-copy-number plasmid) of bacterial culture by centrifugation for 5 minutes at 10,000 x g in a tabletop centrifuge. Pour off the supernatant and blot the inverted tube on a paper towel to remove excess media. (We will harvest the 3ml culture here)

2. Add 250µl of Cell Resuspension Solution and completely resuspend the cell pellet by vortexing or pipetting. It is essential to thoroughly resuspend the cells. If they are not already in a microcentrifuge tube, transfer the resuspended cells to a sterile 1.5ml microcentrifuge tube(s).
Note: To prevent shearing of chromosomal DNA, do not vortex after Step 2. Mix only by inverting the tubes. (bacmid DNA is also huge in size and could be sheared easily, don't vortex or pipette up and down after this step)

3. Add 250µl of Cell Lysis Solution and mix by inverting the tube 4 times (do not vortex). Incubate until the cell suspension clears (approximately 1.5 minutes). Note: It is important to observe partial clearing of the lysate before proceeding to addition of the Alkaline Protease Solution (Step 4); however, do not incubate for longer than 5 minutes.

4. Add 10µl of Alkaline Protease Solution and mix by inverting the tube 4 times. Incubate for 5 minutes at room temperature.
Alkaline protease inactivates endonucleases and other proteins released during the lysis of the bacterial cells that can adversely affect the quality of the isolated DNA. Do not exceed 5 minutes incubation with Alkaline Protease Solution at Step 4, as nicking of the plasmid DNA may occur.

5. Add 350µl of Wizard® Plus SV Neutralization Solution and immediately

mix by inverting the tube 4 times (do not vortex).

6. Centrifuge the bacterial lysate at maximum speed (around 14,000 × g) in a microcentrifuge for 10 minutes at room temperature.

Stop using the promega kit at this step, do not continue with promega protocol, but rather continue with part II below

Part II:
7. Transfer SN from Part I step 6, into new microcentrifuge tube and centrifuge for another 10 min like in step6.
8. Again transfer SN to new tubes, add 0.8ml isopropanol, mix but inverting the tube (remember no vortexing no pipetting)
9. Incubate on ice 15 min
10. Centrifuge for 15 min at RT (Tabletop microcentrifuge)
11. Discard SN (by vacuum suction), add 0.5ml 70% ethanol
12. Invert tubes gently and centrifuge for 5 min at RT (Tabletop microcentrifuge)
13. Discard SN (by vacuum suction) and air dry under hood for 5-10 min
14. Add 40 µl autoclaved milliQ water and allow DNA to resuspend in water without pipetting by leaving the tube 30 min closed under the hood or by putting it 2hrs at 4^{o}C.

At this stage you can take an aliquot for use as template to verify by PCR that your bacmid prep has your insert. Invitrogen has a good description of what primers to use and what to expect in their Bac-to-Bac baculovirus expression system manual under a section called: analyzing recombinant bacmid DNA by PCR

Bacmids are not as stable as plasmids. It is better to use bacmids for transfection the same day they are prepared.

III. Transfection:

We are starting from a suspension culture, but you can start from an adherent culture.

Seed 2ml of .25 to 0.5 million/ml Sf9 cells in a well of a 6 well plate (cells cultured and seeded in Sf900 medium with antibiotic/antimicotic)
Allow cells to attach at 27C for at least 1hr
↓
Meanwhile, Prepare the following solutions in tubes (5ml round-bottom tubes) (under the hood)
Sol .A 5 µl miniprep Bacmid + 100 µl Sf900(w/o ab) (that is without antibiotic antimicotic) Mix by gentle tapping on the tube bottom to create a gentle vortex action in the tube. Use this mixing method through-out the rest of the procedure
Sol .B 6 µl Cellfectin Reagent + 100 µl Sf900(w/o ab)
(Prepare Sol. B for all transfection in advance
ex. 5 samples → (5+1) x 100 µl medium + (5+1) x 6 µl cellfectin
we usually do two controls for all transfections: 1.Cellfectin only 2.Cell only

→Mix A & B , 15-45 min R.T.
↓
Add 0.8 ml Sf900 medium(w/o ab) to each tube of the solution mix above
↓
Wash cells in 6 wells plate with 2 ml Sf900 (w/o ab)
↓
Remove wash medium and overlay the solution mix above onto the cells
Incubate 27^{o}C, 5 hrs
↓
Remove the transfection mixtures and add 2 ml Sf900(w ab)
Incubate 27^{o}C, 72-96 hrs.

At this stage you should have a 100% confluent monolayer in cells only well and transfection wells should show lots of floating cells, swollen nuclei and no 100% confluency. The supernatant of these wells will have the virus. We call this virus P1.

IV. Virus amplification and expression check

In 50 ml flask, add 10ml of 2 millions/ml Sf9 in Sf900 (w ab) and transfer 1 ml of the virus culture from the well into the flask. Incubate at 27^{o}C shaking at 125rpm for 96 hrs. The above is infection to generate P2 virus.

To check expression at this stage, you can take 200µl aliquots at 48hrs, 72 hrs and 96 hrs, spin the aliquot at 2400rpm in table-top microcentrifuge for 5 min, discard SN, resuspend pellet in 75µl water then add 75µl 2XSB, boil 5min and load on gel for coomassie staining or western blot. If you don't see expression, the virus is not good or the virus titer is very low. You need to amplify the virus to increase its titer.

After 96 hrs, you will have 10 ml of P2 virus. Spin down culture, and filter SN (virus solution) with a 0.22 µm filter. To generate P3 virus (to increase titer or to amplify low stock), dilute P2 virus solution 5 to 25 times into the appropriate volume of 2 millions/ml Sf9 culture. P3 virus should be high titer enough to show expression. To determine the exact titer, you need to perform a titer test (plaque assay) descibed by invitrogen.

(Original protocols from Invitrogen; Bac-to-Bac Baculovirus Expression System, Gibco BRL; Bac-to-Bac Baculovirus Expression System. Modified by Gaya Amarashinghe, Junko Umetani and Ayman Ismail.)

Bibliography

Abdul-Manan, N., Aghazadeh, B., Liu, G.A., Majumdar, A., Ouerfelli, O., Siminovitch, K.A., and Rosen, M.K. (1999). Structure of Cdc42 in complex with the GTPase-binding domain of the 'Wiskott-Aldrich syndrome' protein. Nature *399*, 379-383.

Abou-Kheir, W., Isaac, B., Yamaguchi, H., and Cox, D. (2008). Membrane targeting of WAVE2 is not sufficient for WAVE2-dependent actin polymerization: a role for IRSp53 in mediating the interaction between Rac and WAVE2. J Cell Sci *121*, 379-390.

Aghazadeh, B., Lowry, W.E., Huang, X.Y., and Rosen, M.K. (2000). Structural basis for relief of autoinhibition of the Dbl homology domain of proto-oncogene Vav by tyrosine phosphorylation. Cell *102*, 625-633.

Ardern, H., Sandilands, E., Machesky, L.M., Timpson, P., Frame, M.C., and Brunton, V.G. (2006). Src-dependent phosphorylation of Scar1 promotes its association with the Arp2/3 complex. Cell Motil Cytoskeleton *63*, 6-13.

Basu, D., El-Assal Sel, D., Le, J., Mallery, E.L., and Szymanski, D.B. (2004). Interchangeable functions of Arabidopsis PIROGI and the human WAVE complex subunit SRA1 during leaf epidermal development. Development *131*, 4345-4355.

Basu, D., Le, J., El-Essal Sel, D., Huang, S., Zhang, C., Mallery, E.L., Koliantz, G., Staiger, C.J., and Szymanski, D.B. (2005). DISTORTED3/SCAR2 is a putative arabidopsis WAVE complex subunit that activates the Arp2/3 complex and is required for epidermal morphogenesis. Plant Cell *17*, 502-524.

Bear, J.E., Rawls, J.F., and Saxe, C.L., 3rd (1998). SCAR, a WASP-related protein, isolated as a suppressor of receptor defects in late Dictyostelium development. J Cell Biol *142*, 1325-1335.

Bierne, H., Miki, H., Innocenti, M., Scita, G., Gertler, F.B., Takenawa, T., and Cossart, P. (2005). WASP-related proteins, Abi1 and Ena/VASP are required for Listeria invasion induced by the Met receptor. J Cell Sci *118*, 1537-1547.

Billadeau, D.D., Nolz, J.C., and Gomez, T.S. (2007). Regulation of T-cell activation by the cytoskeleton. Nat Rev Immunol *7*, 131-143.

Blanchoin, L., Amann, K.J., Higgs, H.N., Marchand, J.B., Kaiser, D.A., and Pollard, T.D. (2000). Direct observation of dendritic actin filament networks nucleated by Arp2/3 complex and WASP/Scar proteins. Nature *404*, 1007-1011.

Bogdan, S., Grewe, O., Strunk, M., Mertens, A., and Klambt, C. (2004). Sra-1 interacts with Kette and Wasp and is required for neuronal and bristle development in Drosophila. Development *131*, 3981-3989.

Bogdan, S., Stephan, R., Lobke, C., Mertens, A., and Klambt, C. (2005). Abi activates WASP to promote sensory organ development. Nat Cell Biol *7*, 977-984.

Brembu, T., Winge, P., Seem, M., and Bones, A.M. (2004). NAPP and PIRP encode subunits of a putative wave regulatory protein complex involved in plant cell morphogenesis. Plant Cell *16*, 2335-2349.

Carlier, M.F., Nioche, P., Broutin-L'Hermite, I., Boujemaa, R., Le Clainche, C., Egile, C., Garbay, C., Ducruix, A., Sansonetti, P., and Pantaloni, D. (2000). GRB2 links signaling to actin assembly by enhancing interaction of neural Wiskott-Aldrich syndrome protein (N-WASp) with actin-related protein (ARP2/3) complex. J Biol Chem *275*, 21946-21952.

Cheng, H.C., Skehan, B.M., Campellone, K.G., Leong, J.M., and Rosen, M.K. (2008). Structural mechanism of WASP activation by the enterohaemorrhagic E. coli effector EspF(U). Nature *454*, 1009-1013.

Cheng, N.-S. (2008). Formula for the Viscosity of a Glycerol−Water Mixture. Industrial & Engineering Chemistry Research *47*, 3285-3288.

Chhabra, E.S., and Higgs, H.N. (2007). The many faces of actin: matching assembly factors with cellular structures. Nat Cell Biol *9*, 1110-1121.

Co, C., Wong, D.T., Gierke, S., Chang, V., and Taunton, J. (2007). Mechanism of actin network attachment to moving membranes: barbed end capture by N-WASP WH2 domains. Cell *128*, 901-913.

Connolly, B.A., Rice, J., Feig, L.A., and Buchsbaum, R.J. (2005). Tiam1-IRSp53 complex formation directs specificity of rac-mediated actin cytoskeleton regulation. Mol Cell Biol *25*, 4602-4614.

Dahl, J.P., Wang-Dunlop, J., Gonzales, C., Goad, M.E., Mark, R.J., and Kwak, S.P. (2003). Characterization of the WAVE1 knock-out mouse: implications for CNS development. J Neurosci *23*, 3343-3352.

Dai, Z., and Pendergast, A.M. (1995). Abi-2, a novel SH3-containing protein interacts with the c-Abl tyrosine kinase and modulates c-Abl transforming activity. Genes Dev *9*, 2569-2582.

Danson, C.M., Pocha, S.M., Bloomberg, G.B., and Cory, G.O. (2007). Phosphorylation of WAVE2 by MAP kinases regulates persistent cell migration and polarity. J Cell Sci *120*, 4144-4154.

Derivery, E., Fink, J., Martin, D., Houdusse, A., Piel, M., Stradal, T.E., Louvard, D., and Gautreau, A. (2008). Free Brick1 is a trimeric precursor in the assembly of a functional wave complex. PLoS ONE *3*, e2462.

Derivery, E., Lombard, B., Loew, D., and Gautreau, A. (2009). The Wave complex is intrinsically inactive. Cell Motil Cytoskeleton.

Djakovic, S., Dyachok, J., Burke, M., Frank, M.J., and Smith, L.G. (2006). BRICK1/HSPC300 functions with SCAR and the ARP2/3 complex to regulate epidermal cell shape in Arabidopsis. Development *133*, 1091-1100.

dos Remedios, C.G., Chhabra, D., Kekic, M., Dedova, I.V., Tsubakihara, M., Berry, D.A., and Nosworthy, N.J. (2003). Actin binding proteins: regulation of cytoskeletal microfilaments. Physiol Rev *83*, 433-473.

Drenckhahn, D., and Pollard, T.D. (1986). Elongation of actin filaments is a diffusion-limited reaction at the barbed end and is accelerated by inert macromolecules. J Biol Chem *261*, 12754-12758.

Echarri, A., Lai, M.J., Robinson, M.R., and Pendergast, A.M. (2004). Abl interactor 1 (Abi-1) wave-binding and SNARE domains regulate its nucleocytoplasmic shuttling, lamellipodium localization, and wave-1 levels. Mol Cell Biol *24*, 4979-4993.

Eden, S., Rohatgi, R., Podtelejnikov, A.V., Mann, M., and Kirschner, M.W. (2002). Mechanism of regulation of WAVE1-induced actin nucleation by Rac1 and Nck. Nature *418*, 790-793.

Egea, G., Lazaro-Dieguez, F., and Vilella, M. (2006). Actin dynamics at the Golgi complex in mammalian cells. Curr Opin Cell Biol *18*, 168-178.

El-Assal Sel, D., Le, J., Basu, D., Mallery, E.L., and Szymanski, D.B. (2004). Arabidopsis GNARLED encodes a NAP125 homolog that positively regulates ARP2/3. Curr Biol *14*, 1405-1409.

Evangelista, M., Zigmond, S., and Boone, C. (2003). Formins: signaling effectors for assembly and polarization of actin filaments. J Cell Sci *116*, 2603-2611.

Fan, P.D., and Goff, S.P. (2000). Abl interactor 1 binds to sos and inhibits epidermal growth factor- and v-Abl-induced activation of extracellular signal-regulated kinases. Mol Cell Biol *20*, 7591-7601.

Fukuoka, M., Suetsugu, S., Miki, H., Fukami, K., Endo, T., and Takenawa, T. (2001). A novel neural Wiskott-Aldrich syndrome protein (N-WASP) binding protein, WISH, induces Arp2/3 complex activation independent of Cdc42. J Cell Biol *152*, 471-482.

Gautreau, A., Ho, H.Y., Li, J., Steen, H., Gygi, S.P., and Kirschner, M.W. (2004). Purification and architecture of the ubiquitous Wave complex. Proc Natl Acad Sci U S A *101*, 4379-4383.

Goley, E.D., and Welch, M.D. (2006). The ARP2/3 complex: an actin nucleator comes of age. Nat Rev Mol Cell Biol *7*, 713-726.

Grove, M., Demyanenko, G., Echarri, A., Zipfel, P.A., Quiroz, M.E., Rodriguiz, R.M., Playford, M., Martensen, S.A., Robinson, M.R., Wetsel, W.C.*, et al.* (2004). ABI2-deficient mice exhibit defective cell migration, aberrant dendritic spine morphogenesis, and deficits in learning and memory. Mol Cell Biol *24*, 10905-10922.

Hahne, P., Sechi, A., Benesch, S., and Small, J.V. (2001). Scar/WAVE is localised at the tips of protruding lamellipodia in living cells. FEBS Lett *492*, 215-220.

Higgs, H.N., and Pollard, T.D. (2000). Activation by Cdc42 and PIP(2) of Wiskott-Aldrich syndrome protein (WASp) stimulates actin nucleation by Arp2/3 complex. J Cell Biol *150*, 1311-1320.

Hirao, N., Sato, S., Gotoh, T., Maruoka, M., Suzuki, J., Matsuda, S., Shishido, T., and Tani, K. (2006). NESH (Abi-3) is present in the Abi/WAVE complex but does not promote c-Abl-mediated phosphorylation. FEBS Lett *580*, 6464-6470.

Ho, H.Y., Rohatgi, R., Lebensohn, A.M., Le, M., Li, J., Gygi, S.P., and Kirschner, M.W. (2004). Toca-1 mediates Cdc42-dependent actin nucleation by activating the N-WASP-WIP complex. Cell *118*, 203-216.

Huang, C.H., Lin, T.Y., Pan, R.L., and Juang, J.L. (2007). The involvement of Abl and PTP61F in the regulation of Abi protein localization and stability and lamella formation in Drosophila S2 cells. J Biol Chem *282*, 32442-32452.

Huang, C.L., Ueno, M., Liu, D., Masuya, D., Nakano, J., Yokomise, H., Nakagawa, T., and Miyake, M. (2006). MRP-1/CD9 gene transduction regulates the actin cytoskeleton through the downregulation of WAVE2. Oncogene *25*, 6480-6488.

Hummel, T., Leifker, K., and Klambt, C. (2000). The Drosophila HEM-2/NAP1 homolog KETTE controls axonal pathfinding and cytoskeletal organization. Genes Dev *14*, 863-873.

Innocenti, M., Frittoli, E., Ponzanelli, I., Falck, J.R., Brachmann, S.M., Di Fiore, P.P., and Scita, G. (2003). Phosphoinositide 3-kinase activates Rac by entering in a complex with Eps8, Abi1, and Sos-1. J Cell Biol *160*, 17-23.

Innocenti, M., Gerboth, S., Rottner, K., Lai, F.P., Hertzog, M., Stradal, T.E., Frittoli, E., Didry, D., Polo, S., Disanza, A.*, et al.* (2005). Abi1 regulates the activity of N-WASP and WAVE in distinct actin-based processes. Nat Cell Biol *7*, 969-976.

Innocenti, M., Zucconi, A., Disanza, A., Frittoli, E., Areces, L.B., Steffen, A., Stradal, T.E., Di Fiore, P.P., Carlier, M.F., and Scita, G. (2004). Abi1 is essential for the formation and activation of a WAVE2 signalling complex. Nat Cell Biol *6*, 319-327.

Juang, J.L., and Hoffmann, F.M. (1999). Drosophila abelson interacting protein (dAbi) is a positive regulator of abelson tyrosine kinase activity. Oncogene *18*, 5138-5147.

Kawamura, K., Takano, K., Suetsugu, S., Kurisu, S., Yamazaki, D., Miki, H., Takenawa, T., and Endo, T. (2004). N-WASP and WAVE2 acting downstream of phosphatidylinositol 3-kinase are required for myogenic cell migration induced by hepatocyte growth factor. J Biol Chem *279*, 54862-54871.

Kheir, W.A., Gevrey, J.C., Yamaguchi, H., Isaac, B., and Cox, D. (2005). A WAVE2-Abi1 complex mediates CSF-1-induced F-actin-rich membrane protrusions and migration in macrophages. J Cell Sci *118*, 5369-5379.

Kim, A.S., Kakalis, L.T., Abdul-Manan, N., Liu, G.A., and Rosen, M.K. (2000). Autoinhibition and activation mechanisms of the Wiskott-Aldrich syndrome protein. Nature *404*, 151-158.

Kim, Y., Sung, J.Y., Ceglia, I., Lee, K.W., Ahn, J.H., Halford, J.M., Kim, A.M., Kwak, S.P., Park, J.B., Ho Ryu, S.*, et al.* (2006). Phosphorylation of WAVE1 regulates actin polymerization and dendritic spine morphology. Nature *442*, 814-817.

Kitamura, T., Kitamura, Y., Yonezawa, K., Totty, N.F., Gout, I., Hara, K., Waterfield, M.D., Sakaue, M., Ogawa, W., and Kasuga, M. (1996). Molecular cloning of p125Nap1, a protein that associates with an SH3 domain of Nck. Biochem Biophys Res Commun *219*, 509-514.

Kitamura, Y., Kitamura, T., Sakaue, H., Maeda, T., Ueno, H., Nishio, S., Ohno, S., Osada, S., Sakaue, M., Ogawa, W., and Kasuga, M. (1997). Interaction of Nck-associated protein 1 with activated GTP-binding protein Rac. Biochem J *322 (Pt 3)*, 873-878.

Kobayashi, K., Kuroda, S., Fukata, M., Nakamura, T., Nagase, T., Nomura, N., Matsuura, Y., Yoshida-Kubomura, N., Iwamatsu, A., and Kaibuchi, K. (1998). p140Sra-1 (specifically Rac1-associated protein) is a novel specific target for Rac1 small GTPase. J Biol Chem *273*, 291-295.

Kowalski, J.R., Egile, C., Gil, S., Snapper, S.B., Li, R., and Thomas, S.M. (2005). Cortactin regulates cell migration through activation of N-WASP. J Cell Sci *118*, 79-87.

Kunda, P., Craig, G., Dominguez, V., and Baum, B. (2003). Abi, Sra1, and Kette control the stability and localization of SCAR/WAVE to regulate the formation of actin-based protrusions. Curr Biol *13*, 1867-1875.

Kurisu, S., Suetsugu, S., Yamazaki, D., Yamaguchi, H., and Takenawa, T. (2005). Rac-WAVE2 signaling is involved in the invasive and metastatic phenotypes of murine melanoma cells. Oncogene *24*, 1309-1319.

Laue, T.M., Shah, B.D., Ridgeway, R.M., and Pelletier, S.L. (1992). Computer-aided interpretation of analytical sedimentation data for proteins. In Analytical

Ultracentrifugation in Biochemistry and Polymer Science, S.E. Harding, A.J. Rowe, and J.C. Horton, eds. (Cambridge, UK: The Royal Society of Chemistry).

Leng, Y., Zhang, J., Badour, K., Arpaia, E., Freeman, S., Cheung, P., Siu, M., and Siminovitch, K. (2005). Abelson-interactor-1 promotes WAVE2 membrane translocation and Abelson-mediated tyrosine phosphorylation required for WAVE2 activation. Proc Natl Acad Sci U S A *102*, 1098-1103.

Leung, D.W., Morgan, D.M., and Rosen, M.K. (2006). Biochemical properties and inhibitors of (N-)WASP. Methods Enzymol *406*, 281-296.

Machesky, L.M., Atkinson, S.J., Ampe, C., Vandekerckhove, J., and Pollard, T.D. (1994). Purification of a cortical complex containing two unconventional actins from Acanthamoeba by affinity chromatography on profilin-agarose. J Cell Biol *127*, 107-115.

Machesky, L.M., and Insall, R.H. (1998). Scar1 and the related Wiskott-Aldrich syndrome protein, WASP, regulate the actin cytoskeleton through the Arp2/3 complex. Curr Biol *8*, 1347-1356.

Machesky, L.M., Mullins, R.D., Higgs, H.N., Kaiser, D.A., Blanchoin, L., May, R.C., Hall, M.E., and Pollard, T.D. (1999). Scar, a WASp-related protein, activates nucleation of actin filaments by the Arp2/3 complex. Proc Natl Acad Sci U S A *96*, 3739-3744.

Marchand, J.B., Kaiser, D.A., Pollard, T.D., and Higgs, H.N. (2001). Interaction of WASP/Scar proteins with actin and vertebrate Arp2/3 complex. Nat Cell Biol *3*, 76-82.

Matsuo, H., Walters, K.J., Teruya, K., Tanaka, T., Gassner, G.T., Lippard, S.J., Kyogoku, Y., and Wagner, G. (1999). Identification by NMR Spectroscopy of Residues at Contact Surfaces in Large, Slowly Exchanging Macromolecular Complexes. Journal of the American Chemical Society *121*, 9903-9904.

Miki, H., Miura, K., and Takenawa, T. (1996). N-WASP, a novel actin-depolymerizing protein, regulates the cortical cytoskeletal rearrangement in a PIP2-dependent manner downstream of tyrosine kinases. EMBO J *15*, 5326-5335.

Miki, H., Suetsugu, S., and Takenawa, T. (1998). WAVE, a novel WASP-family protein involved in actin reorganization induced by Rac. EMBO J *17*, 6932-6941.

Miki, H., and Takenawa, T. (2002). WAVE2 serves a functional partner of IRSp53 by regulating its interaction with Rac. Biochem Biophys Res Commun *293*, 93-99.

Miki, H., Yamaguchi, H., Suetsugu, S., and Takenawa, T. (2000). IRSp53 is an essential intermediate between Rac and WAVE in the regulation of membrane ruffling. Nature *408*, 732-735.

Mullins, R.D., and Machesky, L.M. (2000). Actin assembly mediated by Arp2/3 complex and WASP family proteins. Methods Enzymol *325*, 214-237.

Nakagawa, H., Miki, H., Ito, M., Ohashi, K., Takenawa, T., and Miyamoto, S. (2001). N-WASP, WAVE and Mena play different roles in the organization of actin cytoskeleton in lamellipodia. J Cell Sci *114*, 1555-1565.

Nakagawa, H., Miki, H., Nozumi, M., Takenawa, T., Miyamoto, S., Wehland, J., and Small, J.V. (2003). IRSp53 is colocalised with WAVE2 at the tips of protruding lamellipodia and filopodia independently of Mena. J Cell Sci *116*, 2577-2583.

Nakanishi, O., Suetsugu, S., Yamazaki, D., and Takenawa, T. (2007). Effect of WAVE2 phosphorylation on activation of the Arp2/3 complex. J Biochem *141*, 319-325.

Nolz, J.C., Gomez, T.S., Zhu, P., Li, S., Medeiros, R.B., Shimizu, Y., Burkhardt, J.K., Freedman, B.D., and Billadeau, D.D. (2006). The WAVE2 complex regulates actin cytoskeletal reorganization and CRAC-mediated calcium entry during T cell activation. Curr Biol *16*, 24-34.

Oikawa, T., Yamaguchi, H., Itoh, T., Kato, M., Ijuin, T., Yamazaki, D., Suetsugu, S., and Takenawa, T. (2004). PtdIns(3,4,5)P3 binding is necessary for WAVE2-induced formation of lamellipodia. Nat Cell Biol *6*, 420-426.

Otsuki, M., Itoh, T., and Takenawa, T. (2003). Neural Wiskott-Aldrich syndrome protein is recruited to rafts and associates with endophilin A in response to epidermal growth factor. J Biol Chem *278*, 6461-6469.

Paavilainen, V.O., Bertling, E., Falck, S., and Lappalainen, P. (2004). Regulation of cytoskeletal dynamics by actin-monomer-binding proteins. Trends Cell Biol *14*, 386-394.

Padrick, S.B., Cheng, H.C., Ismail, A.M., Panchal, S.C., Doolittle, L.K., Kim, S., Skehan, B.M., Umetani, J., Brautigam, C.A., Leong, J.M., and Rosen, M.K. (2008). Hierarchical regulation of WASP/WAVE proteins. Mol Cell *32*, 426-438.

Panchal, S.C., Kaiser, D.A., Torres, E., Pollard, T.D., and Rosen, M.K. (2003). A conserved amphipathic helix in WASP/Scar proteins is essential for activation of Arp2/3 complex. Nat Struct Biol *10*, 591-598.

Pocha, S.M., and Cory, G.O. (2009). WAVE2 is regulated by multiple phosphorylation events within its VCA domain. Cell Motil Cytoskeleton *66*, 36-47.

Pollard, T.D. (1986). Rate constants for the reactions of ATP- and ADP-actin with the ends of actin filaments. J Cell Biol *103*, 2747-2754.

Pollard, T.D. (2007). Regulation of actin filament assembly by Arp2/3 complex and formins. Annu Rev Biophys Biomol Struct *36*, 451-477.

Pollard, T.D., and Borisy, G.G. (2003). Cellular motility driven by assembly and disassembly of actin filaments. Cell *112*, 453-465.

Prehoda, K.E., Scott, J.A., Mullins, R.D., and Lim, W.A. (2000). Integration of multiple signals through cooperative regulation of the N-WASP-Arp2/3 complex. Science *290*, 801-806.

Qurashi, A., Sahin, H.B., Carrera, P., Gautreau, A., Schenck, A., and Giangrande, A. (2007). HSPC300 and its role in neuronal connectivity. Neural Develop *2*, 18.

Rafelski, S.M., and Theriot, J.A. (2004). Crawling toward a unified model of cell mobility: spatial and temporal regulation of actin dynamics. Annu Rev Biochem *73*, 209-239.

Rakeman, A.S., and Anderson, K.V. (2006). Axis specification and morphogenesis in the mouse embryo require Nap1, a regulator of WAVE-mediated actin branching. Development *133*, 3075-3083.

Rameh, L.E., Arvidsson, A., Carraway, K.L., 3rd, Couvillon, A.D., Rathbun, G., Crompton, A., VanRenterghem, B., Czech, M.P., Ravichandran, K.S., Burakoff, S.J.*, et al.* (1997). A comparative analysis of the phosphoinositide binding specificity of pleckstrin homology domains. J Biol Chem *272*, 22059-22066.

Robinson, R.C., Turbedsky, K., Kaiser, D.A., Marchand, J.B., Higgs, H.N., Choe, S., and Pollard, T.D. (2001). Crystal structure of Arp2/3 complex. Science *294*, 1679-1684.

Rogers, S.L., Wiedemann, U., Stuurman, N., and Vale, R.D. (2003). Molecular requirements for actin-based lamella formation in Drosophila S2 cells. J Cell Biol *162*, 1079-1088.

Rohatgi, R., Nollau, P., Ho, H.Y., Kirschner, M.W., and Mayer, B.J. (2001). Nck and phosphatidylinositol 4,5-bisphosphate synergistically activate actin polymerization through the N-WASP-Arp2/3 pathway. J Biol Chem *276*, 26448-26452.

Rozelle, A.L., Machesky, L.M., Yamamoto, M., Driessens, M.H., Insall, R.H., Roth, M.G., Luby-Phelps, K., Marriott, G., Hall, A., and Yin, H.L. (2000). Phosphatidylinositol 4,5-bisphosphate induces actin-based movement of raft-enriched vesicles through WASP-Arp2/3. Curr Biol *10*, 311-320.

Saedler, R., Zimmermann, I., Mutondo, M., and Hulskamp, M. (2004). The Arabidopsis KLUNKER gene controls cell shape changes and encodes the AtSRA1 homolog. Plant Mol Biol *56*, 775-782.

Saller, E., Tom, E., Brunori, M., Otter, M., Estreicher, A., Mack, D.H., and Iggo, R. (1999). Increased apoptosis induction by 121F mutant p53. EMBO J *18*, 4424-4437.

Sano, K., Maeda, K., Oki, M., and Maeda, Y. (2002). Enhancement of protein expression in insect cells by a lobster tropomyosin cDNA leader sequence. FEBS Lett *532*, 143-146.

Schenck, A., Bardoni, B., Langmann, C., Harden, N., Mandel, J.L., and Giangrande, A. (2003). CYFIP/Sra-1 controls neuronal connectivity in Drosophila and links the Rac1 GTPase pathway to the fragile X protein. Neuron *38*, 887-898.

Schenck, A., Bardoni, B., Moro, A., Bagni, C., and Mandel, J.L. (2001). A highly conserved protein family interacting with the fragile X mental retardation protein (FMRP) and displaying selective interactions with FMRP-related proteins FXR1P and FXR2P. Proc Natl Acad Sci U S A *98*, 8844-8849.

Schenck, A., Qurashi, A., Carrera, P., Bardoni, B., Diebold, C., Schejter, E., Mandel, J.L., and Giangrande, A. (2004). WAVE/SCAR, a multifunctional complex coordinating different aspects of neuronal connectivity. Dev Biol *274*, 260-270.

Scita, G., Nordstrom, J., Carbone, R., Tenca, P., Giardina, G., Gutkind, S., Bjarnegard, M., Betsholtz, C., and Di Fiore, P.P. (1999). EPS8 and E3B1 transduce signals from Ras to Rac. Nature *401*, 290-293.

Segur, J.B., and Oberstar, H.E. (1951). Viscosity of Glycerol and Its Aqueous Solutions. Industrial & Engineering Chemistry *43*, 2117-2120.

Sept, D., and McCammon, J.A. (2001). Thermodynamics and kinetics of actin filament nucleation. Biophys J *81*, 667-674.

Sheterline, P., Clayton, J., and Sparrow, J. (1998). Actin, fourth edition edn (Oxford: Oxford University Press).

Shi, Y., Alin, K., and Goff, S.P. (1995). Abl-interactor-1, a novel SH3 protein binding to the carboxy-terminal portion of the Abl protein, suppresses v-abl transforming activity. Genes Dev *9*, 2583-2597.

Silacci, P., Mazzolai, L., Gauci, C., Stergiopulos, N., Yin, H.L., and Hayoz, D. (2004). Gelsolin superfamily proteins: key regulators of cellular functions. Cell Mol Life Sci *61*, 2614-2623.

Soderling, S.H., Binns, K.L., Wayman, G.A., Davee, S.M., Ong, S.H., Pawson, T., and Scott, J.D. (2002). The WRP component of the WAVE-1 complex attenuates Rac-mediated signalling. Nat Cell Biol *4*, 970-975.

Soderling, S.H., Guire, E.S., Kaech, S., White, J., Zhang, F., Schutz, K., Langeberg, L.K., Banker, G., Raber, J., and Scott, J.D. (2007). A WAVE-1 and WRP signaling complex regulates spine density, synaptic plasticity, and memory. J Neurosci *27*, 355-365.

Soderling, S.H., Langeberg, L.K., Soderling, J.A., Davee, S.M., Simerly, R., Raber, J., and Scott, J.D. (2003). Loss of WAVE-1 causes sensorimotor retardation and reduced learning and memory in mice. Proc Natl Acad Sci U S A *100*, 1723-1728.

Sossey-Alaoui, K., Head, K., Nowak, N., and Cowell, J.K. (2003). Genomic organization and expression profile of the human and mouse WAVE gene family. Mamm Genome *14*, 314-322.

Sossey-Alaoui, K., Li, X., and Cowell, J.K. (2007). c-Abl-mediated phosphorylation of WAVE3 is required for lamellipodia formation and cell migration. J Biol Chem *282*, 26257-26265.

Sossey-Alaoui, K., Li, X., Ranalli, T.A., and Cowell, J.K. (2005). WAVE3-mediated cell migration and lamellipodia formation are regulated downstream of phosphatidylinositol 3-kinase. J Biol Chem *280*, 21748-21755.

Soto, M.C., Qadota, H., Kasuya, K., Inoue, M., Tsuboi, D., Mello, C.C., and Kaibuchi, K. (2002). The GEX-2 and GEX-3 proteins are required for tissue morphogenesis and cell migrations in C. elegans. Genes Dev *16*, 620-632.

Steffen, A., Rottner, K., Ehinger, J., Innocenti, M., Scita, G., Wehland, J., and Stradal, T.E. (2004). Sra-1 and Nap1 link Rac to actin assembly driving lamellipodia formation. EMBO J *23*, 749-759.

Stovold, C.F., Millard, T.H., and Machesky, L.M. (2005). Inclusion of Scar/WAVE3 in a similar complex to Scar/WAVE1 and 2. BMC Cell Biol *6*, 11.

Stradal, T., Courtney, K.D., Rottner, K., Hahne, P., Small, J.V., and Pendergast, A.M. (2001). The Abl interactor proteins localize to sites of actin polymerization at the tips of lamellipodia and filopodia. Curr Biol *11*, 891-895.

Stradal, T.E., and Scita, G. (2006). Protein complexes regulating Arp2/3-mediated actin assembly. Curr Opin Cell Biol *18*, 4-10.

Suetsugu, S., Miki, H., and Takenawa, T. (1999). Identification of two human WAVE/SCAR homologues as general actin regulatory molecules which associate with the Arp2/3 complex. Biochem Biophys Res Commun *260*, 296-302.

Takano, K., Toyooka, K., and Suetsugu, S. (2008). EFC/F-BAR proteins and the N-WASP-WIP complex induce membrane curvature-dependent actin polymerization. EMBO J *27*, 2817-2828.

Tam, P.P., and Behringer, R.R. (1997). Mouse gastrulation: the formation of a mammalian body plan. Mech Dev *68*, 3-25.

Tani, K., Sato, S., Sukezane, T., Kojima, H., Hirose, H., Hanafusa, H., and Shishido, T. (2003). Abl interactor 1 promotes tyrosine 296 phosphorylation of mammalian enabled (Mena) by c-Abl kinase. J Biol Chem *278*, 21685-21692.

Torres, E., and Rosen, M.K. (2003). Contingent phosphorylation/dephosphorylation provides a mechanism of molecular memory in WASP. Mol Cell *11*, 1215-1227.

Unsworth, K.E., Way, M., McNiven, M., Machesky, L., and Holden, D.W. (2004). Analysis of the mechanisms of Salmonella-induced actin assembly during invasion of host cells and intracellular replication. Cell Microbiol *6*, 1041-1055.

Wang, C., Navab, R., Iakovlev, V., Leng, Y., Zhang, J., Tsao, M.S., Siminovitch, K., McCready, D.R., and Done, S.J. (2007). Abelson interactor protein-1 positively regulates breast cancer cell proliferation, migration, and invasion. Mol Cancer Res *5*, 1031-1039.

Wang, Q., Kaan, H.Y., Hooda, R.N., Goh, S.L., and Sondermann, H. (2008). Structure and plasticity of Endophilin and Sorting Nexin 9. Structure *16*, 1574-1587.

Weiner, O.D., Rentel, M.C., Ott, A., Brown, G.E., Jedrychowski, M., Yaffe, M.B., Gygi, S.P., Cantley, L.C., Bourne, H.R., and Kirschner, M.W. (2006). Hem-1 complexes are essential for Rac activation, actin polymerization, and myosin regulation during neutrophil chemotaxis. PLoS Biol *4*, e38.

Weissenhorn, W. (2005). Crystal structure of the endophilin-A1 BAR domain. J Mol Biol *351*, 653-661.

Westphal, R.S., Soderling, S.H., Alto, N.M., Langeberg, L.K., and Scott, J.D. (2000). Scar/WAVE-1, a Wiskott-Aldrich syndrome protein, assembles an actin-associated multi-kinase scaffold. EMBO J *19*, 4589-4600.

Yamamoto, A., and Behl, C. (2001). Human Nck-associated protein 1 and its binding protein affect the metabolism of beta-amyloid precursor protein with Swedish mutation. Neurosci Lett *316*, 50-54.

Yamamoto, A., Suzuki, T., and Sakaki, Y. (2001). Isolation of hNap1BP which interacts with human Nap1 (NCKAP1) whose expression is down-regulated in Alzheimer's disease. Gene *271*, 159-169.

Yamazaki, D., Fujiwara, T., Suetsugu, S., and Takenawa, T. (2005). A novel function of WAVE in lamellipodia: WAVE1 is required for stabilization of lamellipodial protrusions during cell spreading. Genes Cells *10*, 381-392.

Yamazaki, D., Suetsugu, S., Miki, H., Kataoka, Y., Nishikawa, S., Fujiwara, T., Yoshida, N., and Takenawa, T. (2003). WAVE2 is required for directed cell migration and cardiovascular development. Nature *424*, 452-456.

Yan, C., Martinez-Quiles, N., Eden, S., Shibata, T., Takeshima, F., Shinkura, R., Fujiwara, Y., Bronson, R., Snapper, S.B., Kirschner, M.W.*, et al.* (2003). WAVE2 deficiency reveals distinct roles in embryogenesis and Rac-mediated actin-based motility. EMBO J *22*, 3602-3612.

Yokota, Y., Ring, C., Cheung, R., Pevny, L., and Anton, E.S. (2007). Nap1-regulated neuronal cytoskeletal dynamics is essential for the final differentiation of neurons in cerebral cortex. Neuron *54*, 429-445.

Zalevsky, J., Lempert, L., Kranitz, H., and Mullins, R.D. (2001). Different WASP family proteins stimulate different Arp2/3 complex-dependent actin-nucleating activities. Curr Biol *11*, 1903-1913.

Zallen, J.A., Cohen, Y., Hudson, A.M., Cooley, L., Wieschaus, E., and Schejter, E.D. (2002). SCAR is a primary regulator of Arp2/3-dependent morphological events in Drosophila. J Cell Biol *156*, 689-701.

Zhang, X., Dyachok, J., Krishnakumar, S., Smith, L.G., and Oppenheimer, D.G. (2005). IRREGULAR TRICHOME BRANCH1 in Arabidopsis encodes a plant homolog of the actin-related protein2/3 complex activator Scar/WAVE that regulates actin and microtubule organization. Plant Cell *17*, 2314-2326.

Zimmermann, I., Saedler, R., Mutondo, M., and Hulskamp, M. (2004). The Arabidopsis GNARLED gene encodes the NAP125 homolog and controls several actin-based cell shape changes. Mol Genet Genomics *272*, 290-296.

Zipfel, P.A., Bunnell, S.C., Witherow, D.S., Gu, J.J., Chislock, E.M., Ring, C., and Pendergast, A.M. (2006). Role for the Abi/wave protein complex in T cell receptor-mediated proliferation and cytoskeletal remodeling. Curr Biol *16*, 35-46.